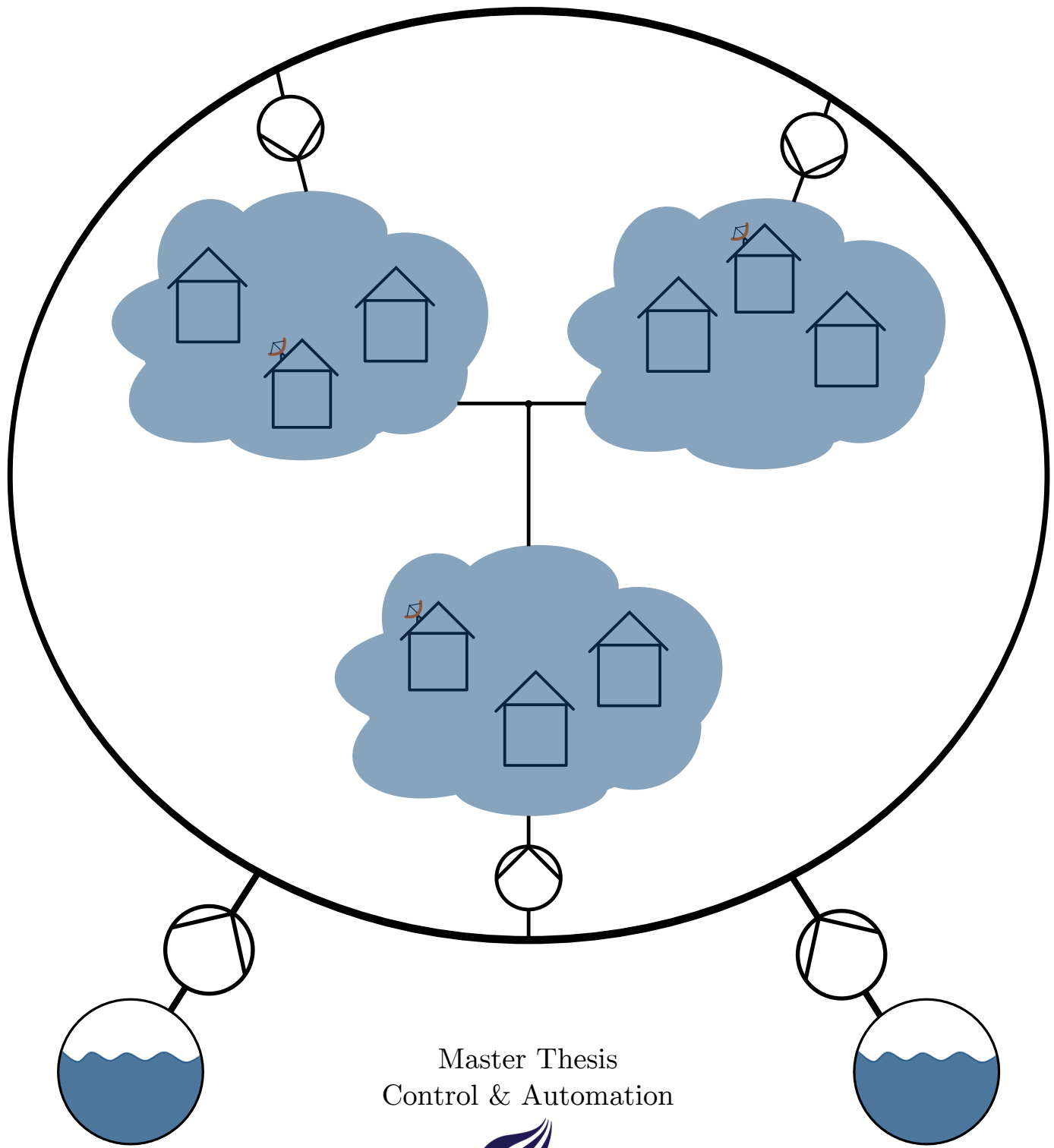


Energy Optimization of Water Distribution Networks

-Using a distributed pumping solution for optimal pressure control



Master Thesis
Control & Automation



AALBORG UNIVERSITY
DENMARK

Aalborg University
The Faculty of Engineering and Science
School of Information and
Communication Technology
Frederik Bajers Vej 7
9220 Aalborg Ø
Tlf.: 9940 9730
Telefax: 9940 9725
<http://www.es.aau.dk>



Subject: Control and Automation
Title: Energy Optimization of Water Distribution Networks
Project period: February 2th – June 3rd 2015
Semester: 10th Semester (P10)
Project group: 1033
Authors:

Mathias Mølgaard

Bjarni Geir Pétursson

Supervisor: Carsten Skovmose Kallsøe & Tom Nørgaard Jensen
Number of copies: 5

Pages: 130
Appendix pages: 21
Attachment: USB - Storage Device

Abstract:

This project covers the development of a power optimal control strategy for a water distribution network.

It is proposed to replace the pressure reducing valves commonly used to regulate pressure, with pumps, throughout the network.

By exploiting the additional freedom for control, obtained by having an over-actuated system, it is possible to reduce the power consumption.

The power optimal controller finds the optimal distribution of pressure boost from the pumps, by means of gradient descent, while still maintaining output pressure.

Furthermore the controller developed only requires knowledge of the distribution networks topology given by a graphical description. It is also designed to use a minimum of communication between the individual pumps within the network.

The results shows that the power optimal controller slowly reduces the power consumption of the distribution network once the system pressure has reached steady-state, thus fulfilling the criteria of the controller.

The contents of this report are freely available, but publication (with specification of source) may only take place after arrangement with the authors.

Preface

Reading Guide

Sources given in the beginning of a section apply to all subsections. Additional sources may be given in subsections. Citations are given in square brackets indicating the author (first) and the year of publication (last two ciphers), i.e. *Robust Model-Based Fault Diagnosis for Dynamic Systems* from 1999 by J. Chen & R. J. Patton is given as [Chen 99]. Figures, equations and tables are numbered according to chapter and location, e.g. third figure in chapter five is numbered 5.3. Units are given in square brackets in symbolic equations and without brackets otherwise.

Symbols, acronyms and general notations used in this report are presented in the nomenclature after this preface. Appendices are placed after the main report, referred to by capital letters, followed by the Bibliography. The attached USB contains relevant data sheets, copies of references found on the Internet, MATLAB and Simulink models and a digital version of this report.

Contents

Preface	iii
Nomenclature	1
1 Introduction	5
1.1 Project Background	5
1.2 Pressure Management	6
1.3 Project Focus	8
I System Analysis	9
2 General Network Model	11
2.1 Water Network Components	11
2.2 Graph Theory	22
3 System Model	25
3.1 Water Wall Introduction	25
3.2 Water Wall Model	27
3.3 Model Implementation	30
3.4 Model Parameters	35
3.5 Model Verification	51
II Control Design	55
4 Steady-state Power Minimization	57
4.1 Control Problem	57
4.2 Pressure Control	58
4.3 Steady-state Optimization Problem	59
4.4 Convexity	60
4.5 Power Optimization	61
4.6 Power Optimization Controller	66
5 Implementation of the Control System	71
5.1 Pressure Controller	71
5.2 Power Optimization Controller	73

III Test And Verification	77
6 Test Results	79
6.1 Water Wall	79
6.2 Simulation	83
7 Project Closure	87
7.1 Conclusion and Discussion	87
7.2 Perspective	90
Appendices	90
IV Appendix	91
A Test System	93
A.1 Test System Components	93
A.2 Test System Topology	95
A.3 Test System Graph	96
A.4 Test System Spanning Tree	97
A.5 Test System Incidence Matrix \mathbf{H}	98
A.6 Test System Incidence Matrix \mathbf{H}_f	99
A.7 Test System Circuit Matrix \mathbf{B}	100
A.8 Test System Circuit Matrix \mathbf{B}_f	100
B Unit Transformation	101
C Water Wall Pump Efficiency	103
D Numerical Analysis of Chord Flows	105
D.1 Equal End-user OD Simulation Results	105
D.2 Unequal End-user OD Simulation Results	108
D.3 Constant Difference Between Supply Pumps Simulation Results	110
E Water Wall Setup Guide	113
V Literature	117
Bibliography	119

Nomenclature

Acronyms

CP	Critical Point
DAQ	Data Acquisition Board
KCL	Kirchoff's current law
KVL	Kirchoff's voltage law
NRMSE	Normalised Root-Mean-Square Error
OD	Opening Degree (Pertaining to valves)
ODE	Ordinary Differential Equation
PMA	Pressure Management Area
PRV	Pressure Reducing Valve
PRBS	Pseudo Random Binary Sequence

Notation

Vectors and Matrices

A vector, \mathbf{v} , is noted

$$\mathbf{v} = \begin{bmatrix} v_1 \\ v_2 \\ v_3 \end{bmatrix} \quad , \quad \mathbf{v} = \begin{bmatrix} v_x \\ v_y \\ v_z \end{bmatrix} \quad \text{or} \quad \mathbf{v} = [v_1 \quad v_2 \quad v_3]^\top \quad (1)$$

A vector, \mathbf{v} , that has the subscript, k , is noted

$$\mathbf{v}_k = \begin{bmatrix} v_{k,1} \\ v_{k,2} \\ v_{k,3} \end{bmatrix} \quad \text{or} \quad \mathbf{v}_k = \begin{bmatrix} v_{k,x} \\ v_{k,y} \\ v_{k,z} \end{bmatrix} \quad (2)$$

A vector, \mathbf{v} , that has the subscript, k , and an index number, i , is noted

$$\mathbf{v}_{k,i} = \begin{bmatrix} v_{k,i,1} \\ v_{k,i,2} \\ v_{k,i,3} \end{bmatrix} \quad \text{for } i = 1, 2, \dots, p \quad \mathbf{v}_k = \left\{ \begin{bmatrix} v_{k,1,1} \\ v_{k,1,2} \\ v_{k,1,3} \end{bmatrix}, \begin{bmatrix} v_{k,2,1} \\ v_{k,2,2} \\ v_{k,2,3} \end{bmatrix}, \dots, \begin{bmatrix} v_{k,p,1} \\ v_{k,p,2} \\ v_{k,p,3} \end{bmatrix} \right\} \quad (3)$$

A matrix, \mathbf{M} , is noted

$$\mathbf{M} = \begin{bmatrix} m_{11} & m_{12} & m_{13} \\ m_{21} & m_{22} & m_{23} \\ m_{31} & m_{32} & m_{33} \end{bmatrix} \quad (4)$$

A matrix, \mathbf{M} , that has the subscript, k , is noted

$$\mathbf{M}_k = \begin{bmatrix} m_{k,11} & m_{k,12} & m_{k,13} \\ m_{k,21} & m_{k,22} & m_{k,23} \\ m_{k,31} & m_{k,32} & m_{k,33} \end{bmatrix} \quad (5)$$

General notation

The time derivative of a variable, x , is given by

$$\frac{dx}{dt} = \dot{x} \quad (6)$$

The upper and lower bounds of a variable, x , are respectively given by

$$\bar{x}, \quad \underline{x} \quad (7)$$

Notation for intervals

$$[a, b] = \{x \in \mathbb{R} | a \leq x \leq b\} \quad (8)$$

Symbols

Symbol	Description	Unit
Network Components		
C_k	The k^{th} component of the distribution network	[.]
n_i	The i^{th} node of the distribution network	[.]
q_k	Flow through the k^{th} component	[m^3/h]
Δp_k	The pressure drop across the k^{th} component	[bar]
$p_{in,k}$	The pressure at the input of the k^{th} component	[bar]
$p_{out,k}$	The pressure at the output of the k^{th} component	[bar]
F	The net force effecting the water inside a pipe	[N]
\mathcal{P}	The linear momentum of water inside a pipe	[$kg \cdot m/s$]
M	The water mass	[kg]
v	The water velocity	[m/s]
A	Cross sectional area	[m^2]
L	Length	[m]
D	Diameter	[m]
Δz	Elevation difference	[m]
p	Pressure	[bar]
ρ	Water density	[kg/m^3]
h_f	Head loss from friction	[m]
h_m	Head loss from form resistance	[m]
f	Pipe friction factor	[.]
k_f	Form factor loss coefficient	[.]
R	Reynolds Number	[.]
T	Temperature	[$^\circ C$]
g	Gravity	[m/s^2]
J_k	Water inertia of the k^{th} component	[kg/m^4]
$\lambda_k(\cdot)$	Function for hydraulic resistance in the k^{th} pipe component	[bar]
$\mu_k(\cdot)$	Function for hydraulic resistance in the k^{th} valve component	[bar]
ζ_k	Pressure drop from elevation difference across the k^{th} component	[bar]
OD	Opening Degree of a valve	[.]
K_{vs}	Conductivity of a fully open valve	[m^3/h]
ω	Pump rotor angular rotation	[rpm]
$\alpha_k(\cdot)$	The pressure boost given by the k^{th} pump	[bar]
P_e	Power consumption for a pump	[W]
τ	Pump torque	[Nm]
η	Pump efficiency	[.]
Graph Theory		
G	Graphical description of a water distribution network	[.]
N	Set of nodes in a graph	[.]
E	Set of edges in a graph	[.]
H	Incidence matrix of a graph	[.]
B	Cycle matrix of a graph	[.]
T	Spanning tree of a graph	[.]
L	Fundamental cycles of a graph	[.]
ℓ_i	i^{th} Chord of a graph	[.]

Symbol	Description	Unit
System Model		
\mathbf{q}	Chord flow vector	$[m^3/h]$
\mathbf{q}_ℓ	Chord flow vector	$[m^3/h]$
$\Delta \mathbf{p}$	Differential pressure vector	$[bar]$
$\lambda(\cdot)$	Vector function for hydraulic resistance in pipe components	$[bar]$
$\mu(\cdot)$	Vector function for hydraulic resistance in valve components	$[bar]$
ζ	Vector of pressure drop from elevation difference across the components	$[bar]$
$\alpha(\cdot)$	Vector of pressure boost given by the pumps	$[bar]$
\mathbf{J}	Inertia matrix	$[kg/m^4]$
Control Design		
$P(\cdot)$	Function of the power consumption of the distribution network	$[W]$
q^*	Equilibrium flow	$[m^3/h]$
ξ	Integral action	$[.]$
γ	Gradient descent gain	$[.]$
$S(\cdot)$	Penalty function	$[.]$

Chapter 1

Introduction

This chapter presents an introduction to the project titled "Energy Optimization of Water Distribution Networks - Using a distributed pumping solution for optimal control".

First a motivation for the project is presented, then existing pressure control and management methods are described. Finally an outline for the focus of the project is given.

1.1 Project Background

Water supply and distribution networks are a vital part of the infrastructure all over the world. The distribution network supplies water to the consumers by maintaining a positive water pressure in the network. The pressure must be sufficiently high for the water to reach all parts of the distribution network, and at the same time, maintaining a minimum water pressure at the end users. This can be achieved by the use of pumping stations placed at key locations throughout the distribution network.

The infrastructure which provides safe drinking water is consuming large amounts of energy throughout its supply chain, consisting of retrieving water from the source, a treatment process and finally distributing water to the consumers. In the U.S. 3-4 % of the total electricity consumption is used for water utilities, with 80 % of the energy used for moving and distributing drinking- and wastewater [Goldstein 02, EPA 13].

Energy losses in the distribution network are caused by a number of factors, e.g. inefficient pumps, resistance within the pipes (especially old pipes with large mineral deposits build-up), poor network design with many bottle necks. Water leakages throughout a distribution network are also a large contributor to the energy loss, where the water lost throughout leakages has to be supplied on top of the consumer demand [Feldman 09]. It is estimated that more than 30 % of the drinking water is lost throughout leakages worldwide, thus just as much energy is wasted. This fact gives a possibility to greatly reduce energy consumption by simply reducing water leakages [Group 06, GIZ 11]. Another reason to try to minimize water loss in the network from an energy perspective, is the energy consumption involved with production and procurement of fresh water, such as desalination or pumping water from aquifers.

Additionally the increased flow necessary in the network to accommodate for water leaks, increases the energy consumption, due to the fact that the pipe friction grows with increasing flow, resulting in higher pressure losses in the network.

Lowering the energy consumption can be done in numerous ways, most of these requires replacing old equipment, e.g. old pumps with more energy efficient models, installing new pipes with lower friction or repairing burst pipes. All of these examples are costly processes since most of the distribution network is placed in the underground within metropolitan areas, thus, requiring intensive work and possibly the necessity of shutting down main traffic arteries for prolonged periods, which renders these approaches not viable in many cases.

Even so, other alternative approaches can be used to reduce the energy consumption, like pressure management within the network and smart operation strategies. Active pressure management can be used to manage the pressure throughout the distribution network to ensure that the customer has the desired pressure, and at the same time, reducing the pressure in the remaining part of the network to the minimum required pressure. This is especially useful at night, when the consumer demand is low, and the pressure in many parts of the distribution network can be lowered and the pumps close to the consumers can maintain the water pressure required by the consumer. With a lower water pressure in the distribution network, energy savings can be obtained, as the pumping stations has to deliver less hydraulic energy to the water, thus reducing their energy consumption. On top of this, a lower pressure also decreases the leakage flow and reduces the probability of new bursts and leakages in the network [GIZ 11, Thornton 07].

1.2 Pressure Management

In short, pressure management is a method to ensure that the customers has a guaranteed minimum water pressure, while simultaneously reducing excessive pressure by reducing the sum of input pressures in the distribution network.

As mentioned previously, the reason why reducing water pressure is beneficial, is that it not only reduces the energy consumption, but also, excessive pressure increases the risk of bursts in the distribution pipes. The flow rate of leaks in the distribution network is also affected by the direct relation between pressure and flow, i.e. with a high water pressure the leakage flow will similarly be high.

Several systems and technologies exists for pressure management where pressure management is usually done by dividing the distribution network into a number of pressure management areas (PMA). A PMA can be a city block, industrial area or any other subsection of the distribution network which is suitable. Each PMA is connected to the remaining network through one or more pressure reduction valves (PRV), which reduces the pressure within the PMA, with the aim of maintaining a minimum pressure at a critical point (CP) within the PMA [GIZ 11, Feldman 09]. There exists many different variants of PRVs, with the most basic being a fixed pressure drop variant. Other PRVs can be time dependent in order to accommodate for the daily variations in water consumption, or flow based such that when the flow is high the pressure drop is small to accommodate for the high demand. Remote controlled PRVs are also a possibility, where the utility service operator monitors and controls the valve. Commonly for all PRVs is that even when fully open they induce a pressure loss, which is an unnecessary waste of energy, for which the pumps in the distribution network has to compensate [GIZ 11].

In figure 1.1 a sketch of a small distribution network, consisting of three PMAs, is shown.

A pumping station supplies water from a reservoir and pressurizes the entire distribution network. The pressure must be high enough for the water to reach and meet the minimum pressure required at the critical point (CP), within the PMA farthest away from the pumping station. The CP in a respective PMA is often defined as the end-user with the highest pressure requirement.

Without PRVs the areas close to the pumping station will experience very large pressures, which is unnecessary and causes increased water loss and potential damage to the distribution network. As shown in figure 1.2, inserting PRVs decrease the pressure within the PMA to be high enough to meet the requirement of the CP, but lower than the pressure in the main water line.

Instead of introducing a pressure loss in the system from the use of PRVs, an other method is proposed, shown in figure 1.3.

Here pumping station are used to provide a pressure boost to the PMAs furthest away from the water reservoir; thus the primary pumping station can operate at a lower pressure to meet the demand at the first CP. The pumping station placed near the second and third PMA will be used to boost the pressure up to the minimum requirements in the respective areas. A diagram showing the pressure distribution over distance is shown in figure 1.4.

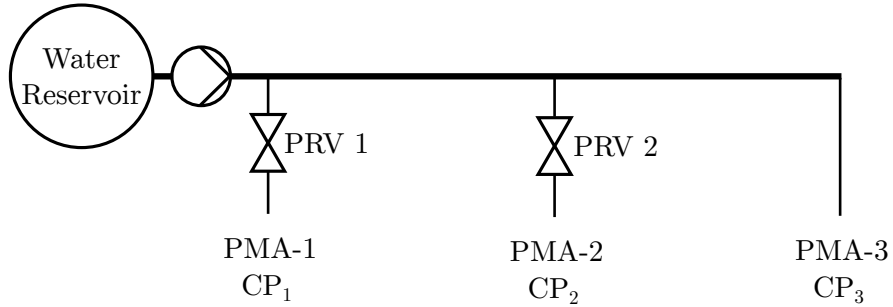


Figure 1.1: A water distribution network containing a water source, a pump and three pressure management areas (PMA) connected to the main water distribution line. The PMAs pressures are controlled with pressure reduction valves (PRV) to meet the pressure requirement at the critical point (CP) within each PMA.

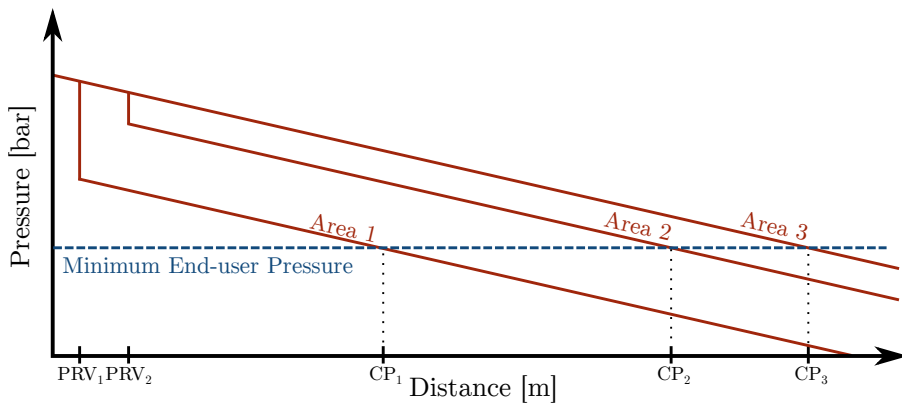


Figure 1.2: A graph of the pressure within the distribution network given in figure 1.1. The pressure is decreasing with distance from the pumping station, PRVs are inducing sudden pressure drops to minimize excessive pressure in the respective PMAs.

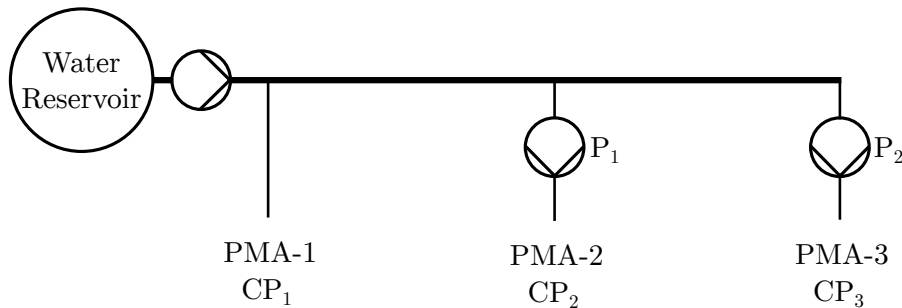


Figure 1.3: A distribution network containing a water source, a pump and three pressure management areas (PMA) which are controlled with pumps used to boost the pressure up to the requirement at the critical point (CP) within the area.

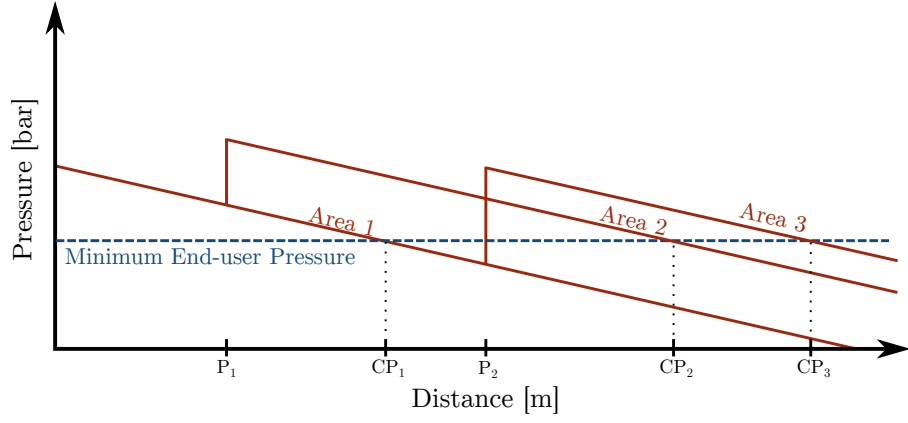


Figure 1.4: A graph of the pressure within the distribution network given in figure 1.3. The pressure is decreasing with distance from the pumping station, pumps gives a pressure boost large enough for the pressure to meet the minimum requirements at the CP within the PMA.

However, problems can occur when exchanging PRVs for pumps. When several pumps are connected to the same PMA or when PMAs are interconnected, instability issues can arise when using feedback control for the pumps. This is generally not a problem when using PRVs, as only the most advanced PRVs are feedback controlled, and most PRVs are either of the time varying type or fixed pressure drop [GIZ 11].

1.3 Project Focus

The focus of this project is to develop a control strategy, for a general class of water distribution networks, which by use of additional pumps in the distribution network is able to reduce the power consumption, without loss of pressure at the consumers. The reduction in power consumption will be obtained by using power optimal pressure regulation within the distribution network. The general class of water distribution networks, are networks with a main supply ring with multiple interconnected PMAs and multiple water source connected to it, including elevation differences of the individual PMAs.

Furthermore it is necessary to keep the requirement for the communication between the pumps in the distribution network at a minim. This requirement arise from the fact that increased communication between pumps, increases the complexity of the system and thereby making implementation more difficult. The use of communication between pumps also introduces additional points which are susceptible of failure, which is to be avoided.

In short: The aim of this report is to develop a distributed control strategy which minimizes the power consumption of a water distribution network. With the control strategy also focusing on minimizing the use of communication between the pumps within the water distribution network.

Part I

System Analysis

Chapter 2

General Network Model

This chapter covers generalized models of water networks. First, the network components are specified. Then, graph theory is introduced and lastly, the water network model is defined from the components using graph theory.

The approach of using a general model is taken to broaden the usability of the work performed here, as the general model is applicable to a wide variety of water distribution networks.

2.1 Water Network Components

One of the main objectives in this project is to design a model which describes a water distributing network. This properties of the network were defined in section 1.3 which can be summarized as: A water network with a grid structure layout, multiple water sources, height difference within the network and multiple pumping stations. An example of such a network is depicted in 2.1 which has the properties listed above apart from multiple water sources. This example water distribution network is used through out this chapter to help explaining the modeling process.

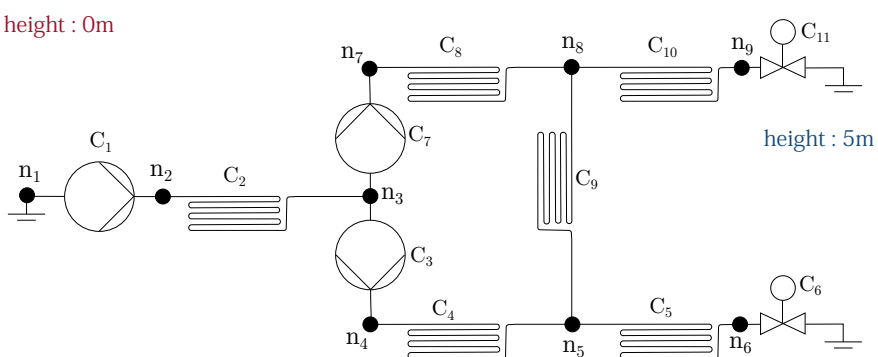


Figure 2.1: A water distribution network example which includes pumps (C_1 , C_2 and C_3), end-user valves (C_6 and C_{11}) and pipes (C_2 , C_4 , C_5 , C_8 and C_{10}) which are distributed at two different heights. Note that the ground sign represents atmospheric pressure and C_1 is considered as the water source pump. Acronyms: C = Component & n = node.

The water network shown in figure 2.1 includes various components where the k^{th} component is characterized by two variables, namely its pressure drop across it, Δp_k , and the water flow though

it q_k . The pressure drop Δp_k is defined as:

$$\Delta p_k = p_{in,k} - p_{out,k} \quad (2.1)$$

where

Δp_k	is the pressure drop across the k^{th} component	[bar]
$p_{in,k}$	is the pressure at the k^{th} component input node	[bar]
$p_{out,k}$	is the pressure at the k^{th} component output node	[bar]

The components are: valves, pipes and pumps, and their models are defined in the following sections.

2.1.1 Pipe Model

A water distribution network is mostly made of pipes and their fittings, it is therefore important to setup a dynamical model which describes how a pipe effects the pressure and flow in a network. One way to model a pipe is to use Newton's second law which states that the net force, F , effecting that water inside the pipe is equal to the rate of change of the water linear momentum, \mathcal{P} [Hunt 95].

$$\frac{d\mathcal{P}}{dt} = F_{net} \quad (2.2)$$

where

\mathcal{P}	is a water linear momentum	[kg m/s]
F_{net}	is a water net force	[N]

By assuming that the pipes are full with water and the water is incompressible, it is possible to rewrite equation 2.2 to its more standard form

$$\frac{d\mathcal{P}}{dt} = \frac{d(M v)}{dt} = M \frac{dv}{dt} = F_{net} \quad (2.3)$$

where

M	is the water mass	[kg]
v	is the water velocity	[m/s]

The forces which affect the water in a pipe, F_{net} , can be written in terms of input-, output- and resistance forces. An illustration of a pipe along with the forces is shown in figure 2.2.

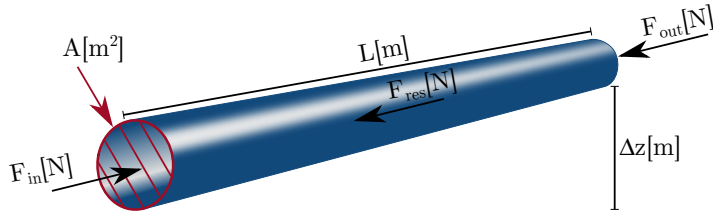


Figure 2.2: Water pipe. Acronyms: L = Length, A = Area, F = Force, res = resistance and Δz = change in height.

As mentioned earlier, the goal is to obtain a component model which includes its pressure drop Δp and the flow q , equation 2.3 is therefore rewritten in the following equations. Note, it is

assumed a constant diameter across the pipe and that the flow is uniformly distributed along its cross section. These assumption make it possible to define only one pipe diameter, D , and cross sectional area, A , for each pipe. Furthermore, water velocity, v , can be written in terms of water flow, q , and cross sectional area, A , hence $v = q/A$

$$\begin{aligned} M_w \frac{dv}{dt} &= F_{in} - F_{out} - F_{res} \\ A L \rho \frac{dv}{dt} &= A p_{in} - A p_{out} - F_{res} \\ A L \rho \frac{d}{dt} \left(\frac{q}{A} \right) &= A p_{in} - A p_{out} - F_{res} \\ \frac{L \rho}{A} \frac{dq}{dt} &= p_{in} - p_{out} - \frac{F_{res}}{A} \\ \frac{L \rho}{A} \frac{dq}{dt} &= \Delta p - \frac{F_{res}}{A} \end{aligned} \quad (2.4)$$

where

M_w	is the water mass	[kg]
v	is the water velocity	[m/s]
F	is a force effecting the water	[N]
A	is the pipe cross areal	[m ²]
L	is the pipe length	[m]
ρ	is the water density	[kg/m ³]
p	is a pressure	[Pa]
Δp	is a pressure drop over a component	[Pa]
q	is the water flow	[m ³ /s]

The factors which cause the resistance force, F_{res} , in a pipe are usually referred as surface resistance, h_f , form resistance, h_m , and lastly head loss, Δz , which is due to change in elevation along the pipe [Swamee 08]. These resistances are given in head, h , which is a way to describe pressure where $p = h \cdot g \cdot \rho$, with g the gravitational acceleration and ρ the fluid density.

Surface Resistance (h_f)

The surface resistance is given by the Darcy-Weisbach equation [Swamee 08]:

$$h_f = f \frac{8 L q_w^2}{\pi^2 g D^5} \quad (2.5)$$

where

h_f	is head loss due to surface resistance	[m]
D	is the pipe diameter	[m]
f	is the pipe friction factor	

The friction factor is dependent on the Reynolds number, \mathbf{R} , which defines the flow type. The Reynold number is given by equation 2.6 where $\mathbf{R} < 2000$ is defined as laminar flow, $\mathbf{R} \approx 2000 - 4000$ as critical flow and $\mathbf{R} > 4000$ as turbulent flow.

$$\mathbf{R} = \frac{v D}{\nu_w} = \frac{4 q}{\pi \nu_w D} \quad (2.6)$$

The kinematic viscosity ν_w in equation 2.6 is given by equation 2.7, where T_w is the water temperature in °C [Swamee 08].

$$\nu_w = 1.792 \cdot 10^{-6} \left(1 + \left(\frac{T_w}{25} \right)^{1.165} \right)^{-1} \quad (2.7)$$

Under normal operation, turbulent flow is the dominating flow type in water distribution networks. This can be shown by applying the typical ranges of the following parameters to equation 2.7 and 2.6: $v = 0.5 - 1.5 \text{ m/s}$, $D = 50 - 1500 \text{ mm}$ and $T_w = 10 - 20^\circ\text{C}$, which result in Reynolds number between 19 000 and 225 000 [Trifunovic 06]. Hence, $\mathbf{R} > 4000$ and consequently the flow is turbulent.

Lastly, the friction factor, f , for a turbulent flow can be found by equation 2.8 [Swamee 08].

$$f = 1.325 \left(\ln \left(\frac{\varepsilon}{3.7D} + \frac{5.74}{\mathbf{R}^{0.9}} \right) \right)^{-2} \quad (2.8)$$

Where ε is the average height of roughness inside a pipe wall which is given by the pipe manufacturer.

Form Resistance (h_m)

A form resistance in a pipe is due to all sort of bends, elbows, valves, enlargements, reducers etc. Basically all form factors which deviate from a straight pipe and also the junction of two pipes of different sizes. These form resistances are also referred as pipe fittings and its head loss, h_f , is calculated by equation 2.9 [Swamee 08].

$$h_m = k_f \frac{8 q_w^2}{\pi^2 g D^4} \quad (2.9)$$

where

h_m	is the head loss due to form resistance	[m]
D	is the pipe diameter	[m]
k_f	is the form-loss coefficient	

The form-loss coefficient k_f can usually be found in the documentation given by the manufacturer, or listed for different materials and general type of fittings in most water distribution network design literature, such as: [Swamee 08].

If there are multiple fittings along a pipe, they can be combined as shown in the following equation.

$$h_m = \sum_{i=1}^n (k_{f,i}) \frac{8 q_w^2}{\pi^2 g D^4} \quad (2.10)$$

Where n is the number of fittings belonging to the pipe model.

Complete Pipe Model

It is now possible to write out the complete pipe model in terms of pressure drop as a function of water flow. Let's rewrite 2.4 by combining it with the surface resistance in equation 2.5, form resistance in equation 2.9 and lastly head loss from change in elevation along the pipe, Δz . Note the relation between head, h , and pressure, p , where $p = h \cdot g \cdot \rho$.

$$\begin{aligned} \frac{L \rho}{A} \frac{dq}{dt} &= \Delta p - h_f g \rho - h_m g \rho - \Delta z g \rho \\ \frac{L \rho}{A} \frac{dq}{dt} &= \Delta p - f \frac{8 L \rho q_w^2}{\pi^2 D^5} - k_f \frac{8 \rho q_w^2}{\pi^2 D^4} - \Delta z g \rho \\ \frac{L \rho}{A} \frac{dq}{dt} &= \Delta p - \left(f \frac{8 L \rho}{\pi^2 D^5} + k_f \frac{8 \rho}{\pi^2 D^4} \right) |q| q - \Delta z g \rho \end{aligned} \quad (2.11)$$

Where the absolute value is applied to the squared flow term, q^2 , to maintain the flow sign, i.e. the flow direction.

Lastly, the units for flow [m^3/s] and pressure [Pa] in equation 2.11 are converted to [m^3/h] and [bar] which are the units used through out this project. The unit transformation procedure is described in appendix B which result in equation 2.12. Note, the symbols for flow, q , and pressure, p , in equation 2.12 are unchanged, however, the units from now on are [m^3/h] and [bar].

$$\frac{L \rho}{A \cdot 10^5 \cdot 3600} \frac{dq}{dt} = \Delta p - \left(f \frac{8 L \rho}{\pi^2 D^5 \cdot 10^5 \cdot 3600^2} + k_f \frac{8 \rho}{\pi^2 D^4 \cdot 10^5 \cdot 3600^2} \right) |q| q - \frac{\Delta z g \rho}{10^5} \quad (2.12)$$

It is worth mentioning that the obtained model in equation 2.12 is the same type of model introduced in [Persis 11, Tahavori 12, DePersis 07, Persis 09].

Equation 2.12 is hereby the complete pipe model. Nonetheless, a more compact notation is introduced in equation 2.13, which is the one used henceforth and it applies to the k^{th} pipe component.

$$J_k \dot{q}_k = \Delta p_k - \lambda_k(q_k) - \zeta_k \quad (2.13)$$

where

$$\begin{aligned} J_k &= \frac{L_k \rho}{A_k \cdot 10^5 \cdot 3600} \\ \lambda_k(q_k) &= \left(f_k \frac{8 L_k \rho}{\pi^2 D_k^5 \cdot 10^5 \cdot 3600^2} + k_{fk} \frac{8 \rho}{\pi^2 D_k^4 \cdot 10^5 \cdot 3600^2} \right) |q_k| q_k \\ \zeta_k &= \frac{\Delta z_k g \rho}{10^5} \end{aligned}$$

Lastly, the general component diagram for a pipe is shown in figure 2.3.

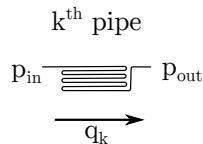


Figure 2.3: Diagram of a pipe and its connecting points in a network. This figure is inspired by [Kallesøe 07].

2.1.2 Valve Model

This section covers the valves which have a variable opening degree (OD), where varying the OD regulates the pressure loss across it. It is assumed that valves are only placed at the water network users since one of the project aims is to use multiple pumping stations instead of PRVs, as discussed in section 1.2. A valve located at an user is denoted as an end-user valve. From a water distribution network point of view, changes in a end-user valve OD is considered as a disturbance and it effects both the network pressure and flow. Other valves that are placed throughout the network with a constant OD are thought as fittings which are included in the pipe model in equation 2.13.

The valve model can be derived in the same matter as the pipe model in equation 2.12. The difference is the length, L , and the change in elevation, Δz , are both assumed zero. These

assumptions resulting in the static equation 2.14 which only contains the pressure loss, Δp , and the form resistance part. This is a fair assumption since the water mass in a valve and its length are relatively small compared to a pipe.

$$0 = \Delta p - k_f \frac{8 \rho q_w^2}{\pi^2 D^4 \cdot 10^5 \cdot 3600} \quad (2.14)$$

Even though it is possible to find a form-loss coefficient, k_f , for all valve types, valve manufacturers provide a more accurate K_{vs} value which is given by equation 2.15 where it may not be mistaken for k_f . The K_{vs} is a valve conductivity value which describes the valves ability to transmit a medium when it is fully open ($OD = 100\%$) where it is a flow expression defined at a 1 bar pressure differential. Equation 2.15 is also under the assumption that the medium flowing through the valve has a liquid specific gravity of $G_l = 1$ and a density of $\rho = 1000 \text{ kg/m}^3$ at a $20^\circ C$ which are indeed properties of water [Boysen 11].

$$K_{vs} = \frac{q}{\sqrt{\Delta p}} \quad (2.15)$$

where

K_{vs}	is the conductivity at a fully open valve	$[\text{m}^3/\text{h}]$
q	is the water flow	$[\text{m}^3/\text{h}]$
Δp	is the pressure drop over the component	[bar]

Equation 2.15 is derived by measuring the flow through a valve in m^3/h when its pressure difference is 1 bar and then by applying the hydrodynamic law which states that the pressure drop, Δp , in a valve is proportional to its squared flow q^2 [Boysen 11]. This derivation is demonstrated in the following equations.

$$\frac{\Delta p_1}{q_1^2} = \frac{\Delta p_2}{q_2^2} \quad \Leftrightarrow \quad \frac{\Delta p_1}{\Delta p_2} = \frac{q_1^2}{q_2^2} \quad \Leftrightarrow \quad q_1 = q_1 \sqrt{\frac{\Delta p_1}{\Delta p_2}}$$

Where $OD = 100\%$, q_2 is measured as k_{vs} at a pressure difference $\Delta p_2 = 1$, one obtains the same result as in equation 2.15.

$$q_1 = k_{vs} \sqrt{\frac{\Delta p_1}{1}} = k_{vs} \sqrt{\Delta p_1} \quad (2.16)$$

More generally, equation 2.16 is written by means of valve conductivity k_v which is a function between a closed valve and a fully open one, hence $k_v(OD) = [0, k_{vs}]$ where OD is a number from zero to one, $OD = [0, 1]$.

$$q = k_v(OD) \sqrt{\Delta p} \quad (2.17)$$

Where the valve conductivity, k_v , dependent on the valve type and design. One can e.g. choose a valve with a k_v function which has a linearising effect on a non-linear system. Figure 2.4 illustrates different k_v functions.

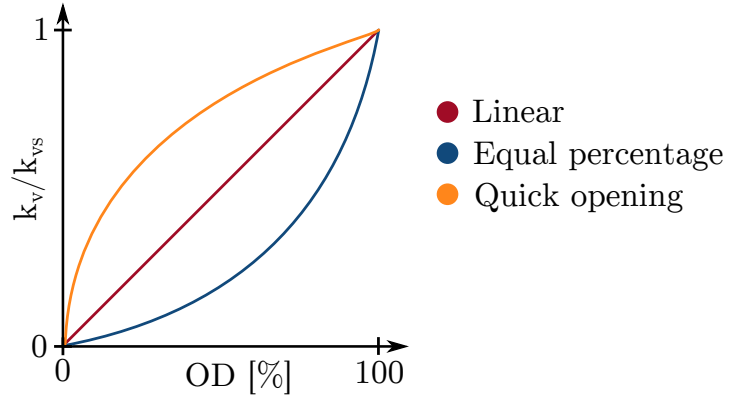


Figure 2.4: The three major types of control valve characteristics: linear, equal percentage and quick opening [Lem 96, GIZ 11].

The goal is to obtain a general component model, consequently, 2.17 is rewritten to the same form as the pipe model in equation 2.12.

$$\begin{aligned}
 q &= k_v(OD)\sqrt{\Delta p} \\
 \sqrt{\Delta p} &= \frac{q}{k_v(OD)} \\
 \Delta p &= \frac{1}{k_v(OD)^2} |q| q \\
 0 &= \Delta p - \frac{1}{k_v(OD)^2} |q| q
 \end{aligned} \tag{2.18}$$

A model for a valve with a variable opening degree is hereby defined in 2.18. A more compact model for the k th valve is defined in the following equation.

$$0 = \Delta p_k - \mu_k(q_k, OD_k) \tag{2.19}$$

where

$$\mu_k(q_k) = \frac{1}{k_{v,k}(OD_k)^2} |q_k| q_k$$

And the general component diagram for a valve is shown in figure 2.5

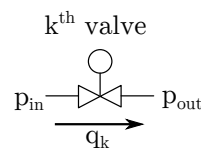


Figure 2.5: Diagram of a valve and its connecting points in a network. This figure is inspired by [Kallesøe 07].

2.1.3 Pump Model

A pump is a component which generates a positive pressure difference in a hydraulic network, thus creating flow. This project only considers a centrifugal pump which is the most common pump type in a water distribution network [DePersis 07]. A model which describes the pressure drop ($\Delta p = p_{in} - p_{out}$) over a centrifugal pump is derived in [Kallesøe 05] where it has shown to fit well with measurements of a real centrifugal pump. The pump model is an algebraic expression and it is presented in equation 2.20.

$$\Delta p = a_{h2} q^2 - a_{h1} q \omega - a_{h0} \omega^2 \quad (2.20)$$

Where a_{h0} , a_{h1} , a_{h2} are constants describing the pump and ω is the rotational speed of the pump. The constants are normally found from measurement data of the pump.

The pump model in equation 2.20 describes the pump differential pressure, Δp , which is dependent on the flow, q , through the pump and rotational speed, ω , of the pump. However, pumping solutions in a distributed water system are usually designed to maintain a constant reference pressure independent on any flow variation, meaning that the pumping solution has a integrated pressure regulator which controls the pump rotational speed. Such a pumping solution is often referred as a booster set which consists of number of pumps connected in parallel to increase the combined flow throughput. Furthermore, the booster set controller chooses how many pumps are active depending on the flow demand and the pumps are set to operate in their combined most efficient way [C. Kallesøe 11]. An example of a booster set with three pumps and their combined pump curves is shown in figure 2.6.

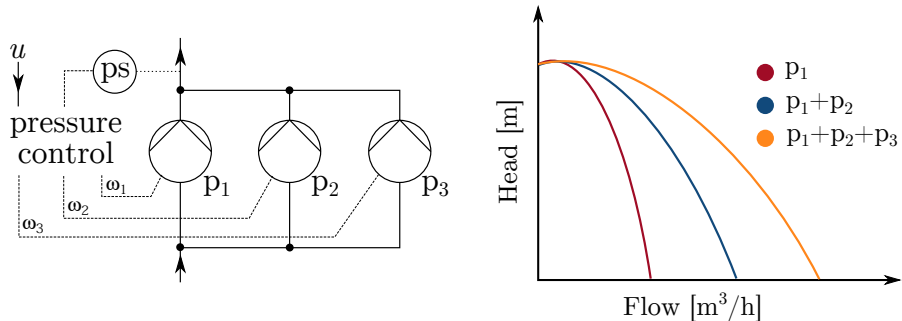


Figure 2.6: Diagram of a booster set with three pumps along with the pumps combined pump curves. The booster set maintains a constant output pressure given by the reference pressure, u , where the controller sets which pumps are active along with their rotational speed ω . This figure is inspired by [C. Kallesøe 11].

Assuming that a pump unit in the water distribution network is indeed a booster set which delivers a constant differential pressure given by u , it is possible to express the k^{th} pump in the network by equation 2.21.

$$0 = \Delta p_k + \alpha_k(u_k) \quad (2.21)$$

where

$$\alpha_k(u_k) = u_k$$

And the general component diagram for a pump is depicted in figure 2.7.

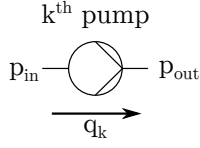


Figure 2.7: Diagram of a pump and its connecting points in a network. This figure is inspired by [Kallesøe 07].

Single Pump Power Consumption

As mentioned earlier in section 1.2, one of the main objectives of this project is to minimize energy usage in a water distribution network, thus making it necessary to state a pump power consumption model. Along with the hydrophilic pump model in equation 2.20, [Kallesøe 05] also derives an expression which describes the torque, τ_e , generated by the electrical circuit of a pump motor. This expression is shown in equation 2.22 and it can be rewritten in terms of electrical power consumption, P_e , by using the relation $P_e = \tau_e \cdot \omega$.

$$\tau_e = -a_{P2} q^2 + a_{P1} q \omega + a_{P0} \omega^2 + B_0 \omega \quad (2.22)$$

$$\begin{aligned} \tau_e \omega &= -a_{P2} q^2 \omega + a_{P1} q \omega^2 + a_{P0} \omega^3 + B_0 \omega^2 \\ P_e &= -a_{P2} q^2 \omega + a_{P1} q \omega^2 + a_{P0} \omega^3 + B_0 \omega^2 \end{aligned} \quad (2.23)$$

Where a_{P0} , a_{P1} , a_{P2} and B_0 are constants describing the pump and ω is the rotational speed and P_e is the electrical power consumption of the pump given in Watt. Lastly, one can add an extra P_0 term to equation 2.23, which is the power consumption of the control hardware placed on the pump, resulting in the following equation.

$$P_e = -a_{P2} q^2 \omega + a_{P1} q \omega^2 + a_{P0} \omega^3 + B_0 \omega^2 + P_0 \quad (2.24)$$

Both B_0 and P_0 along with the constants a_{P0} , a_{P1} , and a_{P2} are usually found from measurement data of a pump. Equation 2.24 describes a single pump electrical power consumption which is later used to calculate the energy efficiency of the pump.

Pump Power Consumption Model And Efficiency

As previously discussed, a booster set is operating in the most energy efficient way which can be achieved by paring speed variable pumps of same size, i.e. identical pumps, where the flow is equally distributed among them [C. Kallesøe 11]. It is assumed the all pumps in the distributed water network are operating as efficiently as possible at a given pressure reference. As a consequence, this project will not focus on how the booster set are controlled but only focus on the booster set total power compunction. The power consumption of the booster set can be found by knowing the pumps energy efficiency. A single pump total efficiency, η , can be calculated from equation 2.25 by applying the pump differential pressure, Δp , given in equation 2.20, the pump electrical power consumption, P_e , given in equation 2.24 and the flow through the pump, q [Grundfos 06].

$$\eta = \frac{P_{\text{hydraulic}}}{P_e} = \frac{-\Delta p \cdot 10^5 \cdot q \cdot 3600^{-1}}{P_e} \cdot 100 \quad (2.25)$$

where

Δp	is the pump differential pressure given by equation 2.20	[bar]
P_e	is the pump electrical power consumption given by equation 2.24	[W]
η	is the pump total efficiency	[%]
q	is the water flow through the pump	[m ³ /h]

An example of efficiency plot for a single and multiple pumps (booster set) are shown in figure 2.8 where the flow through the multiple pumps are equally distributed and all pumps are set to the same rotational speed.

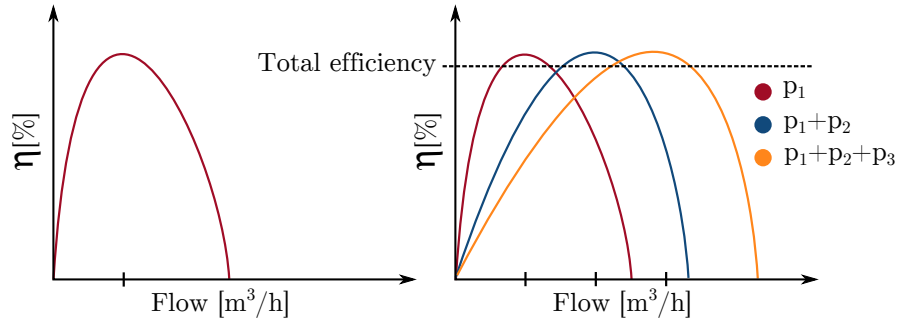


Figure 2.8: Diagram showing the efficiency for a single and multiple pumps (booster set) where the flow through the multiple pumps are equally distributed and all pumps are set to the same rotational speed.

Lastly, by assuming that η is constant, equation 2.21 and equation 2.25 can be combined to the expression in equation 2.26.

$$P_e = u \cdot 10^5 \cdot q \cdot 3600^{-1} \frac{1}{\eta} \quad (2.26)$$

where

P_e	is the pump model electrical power consumption	[W]
u	is the pump model differential pressure set point	[bar]
η	is the pump model total efficiency	[%]
q	is the water flow through the pump model	[m ³ /h]

The power consumption model in equation 2.26 is not applied directly in the component model, however, it is later applied for control purposes as the goal is to minimize the energy usage in a water distribution network.

2.1.4 Component Model

The pump model in equation 2.21, the valve model in equation 2.19 and the pipe model in 2.13 are combined into the following generalized component model.

$$J_k \dot{q}_k = \Delta p_k - \lambda_k(q_k) - \mu_k(q_k, OD_k) + \alpha_k(u_k) - \zeta_k \quad (2.27)$$

Where

$$J_k = \frac{L_k \rho}{A_k \cdot 10^5 \cdot 3600}$$

$$\lambda_k(q_k) = \left(f_k \frac{8 L_k \rho}{\pi^2 D_k^5 \cdot 10^5 \cdot 3600^2} + k_{fk} \frac{8 \rho}{\pi^2 D_k^4 \cdot 10^5 \cdot 3600^2} \right) |q_k| q_k$$

$$\zeta_k = \frac{\Delta z_k g \rho}{10^5}$$

$$\mu_k(q_k) = \frac{1}{k_{v,k}(OD_k)^2} |q_k| q_k$$

$$\alpha_k(u_k) = u_k$$

Equation 2.27 can be used to represents the different component by zeroing the proper terms as shown in table 2.1. Note, the component model is similar to the one introduced in [DePersis 07, Tahavori 12, Knudsen 08]

Component	J_k	λ_k	μ_k	α_k	ζ_k
kth Pipe	J_k	λ_k	0	0	ζ_k
kth Valve	0	0	μ_k	0	0
kth Pump	0	0	0	α_k	0

Table 2.1: The generalized component model parametrization

Lastly, a list of assumptions taken trough the modelling process are listed below.

Assumption 1. *The medium in the network is only water.*

This is a fair assumption where this project focuses on a water distribution network. Also, the pump model in equation 2.20 and valve model in equation 2.15 are only valid for water, and the underling equations in the pipe model shown in equation 2.11 are only valid for liquid.

Assumption 2. *The components are full with water and the water is incompressible.*

This assumption is the basis for rewriting the Newton's second law as done in equation 2.3 where the water mass in the pipes is assumed constant.

Assumption 3. *A pipe in the network has a constant diameter.*

This assumption simplifies the model where change in diameter would require a different model approach than the one presented in section 2.1.1.

Assumption 4. *The flow through a pipe is uniformly distributed along its cross section.*

This assumption allows for rewriting water velocity, v , in terms of water flow, q , and cross sectional area, A , as shown in equation 2.4, hence $v = q/A$

Assumption 5. *The water flow is assumed turbulent.*

The equation behind the pipe friction factor in equation 2.11 are only valid for turbulent flow.

Assumption 6. *The waters density is $\rho = 1000 \text{ kg/m}^3$ and its temperature is assumed 20°C .*

This assumption is necessary for the valve model in equation 2.15 to be valid.

Assumption 7. *The pumps in the network are centrifugal pumps.*

This assumption is the basis for using equation 2.20 which describe the pump type applied in this project.

Assumption 8. *A pump in the network represent a booster set which is operating in its most energy efficient way. Also, the pumps are controlled by a differential pressure set point, u , where booster set total efficiency, η , is assumed constant.*

This assumption allows for controlling a pump by a reference differential pressure, u . Also, the water network control strategy will only focus on how to distribute the pressure actuation among the pumps since the pumps are already set to operate in their most efficient way at a given pressure.

Assumption 9. *A change in elevation, Δz , only occurs in pipes.*

This assumption is made since the physical length of the pumps and valves are small. Also, the differential pressure produced by the component alone is more domination than the effect from the component change in elevation.

The modelling of the components is hereby completed where this section results in the generalized component model in equation 2.27.

2.2 Graph Theory

A graph is a mathematical abstraction which is used to represent a system of connected objects. Graph Theory has many applications in real world problems, e.g. electric circuits or computer networks, with probably the best known problem being the Königsberg bridge problem.

Here a graph theoretical approach is taken to model a hydraulic network. By use of graph theory it is possible to exploit the similarities between electrical circuits and hydraulic networks, with the analogy being that voltage is the pressure and current is the flow. Thereby it is possible to use the much familiar tools from circuit theory on a hydraulic network, specifically Kirchhoff's voltage law (KVL) and current law (KCL) [Desoer 69].

2.2.1 Incidence Matrix

A graph G consists of a set of connection points called nodes, $N = \{n_1, n_2, \dots, n_M\}$, which are interconnected by a set of edges $E = \{e_1, e_2, \dots, e_K\}$. In figure 2.9 a graph of the example distribution network presented in figure 2.1 is shown. The edges represent the individual components of the hydraulic network and the nodes are the connecting points between the components [Deo 74].

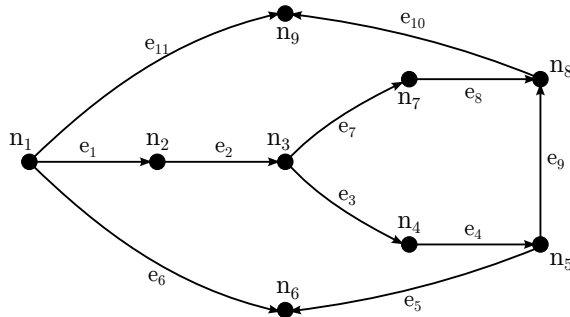


Figure 2.9: The graph G representing the hydraulic network, with 11 edges and 9 nodes.

A reference direction is arbitrarily chosen for each edge, making the graph a directed graph. The incidence matrix \mathbf{H} is as

$$\mathbf{H}_{m,k} = \begin{cases} -1 & , \text{ if the } k^{\text{th}} \text{ edge is incident into the } m^{\text{th}} \text{ node} \\ 0 & , \text{ if the } k^{\text{th}} \text{ edge is not incident to the } m^{\text{th}} \text{ node} \\ 1 & , \text{ if the } k^{\text{th}} \text{ edge is incident out of the } m^{\text{th}} \text{ node} \end{cases} \quad (2.28)$$

The incident matrix for the graph presented in figure 2.9 given in equation 2.29, the direction is chosen such that an edge between two nodes, will be incident into the node with the larger index number and incident out of the node with the lesser index number.

$$\mathbf{H}^{M \times K} = \begin{bmatrix} 1 & 0 & 0 & 0 & 0 & 1 & 0 & 0 & 0 & 0 & 1 \\ -1 & 1 & 0 & 0 & 0 & 0 & 0 & 0 & 0 & 0 & 0 \\ 0 & -1 & 1 & 0 & 0 & 0 & 1 & 0 & 0 & 0 & 0 \\ 0 & 0 & -1 & 1 & 0 & 0 & 0 & 0 & 0 & 0 & 0 \\ 0 & 0 & 0 & -1 & 1 & 0 & 0 & 0 & 1 & 0 & 0 \\ 0 & 0 & 0 & 0 & -1 & -1 & 0 & 0 & 0 & 0 & 0 \\ 0 & 0 & 0 & 0 & 0 & 0 & -1 & 1 & 0 & 0 & 0 \\ 0 & 0 & 0 & 0 & 0 & 0 & 0 & -1 & -1 & 1 & 0 \\ 0 & 0 & 0 & 0 & 0 & 0 & 0 & 0 & 0 & -1 & -1 \end{bmatrix} \quad (2.29)$$

The k^{th} column in the incident matrix corresponding to the connections of the k^{th} component, thus each column will have only two non-zero entries, one positive and one negative. The m^{th} row in the incident matrix represent the connections into and out of the m^{th} node.

2.2.2 Spanning Tree and Cycle Matrix

Assuming that the graph \mathcal{G} is a connected graph, a spanning tree \mathcal{T} exists. If \mathcal{G} is not connected, each subcomponent of \mathcal{G} can be treated as its own separate water distribution network, with individual spanning trees.

A spanning tree is a connected subgraph of \mathcal{G} which contains all the nodes of \mathcal{G} and has no cycles. The number of edges needed to create a spanning tree is always $M - 1$. Each edge used in the spanning tree is called a branch, the remaining edges of \mathcal{G} which are not a part of the spanning tree \mathcal{T} are called chords, denoted ℓ_i . In figure 2.10 a spanning tree \mathcal{T} of \mathcal{G} is drawn, with the gray lines showing the chords of \mathcal{T} [Deo 74].

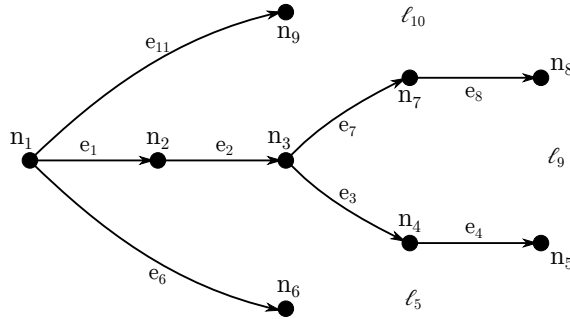


Figure 2.10: A spanning tree \mathcal{T} of the graph \mathcal{G} shown in figure 2.9. Unused edges in the spanning tree are shown in gray and denoted ℓ_i

By adding a chord between two nodes a cycle is created, as there already exists a path between the two nodes formed by the branches of \mathcal{T} . The cycle created by adding a chord is called a fundamental cycle. A cycle created using *more* than one chord is not a *fundamental* cycle, because this cycle consists of several fundamental cycles.

The cycles obtained from \mathcal{T} are denoted \mathcal{L}_i , for $i = 1, 2, \dots, L$ with $L = K - M + 1$, where L is the number of fundamental cycles in \mathcal{G} . A fundamental cycle matrix \mathbf{B} contains all the fundamental

cycles, which is defined as

$$\mathbf{B}_{\mathcal{L},k} = \begin{cases} -1 & , \text{ if the } k^{\text{th}} \text{ edge is in } \mathcal{L}_i \text{ with oppsite direction} \\ 0 & , \text{ if the } k^{\text{th}} \text{ edge is not included in } \mathcal{L}_i \\ 1 & , \text{ if the } k^{\text{th}} \text{ edge is in } \mathcal{L}_i \text{ with matching direction} \end{cases} \quad (2.30)$$

The fundamental cycle matrix has dimensions $L \times K$, where L is the number of fundamental cycles and K is the number of edges. An example of a fundamental cycle matrix is given in equation 2.31, based on the spanning tree in figure 2.10.

$$\mathbf{B}^{L \times K} = \begin{bmatrix} 1 & 1 & 1 & 1 & 1 & -1 & 0 & 0 & 0 & 0 & 0 \\ 1 & 1 & 0 & 0 & 0 & 0 & 1 & 1 & 0 & 1 & -1 \\ 0 & 0 & 1 & 1 & 0 & 0 & -1 & -1 & 1 & 0 & 0 \end{bmatrix} \quad (2.31)$$

2.2.3 Governing Rules

With the incidence and fundamental cycle matrices in place a compact formulation of Kirchhoff's node and loop laws can be made. These define algebraic constraints on the system dynamics.

The loop law (KVL) states that the potential differences across all elements in a closed cycle must sum to zero, equation 2.32.

$$\mathbf{B}\Delta\mathbf{p} = 0 \quad (2.32)$$

Where \mathbf{B} is the fundamental cycle matrix and $\Delta\mathbf{p}$ is a vector containing the pressure differences of all edges in \mathcal{G} , ($\Delta\mathbf{p} = [\Delta p_1, \dots, \Delta p_k]^T$).

The node law (KCL) states that the sum of flows entering a node must equal the sum of flows leaving the node, equation 2.33.

$$\mathbf{H}\mathbf{q} = 0 \quad (2.33)$$

Where \mathbf{H} is the incidence matrix and \mathbf{q} is a vector containing the flows of all edges in \mathcal{G} , ($\mathbf{q} = [q_1, \dots, q_k]^T$).

From the notion in equation 2.33; the sum of all flows into a node must equal the sum of all flows out of the node. The flow in all edges in a graph can be found from the flows through the chords. Each chord form a fundamental cycle loop in the spanning tree of \mathcal{G} , thus the flow through the chord in a fundamental cycle is the superposition of the flows through all edges in that cycle. Likewise the flows through the edges can be found from the superposition of the flows through the chords [Desoer 69].

$$\mathbf{q} = \mathbf{B}^T \mathbf{q}_\ell \quad (2.34)$$

Where \mathbf{q}_ℓ is a vector of the flows through the chords in \mathcal{T} .

Chapter 3

System Model

This chapter cover the modeling of a test-system, named "Water Wall".

First the specifications and physical properties of the Water Wall is introduced. Graph Theory and the component models are used to complete a mathematical model of test system, used for simulation purposes. Finally a comparison between the simulation model and the Water Wall test system is used to verify the mathematical model.

3.1 Water Wall Introduction

The Water Wall pictured in figure 3.1 is a test setup which is placed at Aalborg University's Control and Automation department.

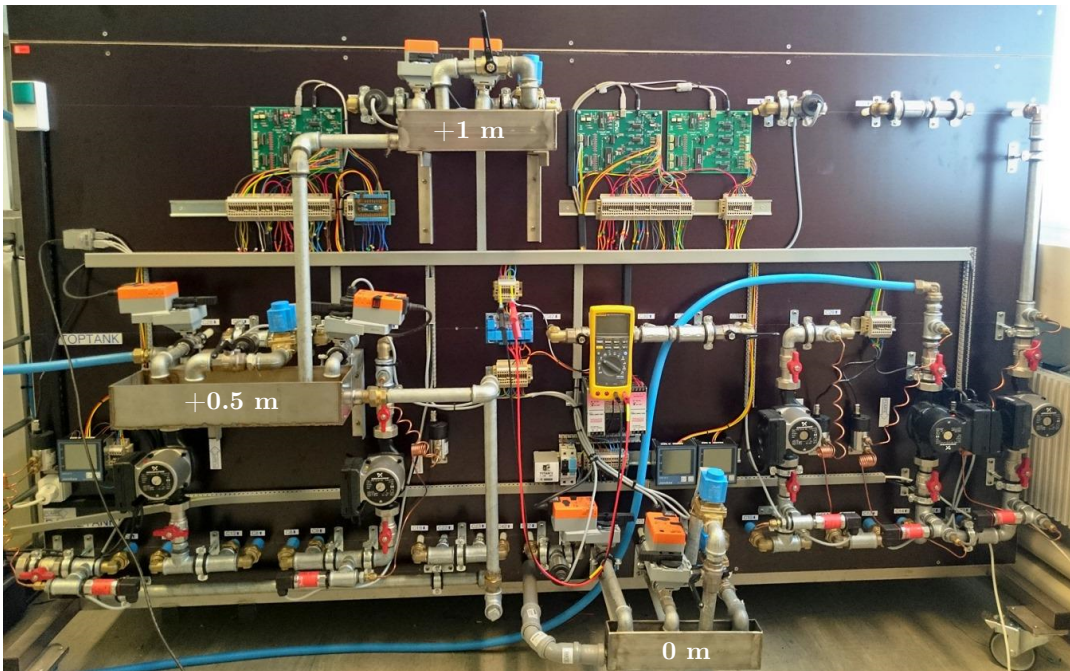


Figure 3.1: The Water Wall which is used to emulate a water distribution network.

The end-users are emulated by motor driven valves (note the orange boxes) where two valves are placed at each geographic hight references which are indicated in the figure. The wall has the AAU-nr.100911

The Water Wall consists of a connection of pumps, pipes and valves which has several different configurations, in order to be used for a large variety of experiments.

In this project, the Water Wall is used to emulate a water distribution network with multiple consumers and water supplies. The Water Wall has a scaling factor of 1:20 compared to a real distribution network. Also, the wall is designed to operate with a pressure around 0.1 bar and water flow of $0.3 \text{ m}^3/\text{h}$ at the end-user valves. A full diagram of the system is presented in Appendix A.2, with a component list given in Appendix A.1. Note that some components of the Water Wall test setup are not used in this project, and only those which are used are shown in the system diagram and the component list.

The Water Wall is connected as a hardware in-the-loop system. It uses a set of data acquisition (DAQ) boards to control and measure valves, pumps and pressure throughout the distribution network.

The DAQ boards are interfacing to Simulink Coder (Real Time Workshop) using a Comedi driver setup on a Linux PC (AAU nr. 804530). A complete setup guide can be found in Appendix E. The drivers written for the Water Wall and the Comedi libraries are found on the project CD.

All sensors which are depicted in the system diagram, figure A.2, are available via the DAQ boards. The sensors measure either differential pressure Δp or relative pressure p . The DAQ boards also give access to the rotational speed input ω of the pumps and the valves opening degree OD . These inputs and measurement points are listed in 3.1.

Inputs				Measurement points							
ω	Comp.	OD	Comp.	Δp	Comp.	p	Comp.	Node	p	Comp.	Node
ω_1	C_2	OD_1	C_{20}	Δp_1	C_2	p_1	$C_{2,4}$	n_2	p_6	$C_{21,22}$	n_{12}
ω_2	C_{16}	OD_2	C_{24}	Δp_2	C_{16}	p_2	$C_{16,14}$	n_9	p_7	$C_{23,24}$	n_{14}
ω_3	C_{18}	OD_3	C_{27}	Δp_3	C_{18}	p_3	$C_{8,18}$	n_4	p_8	$C_{28,29}$	n_{17}
ω_4	C_{25}	OD_4	C_{31}	Δp_4	C_{25}	p_4	$C_{10,25}$	n_6	p_9	$C_{30,31}$	n_{19}
ω_5	C_{32}	OD_5	C_{34}	Δp_5	C_{32}	p_5	$C_{12,32}$	n_8	p_{10}	$C_{35,36}$	n_{22}
		OD_6	C_{38}						p_{11}	$C_{37,38}$	n_{24}

Table 3.1: The Water Wall inputs and sensor outputs which are available via the system DAQ (Data Acquisition) boards. Note, comp. stand for component and when the notation $C_{x,y}$ means between component x and y

In Simulink, the pumps are actuated by a scaled rational speed signal, $\omega = [0, 1]$, where $\omega = 1$ is the maximum rotational speed. The valves are also actuated by a scaled signal, $OD = [0, 1]$, where $OD = 1$ result in a fully open valve. The pressure measurements are all measured in [bar] and note that the pumps are equipped with both a differential pressure sensor and a relative pressure sensor on the suction site.

The Water Wall distribution network consists of three pressure management areas (PMAs). Each PMA has two end-user water outlets, which is shown in the complete system diagram in Appendix A.2. Note in the complete system diagram the ground symbol is used for water intake and outlet points to indicate a node at atmospheric pressure.

The PMAs are placed at different ground elevation levels, 0 m, 0.5 m and 1 m, and each PMA has a single CP (critical point) placed at an end-user in each PMA. A sensor measures the pressure at the CP relative to the atmospheric pressure. The placement of the CP is based on the end-user demand and the pressure loss in the distribution network.

Each PMA has two end-users and two pressure sensors, the CP in each PMA is chosen to be pressure sensor which is pleased directly at the end-user. The CPs are listed in table 3.2

CPs	measurement point	Component	node
CP ₁	p_7	$C_{23,24}$	n_{14}
CP ₂	p_9	$C_{30,31}$	n_{19}
CP ₃	p_{11}	$C_{37,38}$	n_{24}

Table 3.2: The defined CPs (Critical Points) one the Water Wall where the notation $C_{x,y}$ means between component x and y .

In figure 3.2 shows a sketch of the test system distribution network.

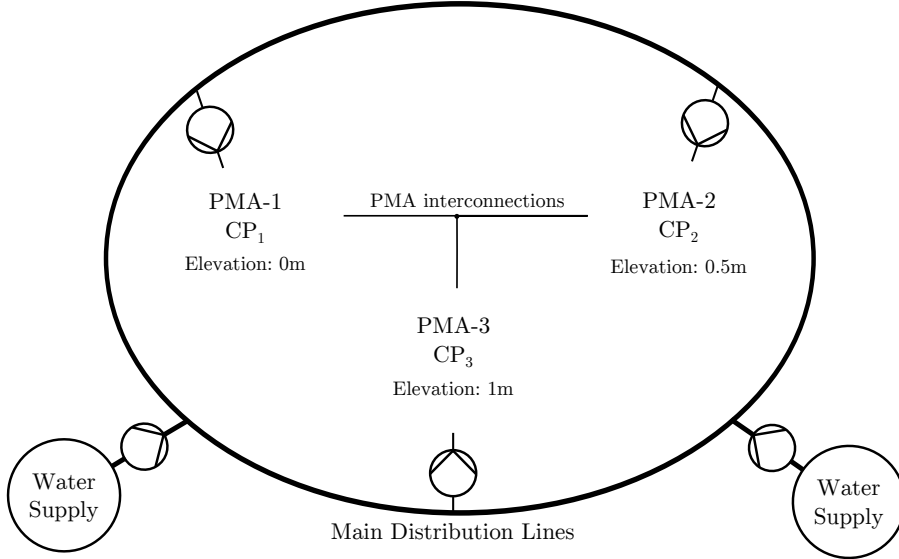


Figure 3.2: Figure of the Water Wall distribution network, with three interconnected pressure management areas each with different elevation and critical point.

The PMAs are connected to the main distribution line with a pump, and all the PMAs are interconnected with a smaller diameter piping than the main distribution line.

Two pumps supply water from a reservoir to the main distribution line at two separate locations.

3.2 Water Wall Model

The Water Wall test system is modeled for simulation and control purposes. The model is based on the component model derived in section 2.1 and uses graph theory to express the algebraic constraints presented in section 2.2.

The Water Wall distribution network is represented by a graph \mathcal{G} , the graph is shown in Appendix A.3. Each edge in \mathcal{G} represents a component of the distribution network. The edge either represents a pump, pipe or valve, and the component model in equation 3.1 is applied to each individual edge of \mathcal{G} .

$$\Delta p_k = J_k \dot{q}_k + \lambda_k(q_k) + \mu_k(q_k, OD_k) - \alpha_k(u_k) + \zeta_k \quad (3.1)$$

Where the subscript m is used to denote for which edge in \mathcal{G} the component belongs to. Recall from section 2.1, that only one of the functions, λ , μ or α can be non-zero for any given edge in \mathcal{G} , with λ and J being non-zero if the edge represents a pipe, μ being non-zero if the edge represents a valve and α being non-zero if the edge represents a pump. ζ is the pressure loss contribution from the elevation difference across an edge, which is zero for all edges that have no change in elevation.

A more compact model can be obtained by using vector notation

$$\Delta \mathbf{p} = \mathbf{J}\dot{\mathbf{q}} + \boldsymbol{\lambda}(\mathbf{q}) + \boldsymbol{\mu}(\mathbf{q}, \mathbf{OD}) - \boldsymbol{\alpha}(\mathbf{u}) + \zeta \quad (3.2)$$

where $\Delta \mathbf{p} = (\Delta p_1, \dots, \Delta p_m)^T$ and each component vector, $\boldsymbol{\lambda}(\mathbf{q}) = (\lambda_1(q_1), \dots, \lambda_m(q_m))^T$, $\boldsymbol{\mu}(\mathbf{q}, \mathbf{OD}) = (\mu_1(q_1, OD_1), \dots, \mu_m(q_m, OD_m))^T$ and $\boldsymbol{\alpha}(\mathbf{q}) = (\alpha_1(u_1), \dots, \alpha_m(u_m))^T$, where the m^{th} vector element equals zero if the m^{th} edge is of another component type than the vector. \mathbf{J} is an $m \times m$ matrix with $\mathbf{J} = \text{diag}\{J_1, \dots, J_m\}$ where all other entries are zero. ζ is a positive value for all edges which has an increase in elevation in the direction of the edge, a negative value if the edge has a decrease in elevation. If there is no change in elevation across the edge the corresponding entry in ζ is zero.

In section 2.2 the algebraic constraints were presented, which are restated here for the convenience of the reader in equation 3.3 and 3.4.

$$\mathbf{B}\Delta \mathbf{p} = 0 \quad (3.3)$$

$$\mathbf{B}^T \mathbf{q}_\ell = \mathbf{q} \quad (3.4)$$

Note that it is always possible to construct the cycle matrix \mathbf{B} such that $\mathbf{B} = [\mathbf{I} \quad \mathbf{F}]$, with \mathbf{I} being an identity matrix of size ℓ (with ℓ being the number of chords) and \mathbf{F} being a suitable matrix of size $\ell \times (n - \ell)$, by choosing the numbering of the edges correctly.

With the correct \mathbf{B} matrix constructed for the Water Wall model it is possible to rewrite equation 3.2 to obtain equation 3.5, by use of the algebraic constraint in equation 3.3.

$$0 = \mathbf{B}\Delta \mathbf{p} = \mathbf{B}\mathbf{J}\dot{\mathbf{q}} + \mathbf{B}\boldsymbol{\lambda}(\mathbf{q}) + \mathbf{B}\boldsymbol{\mu}(\mathbf{q}, \mathbf{OD}) - \mathbf{B}\boldsymbol{\alpha}(\mathbf{u}) + \mathbf{B}\zeta \quad (3.5)$$

Using the algebraic relation in equation 3.4 equation 3.6 can be obtained.

$$0 = \mathbf{B}\mathbf{J}\mathbf{B}^T \dot{\mathbf{q}}_\ell + \mathbf{B}\boldsymbol{\lambda}(\mathbf{B}^T \mathbf{q}_\ell) + \mathbf{B}\boldsymbol{\mu}(\mathbf{B}^T \mathbf{q}_\ell, \mathbf{OD}) - \mathbf{B}\boldsymbol{\alpha}(\mathbf{u}) + \mathbf{B}\zeta \quad (3.6)$$

Which is then rewritten to

$$\mathbf{B}\mathbf{J}\mathbf{B}^T \dot{\mathbf{q}}_\ell = -\mathbf{B}\boldsymbol{\lambda}(\mathbf{B}^T \mathbf{q}_\ell) - \mathbf{B}\boldsymbol{\mu}(\mathbf{B}^T \mathbf{q}_\ell, \mathbf{OD}) + \mathbf{B}\boldsymbol{\alpha}(\mathbf{u}) - \mathbf{B}\zeta \quad (3.7)$$

To isolate the independent flow variables $\dot{\mathbf{q}}_\ell$, which is the flows through the chords, the matrix $\mathbf{J} = \mathbf{B}\mathbf{J}\mathbf{B}^T$ must be invertible.

$$\dot{\mathbf{q}}_\ell = \mathbf{J}^{-1}(-\mathbf{B}\boldsymbol{\lambda}(\mathbf{B}^T \mathbf{q}_\ell) - \mathbf{B}\boldsymbol{\mu}(\mathbf{B}^T \mathbf{q}_\ell, \mathbf{OD}) + \mathbf{B}\boldsymbol{\alpha}(\mathbf{u}) - \mathbf{B}\zeta) \quad (3.8)$$

By showing that \mathbf{J} is a positive definite matrix, a sufficient condition for \mathbf{J} being invertible has been met [Horn 85].

First note that \mathbf{J} can be written on the form

$$\mathbf{J} = \mathbf{B}\mathbf{J}\mathbf{B}^T = [\mathbf{I} \quad \mathbf{F}] \begin{bmatrix} \mathbf{J}_\ell & 0 \\ 0 & \mathbf{J}_F \end{bmatrix} \begin{bmatrix} \mathbf{I} \\ \mathbf{F}^T \end{bmatrix} \quad (3.9)$$

Where $\mathbf{J}_\ell = \text{diag}\{J_1, \dots, J_\ell\}$ is the inertia of the chords of \mathcal{G} and $\mathbf{J}_F = \text{diag}\{J_{\ell+1}, \dots, J_m\}$ is the inertia matrix of the remaining components. As both \mathbf{J}_ℓ and \mathbf{J}_F are diagonal matrices \mathbf{J} is a symmetric matrix.

To make sure that all elements of \mathbf{J}_ℓ are strictly positive the spanning tree \mathcal{T} must allow all chords to be picked as pipe components. For the Water Wall a Spanning Tree is presented in Appendix A.4 where all chords have been picked as pipes, thus $\mathbf{J}_\ell > 0$. The remaining part, $\mathbf{F}\mathbf{J}_F\mathbf{F}^T$, is nonnegative in all of its matrix elements, $\mathbf{F}\mathbf{J}_F\mathbf{F}^T \geq 0$. Which gives that

$$\mathbf{x}^T \mathbf{J} \mathbf{x} > 0, \quad \text{for all } \mathbf{x} \neq 0 \quad (3.10)$$

Thus \mathbf{J} is invertible if there exists a spanning tree where it is possible to pick all chords as pipe elements.

The chosen chords also defines the independent variables, which for the Water Wall model is

$$\mathbf{q}_\ell = [q_{c9}, q_{c13}, q_{c21}, q_{c23}, q_{c26}, q_{c28}, q_{c30}, q_{c33}, q_{c35}, q_{c37}]^T \quad (3.11)$$

3.2.1 Model Relations

With a system model established it is possible to set up a set of relations from the independent variable, \mathbf{q}_ℓ .

First of all the flows through every component in the distribution network can be calculated from the cycle matrix and the independent flows.

$$\mathbf{q} = \mathbf{B}^T \mathbf{q}_\ell \quad (3.12)$$

The pressure difference across each component is calculated from the model equation

$$\Delta \mathbf{p} = \mathbf{J} \dot{\mathbf{q}} + \boldsymbol{\lambda}(\mathbf{q}) + \boldsymbol{\mu}(\mathbf{q}, \mathbf{OD}) - \boldsymbol{\alpha}(\mathbf{u}) + \boldsymbol{\zeta} \quad (3.13)$$

The flow rate of change for the chords, $\dot{\mathbf{q}}_\ell$, is found in equation 3.8, inserting this into equation 3.13 and using the relation in equation 3.12 the following expression can be obtained.

$$\begin{aligned} \Delta \mathbf{p} = & \mathbf{J} \mathbf{B}^T (\mathbf{B} \mathbf{J} \mathbf{B}^T)^{-1} (-\mathbf{B} \boldsymbol{\lambda}(\mathbf{B}^T \mathbf{q}_\ell) - \mathbf{B} \boldsymbol{\mu}(\mathbf{B}^T \mathbf{q}_\ell, \mathbf{OD}) + \mathbf{B} \boldsymbol{\alpha}(\mathbf{u}) - \mathbf{B} \boldsymbol{\zeta}) \\ & + \boldsymbol{\lambda}(\mathbf{B}^T \mathbf{q}_\ell) + \boldsymbol{\mu}(\mathbf{B}^T \mathbf{q}_\ell, \mathbf{OD}) - \boldsymbol{\alpha}(\mathbf{u}) + \boldsymbol{\zeta} \end{aligned} \quad (3.14)$$

Which can be rewritten in a shorter form

$$\Delta \mathbf{p} = (\mathbf{I} - \mathbf{J} \mathbf{B}^T (\mathbf{B} \mathbf{J} \mathbf{B}^T)^{-1} \mathbf{B})(\boldsymbol{\lambda}(\mathbf{B}^T \mathbf{q}_\ell) + \boldsymbol{\mu}(\mathbf{B}^T \mathbf{q}_\ell, \mathbf{OD}) - \boldsymbol{\alpha}(\mathbf{u}) + \boldsymbol{\zeta}) \quad (3.15)$$

The difference pressure can also be found using the incidence matrix and the pressure at each node.

$$\Delta\mathbf{p} = \mathbf{H}^T \mathbf{p} \quad (3.16)$$

With the rank of the incidence matrix for a connected graph always being $n - 1$, it is possible to remove one row, i.e. a node, from \mathbf{H} without losing rank [Deo 74]. The reduced incidence matrix is denoted \mathbf{H}_r .

It is then possible to define a node, \mathbf{H}_0 , as the reference node with reference pressure \mathbf{p}_0 , and remove this from \mathbf{H} to obtain \mathbf{H}_r . The pressure of the remaining nodes can then be calculated relative to the reference node, which should be chosen as a node with a known absolute pressure. Inserting the reduced incidence matrix and the reference pressure into equation 3.16, equation 3.17 is obtained.

$$\Delta\mathbf{p} = \mathbf{H}_r^T \mathbf{p}_r + \mathbf{H}_0^T \mathbf{p}_0 \quad (3.17)$$

By isolating \mathbf{p}_r the pressure at each node is calculated as

$$(\mathbf{H}_r^T)^\dagger \Delta\mathbf{p} = (\mathbf{H}_r^T)^\dagger \mathbf{H}_r^T \mathbf{p}_r + (\mathbf{H}_r^T)^\dagger \mathbf{H}_0^T \mathbf{p}_0 \quad (3.18)$$

$$\mathbf{p}_r = (\mathbf{H}_r^T)^\dagger \Delta\mathbf{p} + (\mathbf{H}_r^T)^\dagger \mathbf{H}_0^T \mathbf{p}_0 \quad (3.19)$$

Where $(\mathbf{H}_r^T)^\dagger$ is the pseudo inverse of \mathbf{H}_r^T , such that $\mathbf{I} = (\mathbf{H}_r^T)^\dagger \mathbf{H}_r^T$.

In the Water Wall model the reduced incidence matrix, \mathbf{H}_r , is formed by removing the first row of \mathbf{H} , corresponding to the first node of \mathcal{G} . This is convenient as this node is known to have ambient pressure (≈ 1 bar) at all times. Otherwise it would be suitable to choose a node which has a pressure transducer installed to give an absolute pressure reading.

3.3 Model Implementation

The model as described in section 3.2 is implemented in Simulink as an S-function block where the combination of equation 3.16 and equation 3.19 are applied to calculate the relative pressures in the system. A simple diagram of the implementation is shown in figure 3.3.

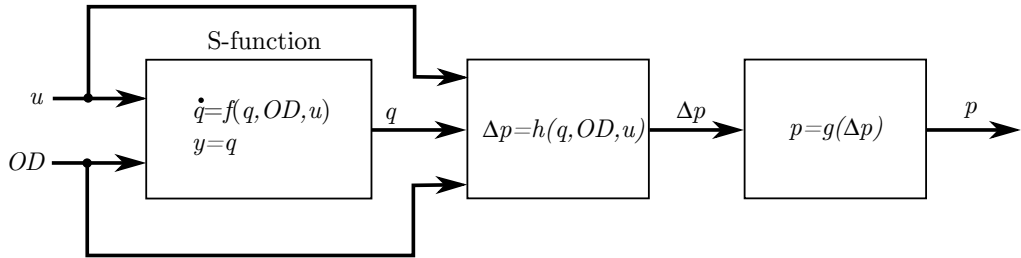


Figure 3.3: Simple implementation demonstration of the model equation described in section 3.2 and how equation 3.16 and equation 3.19 are applied to calculate the relative pressures in the system .

The model is implemented as a discrete time model which is solved by applying Forward-Euler as shown in equation 3.20 .

$$q_n = q_{n-1} + Ts \cdot f(t_{n-1}, q_{n-1}) \quad (3.20)$$

$$\dot{q} = f(t, q) \quad (3.21)$$

In order for the model to work some restrictions have been imposed on the valve components opening degrees. When closing a valve, the resistance value μ in equation 2.19 grows very rapidly towards infinity, thus rendering the solution infeasible due to numerical error. By recalling equation 2.19 in equation 3.22, one can see that small values of $k_v(OD)$ result in a big μ and if $k_v(OD) = 0$, the equation becomes invalid.

$$\mu_k(q) = \frac{1}{k_v(OD)^2} |q| q \quad (3.22)$$

Consequently, the opening degree has been restricted to the interval 35 % to 100 % ($OD = [0.35, 1]$). This restriction is not unrealistic, as an aggregated end-user, the consumption is never zero.

In the Water Wall test system, the pumps experience hysteresis at low speeds and since the pump model in section 2.1.3 does not take that into account, a restriction of the minimum pump rotation speed is imposed at $\omega = 0.16$. The value of 0.16 is given by the pump data material [Grundfos 10]. Similarly, the maximum speed of the pumps are reached at a $\omega = 0.9$, thus the operational interval for the pump speed is restricted to $\omega = [0.16, 0.9]$.

Along with the pumps speed restriction and the defined range of the valves opening degree, one has to take into account how fast these actuators can react. The valves located on the water wall test system are equipped with an rotary actuator which take 9 seconds to fully open the valves from their closed position [Belmio 10]. While the pumps take around 1 second to reach their top speed from a stop position according to Grundfos. These slew rates are therefore implemented in the simulation to ensure that the pumps and valves models behave in the same way as the physical components in water wall test system.

Finally, as a result of the graph theoretical modelling approach, the water distribution network has been modelled as a closed loop as opposite to a tree structure. Meaning that all physical nodes open to atmospheric pressure share the same node in the underlying network graph. This results in the possibility for water, in the simulation model, to flow into the distribution network from the water outlet and to deposit water into the reservoir.

3.3.1 Valve Conductivity Function $k_v(OD)$

Before it is possible to implement the model, the valve conductivity function $k_v(OD)$ needs to be defined. The valves found on the Water Wall are all identical and they are listed in table A.4 in appendix A.1. They share the same valve characteristic curve which is shown in figure 3.4.

Note that the valve is closed when the valve actuator is positioned between $\theta_{OD} = 0^\circ$ and $\theta_{OD} = 15^\circ$. The valve characteristic curve in figure 3.4 is given by the below definition of $k_v(OD)$.

$$k_v(OD) = \begin{cases} 0 & \text{if } \theta_{OD}\theta_{off} < 0 \\ k_{vs} \frac{\theta_{OD} - \theta_{off}}{\theta_{max} - \theta_{off}} n_{gl} e^{1-n_{gl}} & \text{if } \frac{\theta_{OD} - \theta_{off}}{\theta_{max} - \theta_{off}} \leq \frac{1}{n_{gl}}, \quad \theta_{OD} = OD \cdot \theta_{max} \\ k_{vs} e^{n_{gl} \frac{\theta_{OD} - \theta_{off}}{\theta_{max} - \theta_{off}} - 1} & \text{if } \frac{\theta_{OD} - \theta_{off}}{\theta_{max} - \theta_{off}} \geq \frac{1}{n_{gl}} \end{cases}$$

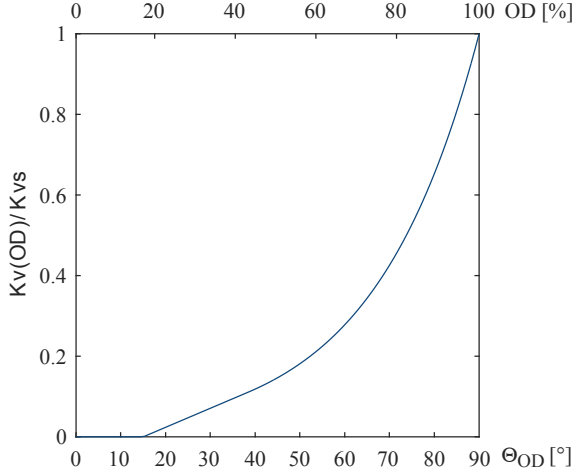


Figure 3.4: Belimo R2015-1-S1 valve characteristic plot [Belimo 11, Belimo 14]. Acronyms: OD = opening degree, θ_{OD} = opening degree angle of rotation.

where

θ_{OD}	is the opening degree angle of rotation	[${}^\circ$]
θ_{off}	angle of rotation at which the valve opens	[${}^\circ$]
θ_{max}	is the angle of rotation when the valve is fully open	[${}^\circ$]
n_{gl}	is the valve characteristic curve factor	
OD	is the valve opening degree ($OD = [0, 1]$)	

The $k_v(OD)$ calculation for this particular valve is defined in [Keller 11] where the characteristic is designed to be linear in the lower opening range when

$$0 < \frac{\theta_{OD} - \theta_{off}}{\theta_{max} - \theta_{off}} \leq \frac{1}{n_{gl}}$$

which improves the control characteristic in the lower partial load range [Belimo 14]. After the linear part, when

$$\frac{\theta_{OD} - \theta_{off}}{\theta_{max} - \theta_{off}} \geq \frac{1}{n_{gl}} \quad (3.23)$$

the valve characteristic is similar to the non-linear equal percentage characteristic presented in figure 2.4 in section 2.1.2.

3.3.2 Pump Speed Controller Design

As mentioned in the beginning of section 3.3, the pumps located on the Water Wall test system are actuated by a relative speed signal ω in $[0.16, 0.9]$. However, the input in the model is the differential pressure u across the pump. Consequently, a speed controller is designed for the pumps. After the controller is designed, it is implemented into the Simulink environment which communicates with the Water Wall via the DAQ boards.

The speed controller implementation for one pump is illustrated in figure 3.5 where the control signal u is the pump differential pressure set point.

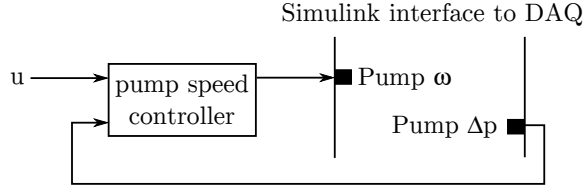


Figure 3.5: Illustration of the pump speed controller implementation in Simulink which communicates with the Water Wall test system via DAQ (Data Acquisition) boards.

The controller shown in figure 3.5 is a PI-controller with an implemented saturation block which limits the pumps speed signal between $\omega_{\min} = 0.16$ and $\omega_{\max} = 0.9$. Additionally, a back-calculation anti windup scheme is implemented as well to prevent the error, $u - \text{Pump } \Delta p$, being integrated when the controller output, ω , is saturated [Franklin 10].

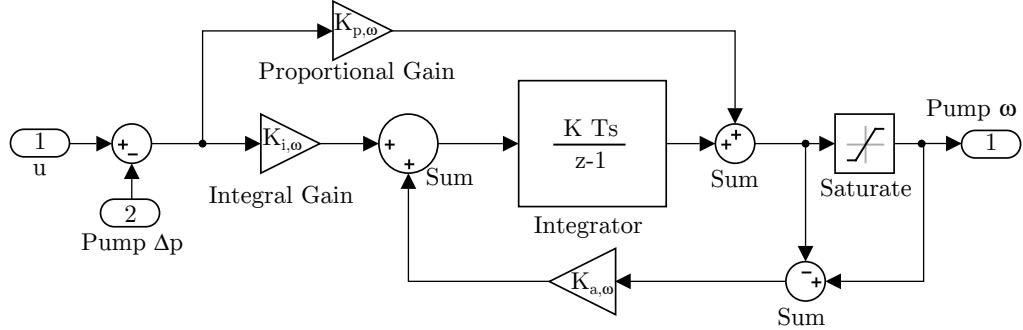


Figure 3.6: The pump speed controller.

The resulting performance of the controller is shown in figure 3.7, where one can see the set point signal u and how the pumps differential pressures follow u .

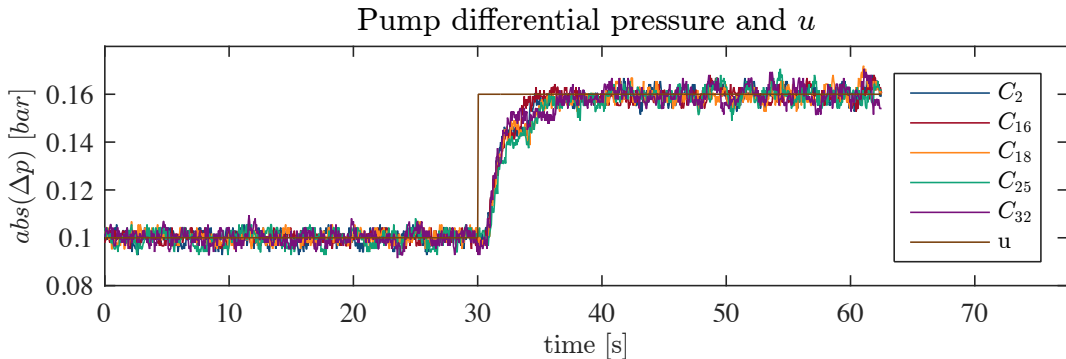
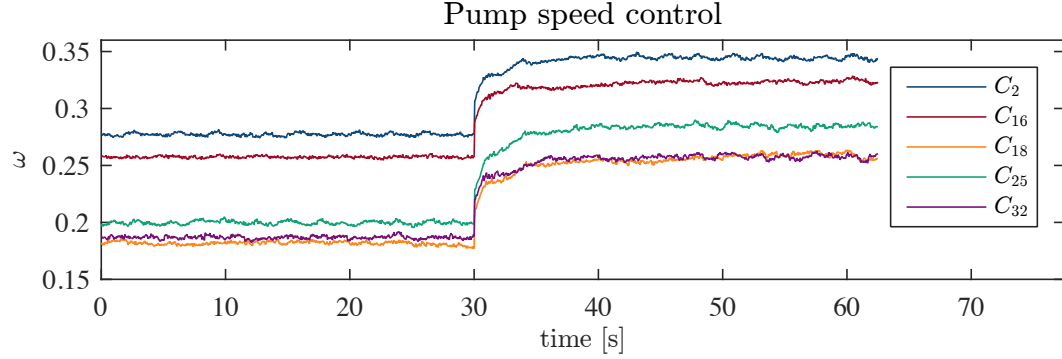


Figure 3.7: The pumps input signal which is applied in the parameter estimation.

The delay that one can observe in figure 3.7 is primary caused by the pump reaction time[Kallesøe 15]. The speed signal ω for each pump is shown in figure 3.8.

**Figure 3.8:** The pump speed controller outputs

The speed signals are also analysed to ensure that they stay in the interval $[0.16, 0.9]$. The pumps C_2 and C_{16} require the largest ω as they, individually, deliver the largest flow of all five pumps. This is due to the fact that the combined flow through C_2 and C_{16} is equal to the combined flow through C_{18} , C_{25} and C_{32} .

From figure 3.7, one can observe that the pumps differential pressure is not completely stable. In fact, the pumps differential pressure measurement have the same variation when the ω is completely stable. This variation is assumed to be caused by sensor noise.

Because of the variation in the pump differential pressure measurements and the delay observed in figure 3.7, the tuning process of the controller is a compromise between a fast rise time and disturbance rejection. The tuning process is described in the following points which is a similar to the Ziegeler-Nichols tuning method [Franklin 10].

- First, the proportional gain $K_{p,\omega}$ is tuned until the oscillation in the measured Δp starts to increase. The additional oscillation is due to the delay observed in figure 3.7 which is not taken into account in the controller design.
- Then, the integration gain $K_{i,\omega}$ which ensures no steady state error is tuned in the same way as the proportional gain $K_{p,\omega}$.
- Lastly, The back-calculation coefficient $K_{a,\omega}$ is set as $K_{a,\omega} = K_{i,\omega}$ since it is recommended to choose it $K_{a,\omega} \leq K_{i,\omega}$ [KJ Astrom 94]. The controller is also tested when ω is saturated where the error, $u - \text{Pump } \Delta p$, becomes zero almost instantly. Hence, no further tuning of $K_{a,\omega}$ is necessary.

The values of $K_{p,\omega}$ and $K_{r,\omega}$ result in a acceptable rise time and are therefore kept. The pump speed controller parameters are shown in table 3.3.

Components	$K_{p,\omega}$	$K_{i,\omega}$	$K_{a,\omega}$	ω_{\max}	ω_{\min}
$C_2, C_{16}, C_{18}, C_{25}, C_{32}$	0.5	0.5	0.5	0.16	0.9

Table 3.3: The pump components which utilize the speed controller shown in figure 3.6 and the controller parameters.

Through the tuning process of the controller, all of the opening degree is kept the same, namely $OD = 0.7$.

3.4 Model Parameters

To complete the model presented in section 3.2, all parameters pertaining to the system components have to be stated. Generally, model parameters can be found in data sheets or via measurements. However, if a parameter is unknown or its given value carries a great uncertainty, parameter estimation becomes necessary. This section starts by covering the known parameters and how they are found, followed by an estimation method used to find the remaining parameters.

3.4.1 Known Parameters

The parameters which are considered known for each component are listed below.

- A list of the pumps located on the water wall depicted in figure 3.1 is found in appendix A.1. Table A.5 lists all the pumps along with their constants a_{h0} , a_{h1} , a_{h2} , a_{p0} , a_{p1} , a_{p2} , B_0 and P_0 provided by Grundfos.
- The valves which are located on the water wall are listed in table A.4 in appendix A.1 along with their conductivity values k_{vs} , their valve characteristic curve factor n_{gl} and the angle of rotation values which define when the valve starts to open and when it is fully open, θ_{off} and θ_{max} . These values are found in the valves data sheet [Belimo 11, Belimo 14].
- All pipes in the system have five parameters. The parameters are the pipe diameter D , their length L , the average roughness hight of the pipe inner walls ε , the total form-loss coefficient, k_f , of the pipe fittings and lastly, the head loss from change in elevation along the pipe, Δz .

Only the length of the pipes, their diameter and head losses due to change in elevation are considered known, they are given by the water wall system diagram in figure A.2 and they are also listed in table A.1 found in appendix A.1.

3.4.2 Unknown Parameters

The parameters left unknown are the pipe interior average roughness hight ε , the total form-loss coefficient, k_f , of the pipe fittings and lastly, Δz for both C_4 and C_{14} are estimated because of an assumption made in the modelling process. This assumption is demonstrated when Δz for both C_4 and C_{14} is explained.

Estimation of ε and k_f

Even though one can find ε via the pipe data sheet, it is only valid for a new pipe as over time and depending on the material, pipes can rust. Also, the inside walls will collect particles from the water e.g. calcium. The form-loss coefficient, k_f , is also hard to determine since the exact number and the size of the fittings in a real water distribution system is not always known. It is though not necessary, or possible, to estimate both of the constants since they enter the pipe model in the same place. Recall the λ term from the pipe model in equation 2.27 and note that the pipe friction factor f is assumed constant where it depends on ε and D .

$$\begin{aligned}\lambda(q) &= \left(f \frac{8 L \rho}{\pi^2 D^5 \cdot 10^5 \cdot 3600^2} + k_f \frac{8 \rho}{\pi^2 D^4 \cdot 10^5 \cdot 3600^2} \right) |q| q \\ \lambda(q) &= \left(f \frac{L}{D} + k_f \right) \frac{8 \rho}{\pi^2 D^4 \cdot 10^5 \cdot 3600^2} |q| q\end{aligned}\quad (3.24)$$

It is clear from the above equation, that tuning only either f or k_f will have the same result for $\lambda(q)$. Consequently, only k_f needs to be estimated.

Note, by only estimating k_f one may not obtain the true k_f value since f is unknown. The relation between the estimated k_f , assuming correct estimation, and equation 3.24 is shown below.

$$f_{\text{init}} \frac{L}{D} + k_{f,\text{est}} = f_{\text{true}} \frac{L}{D} + k_{f,\text{true}} \quad (3.25)$$

$$k_{f,\text{est}} = f_{\text{true}} \frac{L}{D} + k_{f,\text{true}} - f_{\text{init}} \frac{L}{D}$$

where

- f_{init} is the friction factor which is calculated from the initial guess of ε .
- f_{true} is the friction factor which is calculated from the true and unknown ε .
- $k_{f,\text{est}}$ is the estimated k_f
- $k_{f,\text{true}}$ is the true and unknown k_f

Estimation of Δz for C_4 and C_{14}

The following demonstrations are only shown for C_2 where the same setup and assumption apply for C_{16} . In the system diagram, figure A.2, found in appendix A.2, it is assumed that the inlet of both C_2 and C_{16} are connected directly to the water supply at atmospheric pressure. This assumption is demonstrated in figure 3.9 where one can see where the pump, C_2 , is connected to the ground symbol which represents atmospheric pressure.

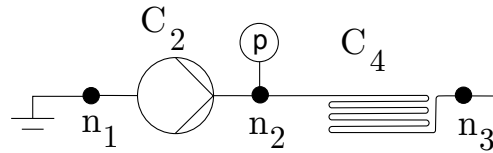


Figure 3.9: Assumed setup of C_2 and C_4 which shows how they are implemented in the system model.

In reality, the pumps are connected to the water supply through a pipe where the water surface level is not in the same line of hight as the pump. The real setup is demonstrated in figure 3.10.

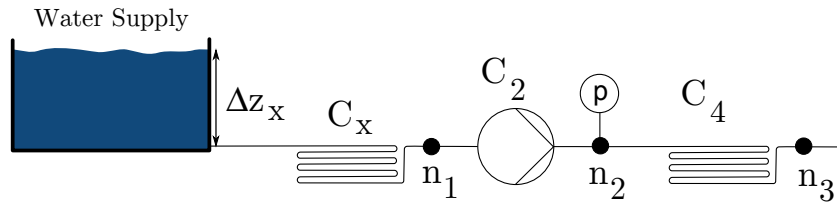


Figure 3.10: How C_2 is connected to the water supply on the real test system.

To compensate for the additional pipe, C_x , and the change in elevation, Δz_x , the properties of C_x and the Δz_x are combined into the C_4 pipe, resulting in figure 3.11. Note that Δz_x is assumed constant since the Water Wall test system is in a closed loop.

First, the length of C_x is added to the length of C_4 assuming the C_x diameter is the same as C_4 and since it is possible to measure the length of C_x on the real test system, it is considered un-necessary to estimate it. Even though it is also possible to measure Δz_x , any measurement error will effect the pressure in the whole system. Hence, it is considered necessary to estimate Δz in C_4 which corresponds to Δz_x . Lastly, the arguments behind the necessity of estimation Δz in C_4 , also applies for Δz in C_{14} .

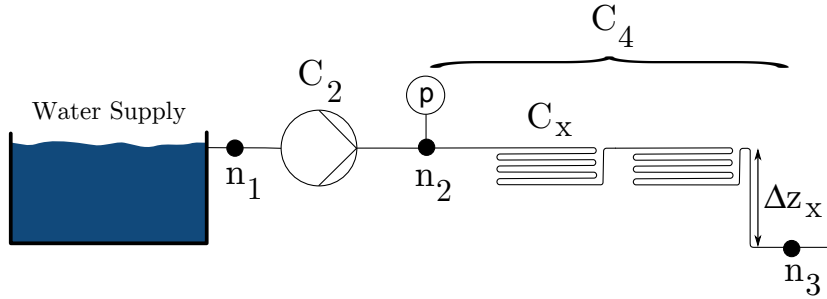


Figure 3.11: How C_x and Δz_x , which are not taken into account in the modelling processes, are compensated for by implementing their properties into the pipe C_4 .

The following notes are made while comparing figure 3.10 and figure 3.11.

- One can consider that figure 3.10 represent a part of the real test system and figure 3.11 shows how that part is implemented in the model.
- The pressure in n_3 is the same in both figure which means that pressure in the remaining model is not effected by the C_x and Δz_x compensation.
- However, the pressure in n_2 is not the same in both figures, meaning that the measurement from the sensor placed at n_2 can not be used to compare the real test system and the model.

3.4.3 Parameter Estimation

Generally, parameter estimation is performed by applying input data on a model with the unknown parameters. The input data also has matching output data that is generated by the system which should reflect the system dynamic properties of the model. Once the input data is applied to the model, the model output and the system output are compared. It is at this stage where the parameters are tuned and the goal is to match the outputs as close as possible. The model simulation is executed multiple times where at each iteration the parameters are tuned until the best possible fit is achieved. The last step is to verify the resulting parameters by applying new input data to the model. Then the new output from the model and the system should still match. [Ljung 87, Petursson 15].

Parameter Initial Guess

When applying any kind of parameter estimation method, a good initial guess of the parameters can help speed up the process.

The initial values for the average roughness height, ε , of the pipe interior is found in the pipe data sheets [Wavin 15] and [Wavin 12]. Their values are listed in table A.1 located in appendix A.1.

By studying the fittings on each pipe located on the water wall introduced in section 3.1, it is possible to make a initial guess of the form-loss coefficients, k_f . A list of different fittings found on the water wall along with their individual k_f values is given in table A.2. The values are found in [Polypipe 08] and [Fischer 11]. Table A.1 lists the different fittings found on each pipe on the water wall.

Lastly, Δz for the pipes C_4 and C_{14} , which are connected to the pumps C_1 and C_{16} , are initially set from physical measurements. The hight measurements are taken between the pumps inlet and the water supply surface level as illustrated in figure 3.10.

The Estimation Data

In a parameter estimation and model verification process, it is important to design an input signal that excites all the dynamics which one is interested to model. Generally, the signal should contain changes both in frequency and in amplitude in all inputs. This type of signal can be generated by using low pass filtered white noise or a PRBS (Pseudo Random Binary Sequence) with varying amplitude [Ljung 87].

However, in this particular case, the unknown parameters only enters on the right hands side of model which is show in equation 3.26, meaning that they can be determined from steady-state conditions.

$$\mathbf{B}\mathbf{J}\mathbf{B}^T \dot{\mathbf{q}}_\ell = -\mathbf{B}\boldsymbol{\lambda}(\mathbf{B}^T \mathbf{q}_\ell) - \mathbf{B}\boldsymbol{\mu}(\mathbf{B}^T \mathbf{q}_\ell, \mathbf{OD}) + \mathbf{B}\boldsymbol{\alpha}(\mathbf{u}) - \mathbf{B}\boldsymbol{\zeta} \quad (3.26)$$

As it is possible to focus only on the steady-state conditions, the frequency of the input signal is not of concern and it is only necessary to focus on the signal amplitude. Hence, the estimation input signal has the following properties:

- All input signals vary in amplitude.
- All input signals hold a steady amplitude for minimum 25 seconds to ensure that the system reaches steady state between signal steps. The 25 second period is found to be an appropriate amount of time to ensure that the system output signal is dominated by steady state measurements.
- The input signal may not result in a system relative pressure over 0.16 bar since the pressure sensors in the system have a operation range of p in $[0, 0.16]$ bar.
- The input signal may not result in saturation in the pump speeds ω . This is important as if the pumps are saturated, the set point signal, u , is no longer equal to the actual differential pressure across the pump.

The estimation signal for the valves is shown in figure 3.12.

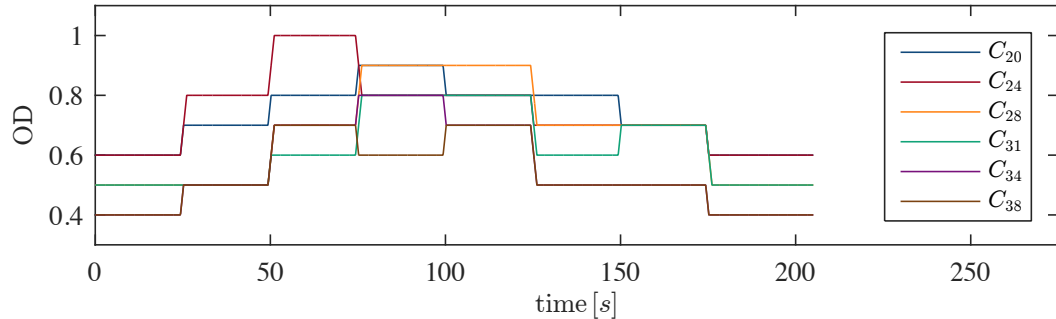


Figure 3.12: The valve input signal which is used in the parameter estimation.

And the estimation signals for the pumps is shown in figure 3.13. The input signals shown figure 3.13 and 3.12 have the same amplitude in the beginning and in the end. Consequently, one expects that the outputs have the same steady state values in their beginning and end.

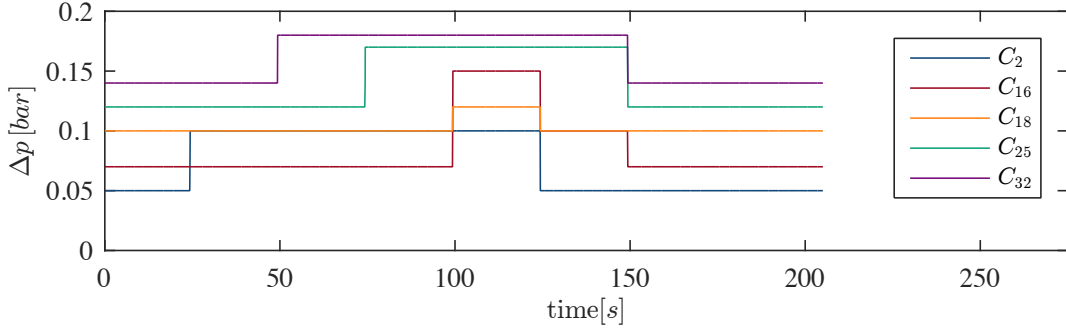


Figure 3.13: The pumps input signal which is used in the parameter estimation.

The outputs which are used in the parameter estimation are only the relative pressure measurements since the differential pressure measurements are equal to the input signal u in steady state. Also, the pressure measurements p_1 and p_2 belonging to C_2 and C_{16} are neglected as discussed in section 3.4.2. The measurements applied in the parameter estimation are listed in table 3.4.

Estimation outputs					
p	Comp.	Node	p	Comp.	Node
p_3	$C_{8,18}$	n_4	p_7	$C_{23,24}$	n_{14}
p_4	$C_{10,25}$	n_6	p_8	$C_{28,29}$	n_{17}
p_5	$C_{12,32}$	n_8	p_9	$C_{30,31}$	n_{19}
p_6	$C_{21,22}$	n_{12}	p_{10}	$C_{35,36}$	n_{22}
			p_{11}	$C_{37,38}$	n_{24}

Table 3.4: The pressure measurement points used as parameter estimation outputs.
Note, comp. stand for component and when the notation $C_{x,y}$ means between component x and y

The resulting pressure measurement taken on the test system are shown in the following plots.

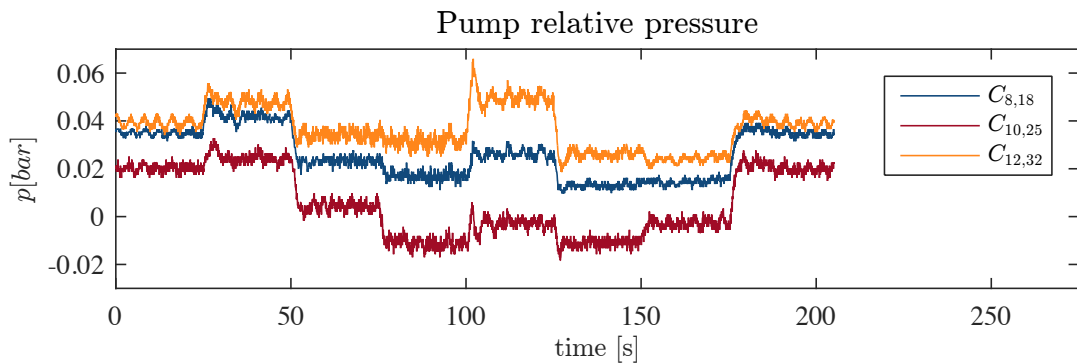


Figure 3.14: Pump inlet pressure measurements which are part of the estimation data.

Figure 3.14 and 3.15 show how the pressure in the system varies while the pumps and the valves are actuated by the signals shown in figure 3.12 and 3.13. As expected, the pressure measurements have the same steady state values in their beginning and end. After the parameters are estimated in the upcoming section, the signals shown in figure 3.14, 3.15, 3.12 and 3.13 are used to evaluate how correct those parameters are. However, these exact signals are not directly applied in the

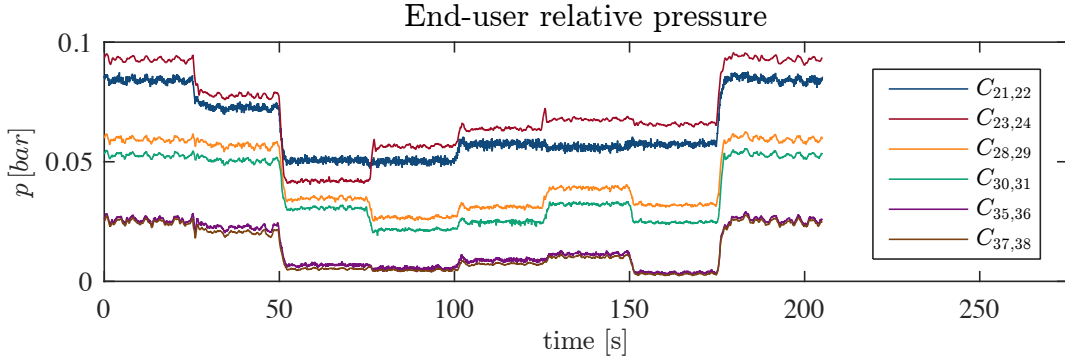


Figure 3.15: End-user pressure measurements which are part of the estimation data.

estimation process. Instead of using the whole sequence, which is just over 200 s long, chosen parts of the signals are used instead. The above signals can be divided into seven different parts where the measurements are in steady state. Each signal part includes a specific time frame of the signals shown in figure 3.14, 3.15, 3.12 and 3.13. The start and stop time of the parts are shown in table 3.5.

Signal parts	Part 1	Part 2	Part 3	Part 4	Part 5	Part 6	Part 7
Start time	4.5 s	30.6 s	55.8 s	79.1 s	106.4 s	128.9 s	157 s
Stop time	12 s	38.1 s	63.3 s	86.6 s	113.9 s	136.4 s	163.5 s

Table 3.5: The time frame of the signal parts which are applied in the parameter estimation process.

The signals parts are treated as seven difference estimation signals and since their combined signal length has been reduce by a factor of four from the original estimation data, the estimation process time is also reduced. The parts are choose where the pressure measurement are in steady state and since the model can not be fitted to the sensor noise which can be observed in 3.14 and 3.15, the mean value of the steady state measurements are used instead of the measurement itself. By applying the mean of the measurement and not the true measurement, will also reduce the amount of time it takes to estimate the parameters.

The signal parts which are taken from pump and valve inputs signals are shown in figure 3.16 and figure 3.17. Note, the signal parts are plotted together even though they are treated as seven different signals.

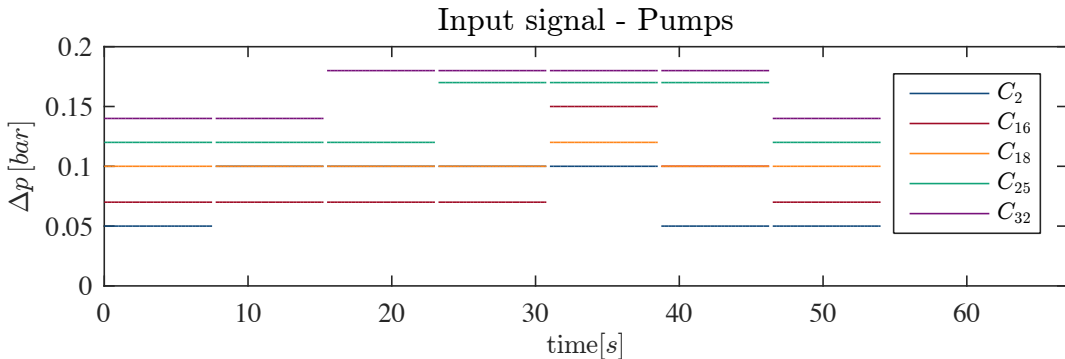


Figure 3.16: The valve input signal which is used in the parameter estimation.

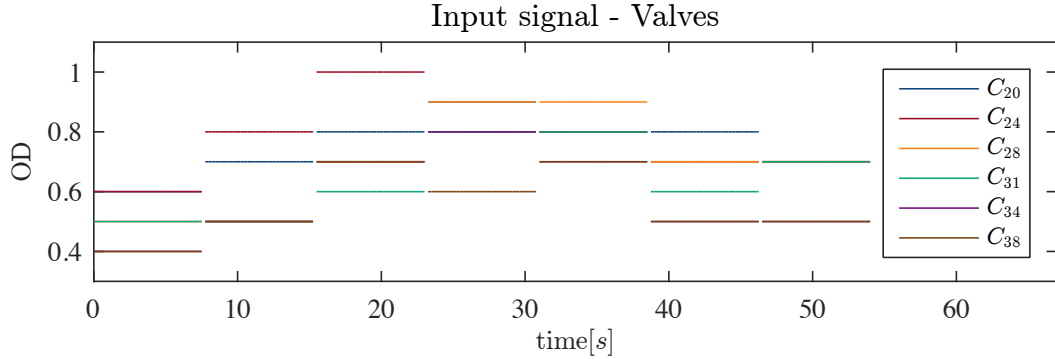


Figure 3.17: The pumps input signal which is used in the parameter estimation.

And lastly, the signal parts where one can see the mean value of the pressure measurements are depicted in figure 3.18 and 3.19.

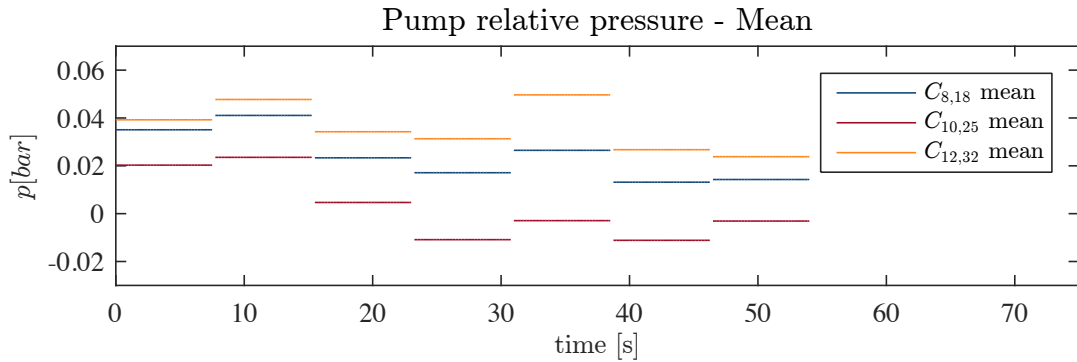


Figure 3.18: The valve input signal which is used in the parameter estimation.

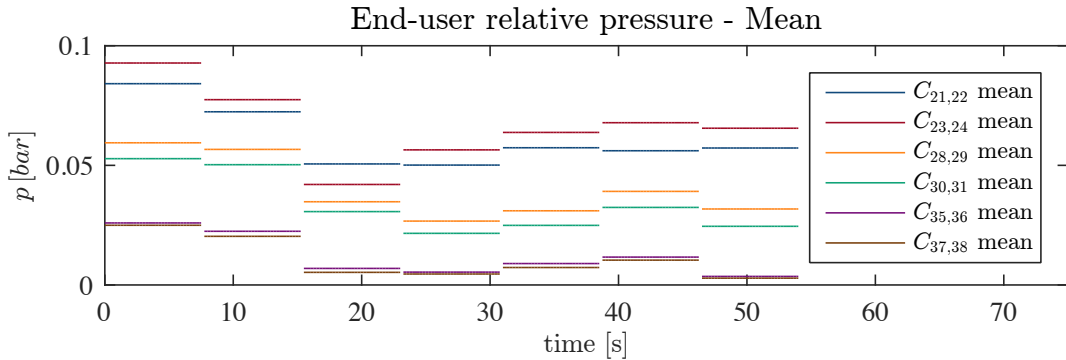


Figure 3.19: The pumps input signal which is used in the parameter estimation.

The estimation data is hereby designed. The data which is applied while computing the parameters are shown in figure 3.16, 3.17, 3.18 and 3.19. The estimation data which is used to evaluate the parameters correctness are shown in figure 3.14, 3.15, 3.12 and 3.13.

The Estimation Method

The parameters are estimated by applying the **Trustregion Reflective Newton** which is a part of the MATLAB Nonlinear Gray Box Model Estimation toolbox. First, the model is defined as a

`idnlgey` which stands for a *Nonlinear ODE (grey-box model) with unknown parameters* and the function `pem` (Prediction error estimate) is used to execute the estimation.

The toolbox configuration setup is kept as default where **Trustregion Reflective Newton** is automatically set as the estimation method and since it gives acceptable results, no further tuning is performed. Also, any deeper understanding of the estimation algorithm is considered out of this project scope.

Note that weighing of the outputs is considered non-necessary since all measurements have the same unit and are considered equally important to obtain correct parameters.

The Estimation Results - The First Attempt

The resulting parameters obtained from the parameter estimation are listed table 3.6.

Parameters	$C_4(k_f)$	$C_8(k_f)$	$C_9(k_f)$	$C_{10}(k_f)$	$C_{11}(k_f)$	$C_{12}(k_f)$	$C_{13}(k_f)$	$C_{14}(k_f)$
Init. value	4.42	3.92	0.51	3.11	1.81	3.63	0.51	1.81
Est. value	579	186	435	438	563	202	283	889
Parameters	$C_{19}(k_f)$	$C_{21}(k_f)$	$C_{22}(k_f)$	$C_{23}(k_f)$	$C_{26}(k_f)$	$C_{28}(k_f)$	$C_{29}(k_f)$	$C_{30}(k_f)$
Init. Value	3.57	1.46	7.68	2.55	2.77	0.81	2.26	2.10
Est. Value	259	67	108	42	10	92	104	155
Parameters	$C_{33}(k_f)$	$C_{35}(k_f)$	$C_{36}(k_f)$	$C_{37}(k_f)$	$C_{39}(k_f)$	$C_{42}(k_f)$	$C_4(\Delta Z)$	$C_{14}(\Delta Z)$
Init. Value	2.27	3.07	2.26	3.27	2.27	2.77	-0.11	0.4
Est. Value	447	44	0	33	345	0	-0.1524	0.5937

Table 3.6: The parameter estimation resulting parameters along with their initial values. The initial parameters are the same as introduced in table A.1 in appendix A.1.

The resulting parameters seem to be unrealistically high and much higher than the original parameters. To get a better understanding of what values of K_f are to expect, $\lambda(q)$ is computed for different values of K_f in figure 3.20. The equation for $\lambda(q)$ is given in equation 2.12 where it results in the pipe pressure drop under steady state.

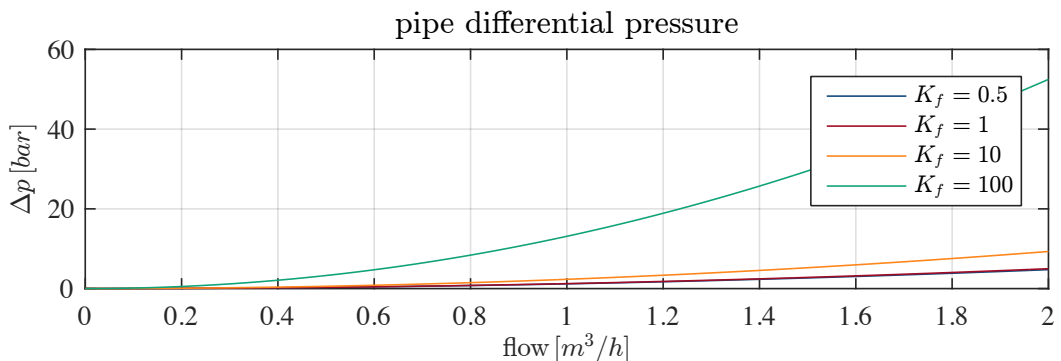


Figure 3.20: The pressure drop over a pipe for different K_f values. The pipe has the following parameters: $L = 10 \text{ m}$, $D = 0.01 \text{ m}$, $\epsilon = 7e - 6$

From figure 3.20, it is obvious that K_f values around and over 100 are not correct and even values that are over 10 seems unrealistic for the system. However, to figure out what is causing the parameter estimation process to result in such unrealistic K_f values, the next step in the estimation process is taken.

The next step in the parameter estimation process is to compare the model output with the test setup measurements. The comparison is done using the MATLAB function `compare`, which plots a visual comparison of the signals along with computing a fitting percentage, `fit`, that indicates how close the model output is to the test system measurements. The `fit` value represents an NRMSE (The normalized root-mean-square error) which MATLAB defines as equation 3.27. Equation 3.27 shows how to compute a `fit` from two signal vectors, one which is the model output \hat{y} and the second one is the validation output data y .

$$\text{fit} = 100 \left(1 - \frac{\|\mathbf{y} - \hat{\mathbf{y}}\|}{\|\mathbf{y} - \mathbf{y}_1 \cdot \text{mean}(\mathbf{y})\|} \right) = 100 \left(1 - \frac{\sqrt{\sum_{i=1}^a (y_i - \hat{y}_i)^2}}{\sqrt{\sum_{i=1}^a (y_i - \text{mean}(y))^2}} \right) \quad (3.27)$$

where

- \mathbf{y} is a single validation output data vector.
- $\hat{\mathbf{y}}$ is the model output vector.
- \mathbf{y}_1 is a vector of ones which has the same length as \mathbf{y} .
- y_i is a single element in the validation output data vector.
- \hat{y}_i is a single element in the model output data vector.
- a is the number of samples in both the model and the validation output data vector.
- fit is a NRMSE fitting percentage.

From equation 3.27, one can see that it results in a 100 % `fit` only when $\mathbf{y} - \hat{\mathbf{y}} = 0$ and if $(\mathbf{y} - \hat{\mathbf{y}}) > (\mathbf{y} - \text{mean}(\mathbf{y}))$, the `fit` becomes negative. However, what is more interesting, is the fact that a `fit` percentage close to zero is not necessarily a bad fit since it only means that $\text{mean}(\mathbf{y}) = \hat{\mathbf{y}}$. A demonstration of a `fit` which is close to zero is illustrated in figure 3.21.

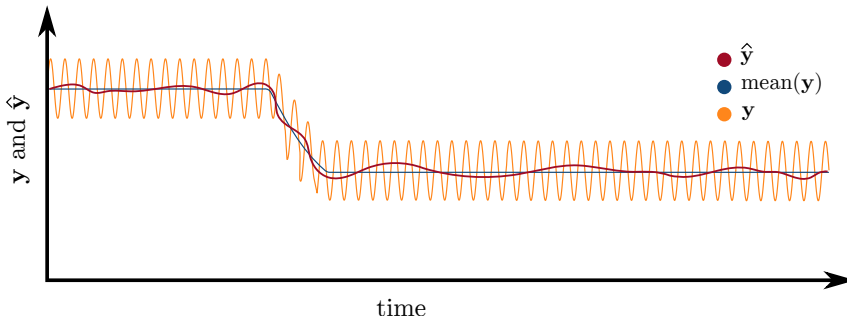


Figure 3.21: Demonstration of a model output signal, \hat{y} , that is close to the mean of the validation data output signal, $\text{mean}(y)$.

The oscillation in \hat{y} is meant to demonstrate sensor noise or e.g. dynamic behaviour which has not been considered in the model. Depending on the necessity of the model correctness and the purpose of the model, one can conclude that the model which generated \hat{y} can indeed be used to represent the system behind the validation data y , even though their `fit` is close to zero. Hence, it is not possible to state if the model is correct by the `fit` value alone. The focus is more on how much the `fit` improves after the parameter estimation. The final verification of the parameter estimation is performed by a visual analysis of the output signals together.

The fitting percentage for each of the model outputs, before and after estimation, is listed in table 3.7.

Measurement point	$C_{8,18}$	$C_{10,25}$	$C_{12,32}$	$C_{21,22}$	$C_{23,24}$
fit - Before	p_3	p_4	p_5	p_6	p_7
fit - After	-252%	-275%	-159%	-534%	-362%
Measurement point	$C_{28,29}$	$C_{30,31}$	$C_{35,36}$	$C_{37,38}$	
fit - Before	p_8	p_9	p_{10}	p_{11}	
fit - After	-471%	-545%	-662%	-682%	
	30%	10%	18%	-1%	

Table 3.7: The fitting percentage, **fit**, before and after the parameter estimation.
Note, the notation $C_{x,y}$ means between component x and y

From table 3.7 one can see how the **fit** improves by using the estimated parameters even though their values are unusually high.

The following figures plot the test system measurements along with the model outputs which are defined in table 3.4. The model outputs are computed by using the estimated parameters. Figure 3.22 shows the pressures at the pumps inlet.

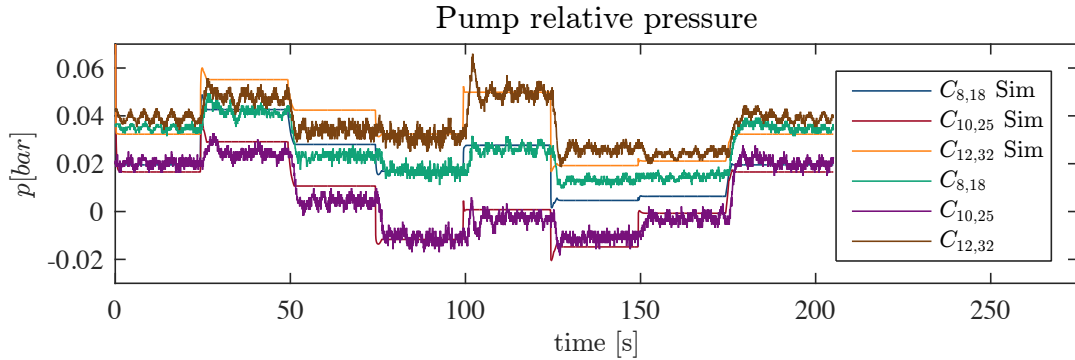


Figure 3.22: Estimation data results showing the actual and simulated relative pressure at the pumps inlet.

Figure 3.23, 3.24, and 3.25 show the pressures at or close to the end-user valves.

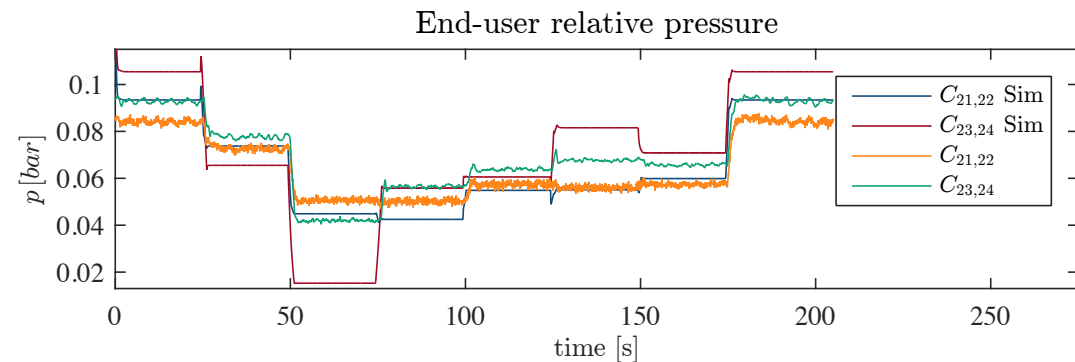


Figure 3.23: Estimation data results showing the actual and simulated relative pressure close to the end-user valves.

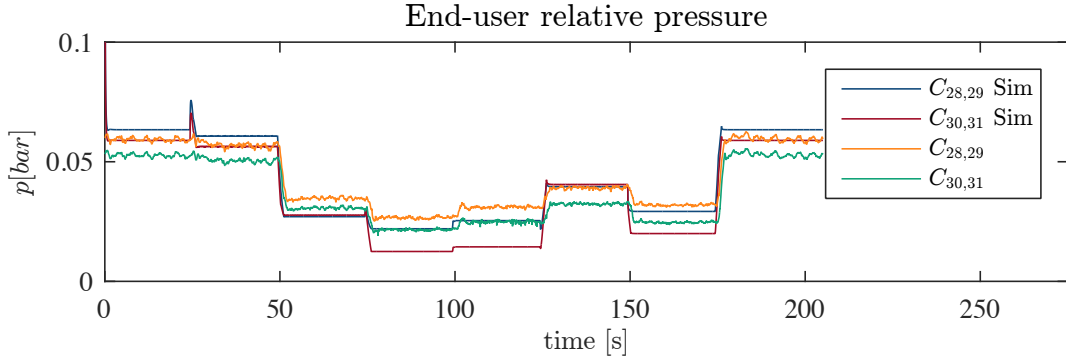


Figure 3.24: Estimation data results showing the actual and simulated relative pressure close to the end-user valves.

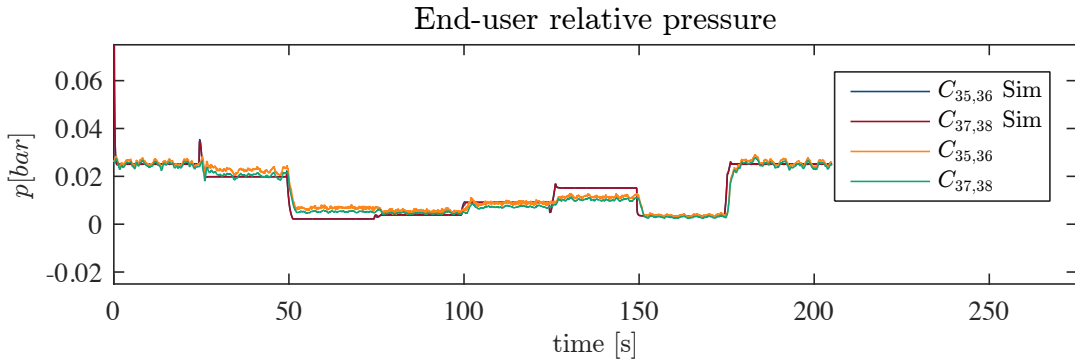


Figure 3.25: Estimation data results showing the actual and simulated relative pressure close to the end-user valves.

From figure 3.22, 3.23, 3.24, and 3.25, one can observe that the model outputs and the real test system measurements have a close fit, despite the high K_f values. The following conclusions can be made from plots presented above and the estimated K_f values.

- The parameter estimation process seems to work since the model outputs and the real test system measurements have a close fit.
- The high values of the estimated parameters indicate that there is a modelling error and/or the measurements from the test system are not accurate.
- If the measurements are not correct, the estimation process tries to force the model to give the same outputs by over tuning the K_f values.
- Since the purpose of the parameter estimation process is to correct the pipe components, one should focus on the valve model and evaluate how it can effect the above results. Even though the valve model is considered known as all its parameters are given by its producer, a small model error can have a relatively big effect. This error could origin from the fact that the valve OD is mapped to a K_v value through an exponential function as shown in figure 3.4 in section 3.3.1. Consequently, if the model is not correct, small displacement of the exponential curve can have a relatively big effect on the pressure drop over the valve.

Because of the last consideration, a second parameter estimation attempt is computed where all the valves are fully open, $\text{OD}=100\%$. This means that the function, $K_v(\text{OD})$, which includes the

exponential term is no longer part of the valve model. The valve model is recalled in equation 3.28 where it can be rewritten since the $OD = 1$.

$$\Delta p = \frac{1}{k_v(OD)^2} |q| q \Big|_{OD=1} = \frac{1}{k_{vs}^2} |q| q \quad (3.28)$$

From equation 3.28, one can see that a fully open valve only has one parameter, namely K_{vs} which is considered as a known parameter in the second estimation attempt.

The Estimation Results - The Second Attempt

As described in the first parameter estimation attempt, second attempt is computed where all valves are fully open. As the fully open valves result in flow increase in the system and a pressure drop at the end-user valves, it became necessary to increase the differential pressure over the pumps. The new input signals for the pumps is shown in 3.26.

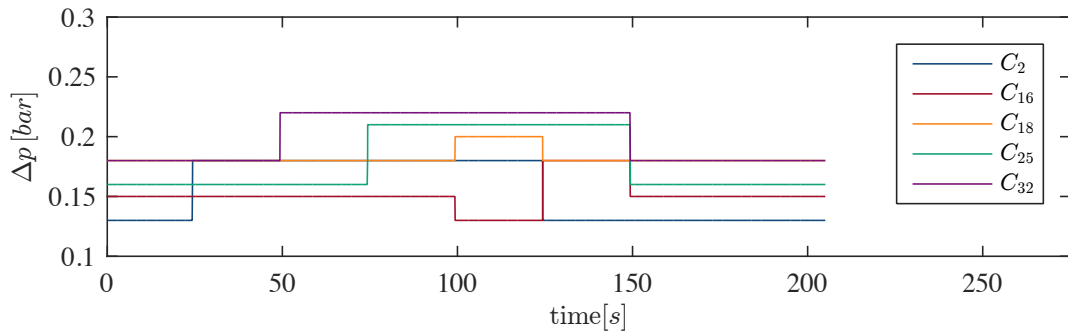


Figure 3.26: The pumps input signal which is used in the parameter estimation.

The second parameter estimation attempt is computed in the same way as the first attempt where it estimation data is divided into seven parts. The only real difference is the input signals applied to the valves and the pumps.

The resulting parameters obtained from the second attempt of the parameter estimation are listed table 3.8.

Parameters	$C_4(k_f)$	$C_8(k_f)$	$C_9(k_f)$	$C_{10}(k_f)$	$C_{11}(k_f)$	$C_{12}(k_f)$	$C_{13}(k_f)$	$C_{14}(k_f)$
Init. value	4.42	3.92	0.51	3.11	1.81	3.63	0.51	1.81
Est. value	6.6318	0.8662	0.5167	3.1507	9.3948	11.2659	2.2854	1.8353
Parameters	$C_{19}(k_f)$	$C_{21}(k_f)$	$C_{22}(k_f)$	$C_{23}(k_f)$	$C_{26}(k_f)$	$C_{28}(k_f)$	$C_{29}(k_f)$	$C_{30}(k_f)$
Init. Value	3.57	1.46	7.68	2.55	2.77	0.81	2.26	2.10
Est. Value	0.1528	1.4000	15.8396	5.9887	2.7552	0.7640	37.6350	41.7320
Parameters	$C_{33}(k_f)$	$C_{35}(k_f)$	$C_{36}(k_f)$	$C_{37}(k_f)$	$C_{39}(k_f)$	$C_{42}(k_f)$	$C_4(\Delta Z)$	$C_{14}(\Delta Z)$
Init. Value	2.27	3.07	2.26	3.27	2.27	2.77	-0.11	0.4
Est. Value	8.7924	2.9197	25.1453	28.4461	3.5472	2.8056	0.4350	0.6278

Table 3.8: The parameter estimation resulting parameters along with their initial values. The initial parameters are the same as introduced in table A.1 in appendix A.1.

The estimated parameters from the second attempt seem more realistic. However the Δz parameters seems to be estimated incorrectly and K_f values are still estimated to be above 30 which again seems unrealistic.

The fitting percentage for each of the model outputs, before and after estimation, is listed in table 3.9.

Measurement point	$C_{8,18}$	$C_{10,25}$	$C_{12,32}$	$C_{21,22}$	$C_{23,24}$
fit - Before	p_3	p_4	p_5	p_6	p_7
fit - After	-780%	-1074%	-557%	-2444%	-2955%
	-16%	28%	34%	2%	15%
Measurement point	$C_{28,29}$	$C_{30,31}$	$C_{35,36}$	$C_{37,38}$	
fit - Before	p_8	p_9	p_{10}	p_{11}	
fit - After	-1717%	-1978%	-1506%	-1578%	
	32%	23%	61%	34%	

Table 3.9: The fitting percentage, **fit**, before and after the parameter estimation.

Note, the notation $C_{x,y}$ means between component x and y

Even though that the **fit** improves dramatically by using the estimated parameters, one is concerned about how poor the **fit** is for the original parameters. To gain a better understanding on how the model performances with the new estimated parameters, plots are made which show the test system and the model outputs. Figure 3.27 shows the pressures at the pumps inlet.

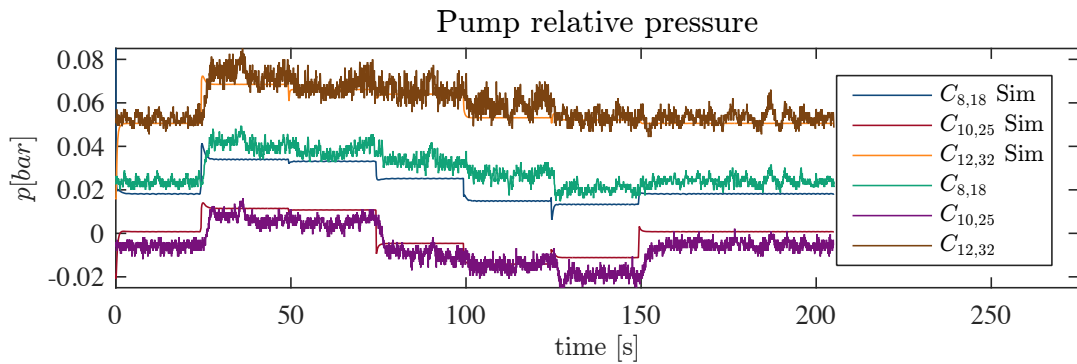


Figure 3.27: Estimation data results showing the actual and simulated relative pressure at the pumps inlet.

Figure 3.28, 3.29, and 3.30 show the pressures at or close to the end-user valves.

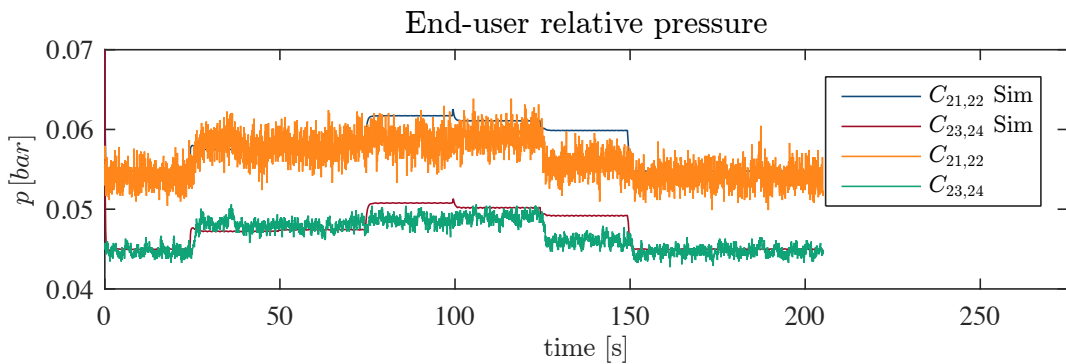


Figure 3.28: Estimation data results showing the actual and simulated relative pressure close to the end-user valves.

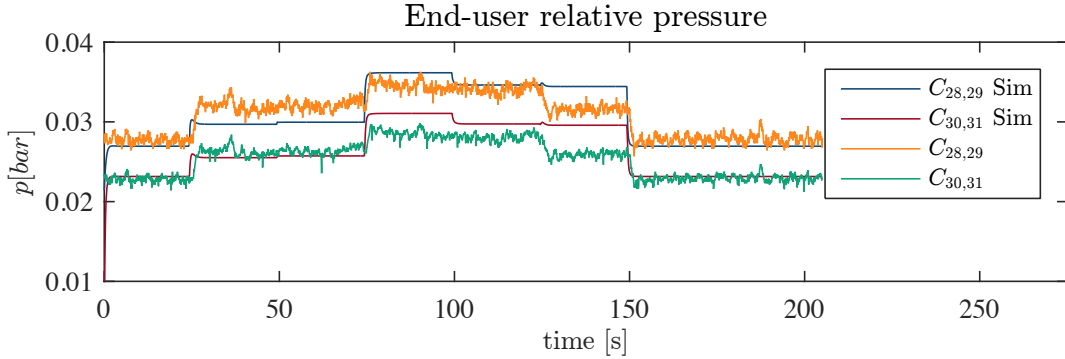


Figure 3.29: Estimation data results showing the actual and simulated relative pressure close to the end-user valves.

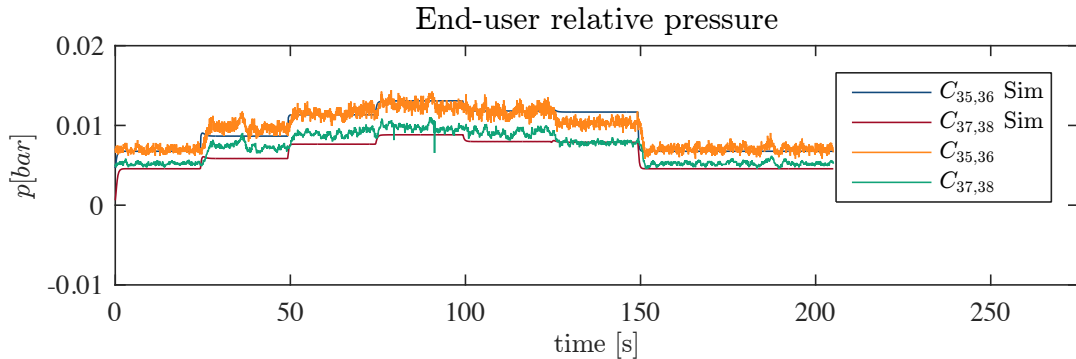


Figure 3.30: Estimation data results showing the actual and simulated relative pressure close to the end-user valves.

From figure 3.27, 3.28, 3.29, and 3.30, one can see that the model outputs and the real test system measurements have a close fit. It also seems that the correct parameters are found where the valve model is needs to bee tuned. Hoverer, late in the project period, it was discovered that some of the pump differential pressure sensors in the Water Wall test system where incorrectly implemented. Consequently, the input signal for the pumps C_{18} , C_{25} and C_{32} was never equal to the real differential pressure over those pumps.

This finding does also explain why the original parameters resulted in such a poor **fit** in table 3.7 and 3.9 . The consequence of this finding and what parameters are used in the rest of the project are discussed in the following section.

The Applied Parameters

As discussed before, the differential pressure sensors for the pumps C_{18} , C_{25} and C_{32} where incorrectly implemented. Figure 3.31 shows how the controller is impeditments into Simulink and how the DAQ is connected to one of the pumps.

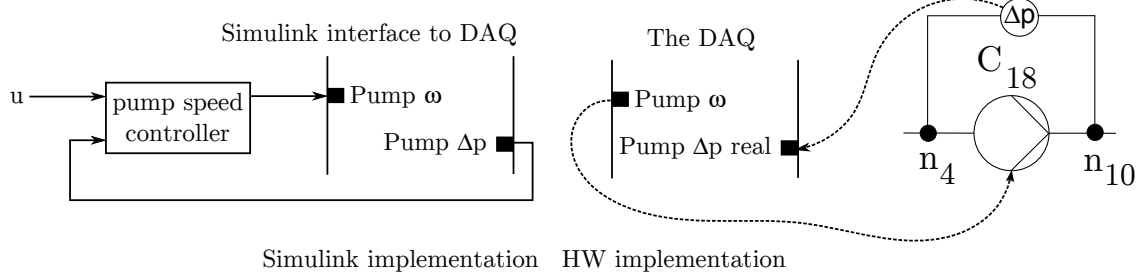


Figure 3.31: Illustration of the pump speed controller implementation in Simulink which communicates with the Water Wall test system via DAQ (Data Acquisition) boards.

The consequence is that the true pressure over the pump is not equal to the pump Δp which is feed back to the controller in Simulink. This means that through the parameter estimation process, the real pumps and the model pumps have received the same u signal, however, they did not deliver the same differential pressure. Due to time constraints it is not possible to redo the parameter estimation, to obtain parameters using the correctly implemented pressure sensors. Instead the initial pipe parameters are applied which where found by means of studying the physical system as discussed in 3.4.3.

Additionally, the implementation of the sensor is corrected and the design of the pump speed controller was revisited to ensure that it is still performing as it did when it was designed.

In order to analyze the performance of the initial parameters, new measurements are made from the test system by using the same input data as used in the parameter estimation first attempt. That is, the input data which actuates both the pumps and valves that are shown in figure 3.13 and 3.12.

First, the **fit** for initial parameters is computed and shown in table 3.10.

Measurement point	$C_{8,18}$	$C_{10,25}$	$C_{12,32}$	$C_{21,22}$	$C_{23,24}$
fit	p_3	p_4	p_5	p_6	p_7
	-282%	-252%	-261%	-298%	-191%
Measurement point	$C_{28,29}$	$C_{30,31}$	$C_{35,36}$	$C_{37,38}$	
fit	p_8	p_9	p_{10}	p_{11}	
	-225%	-282%	-243%	-251%	

Table 3.10: The fitting percentage **fit** where the initial model parameters are applied. Note, the notation $C_{x,y}$ means between component x and y

From table 3.10, one can see that in total the **fit** percentage has improved from the "fit-Before" presented in table 3.7. This indicates that the calculated initial parameters are not far from the real parameters.

To gain a better understanding on how the model performances with the initial parameters and where sensors are implement correctly, plots are made which show the test system and the model outputs. Figure 3.32 shows the pressures at the pumps inlet.

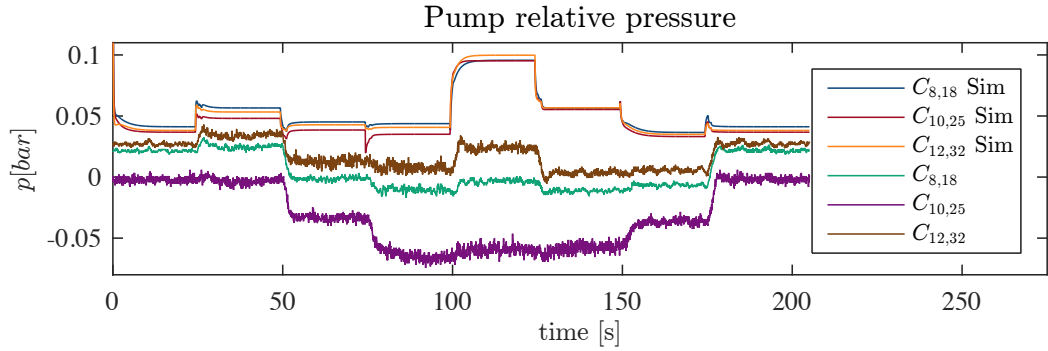


Figure 3.32: Estimation data results showing the actual and simulated relative pressure at the pumps inlet.

Figure 3.33, 3.34, and 3.35 show the pressures at or close to the end-user valves.

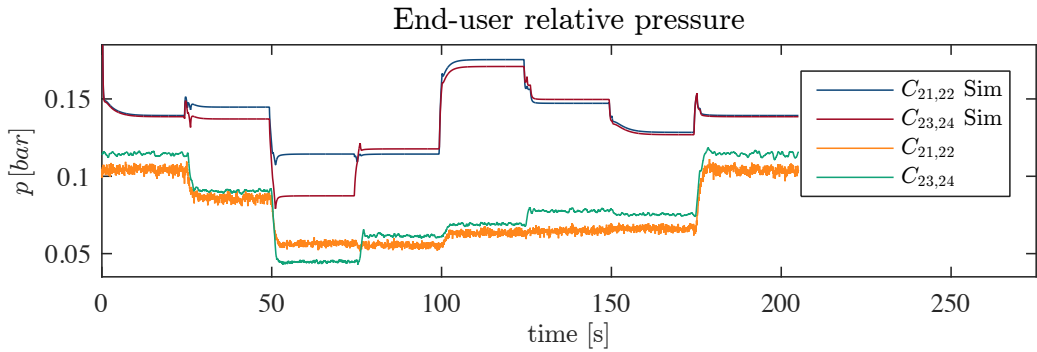


Figure 3.33: Estimation data results showing the actual and simulated relative pressure close to the end-user valves.

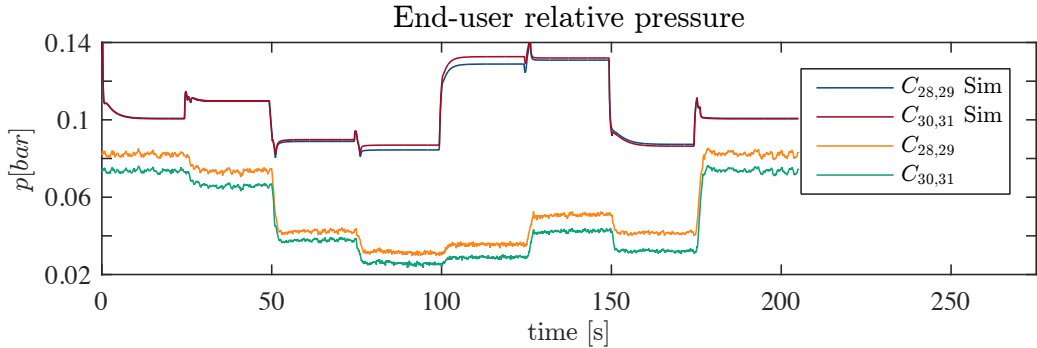


Figure 3.34: Estimation data results showing the actual and simulated relative pressure close to the end-user valves.

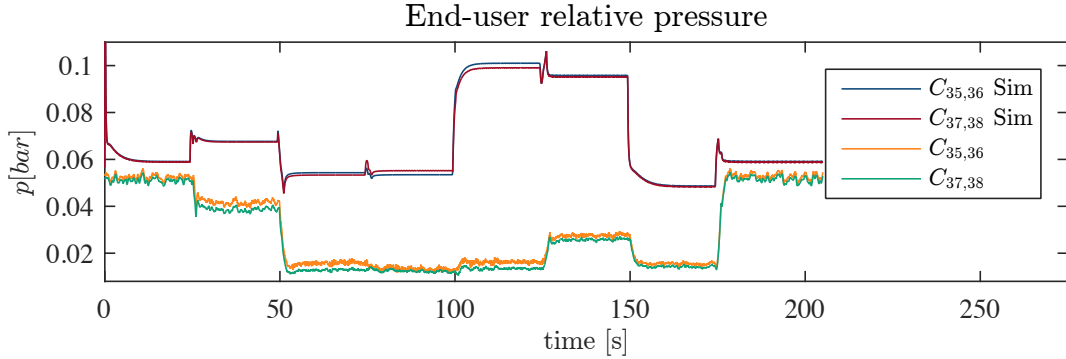


Figure 3.35: Estimation data results showing the actual and simulated relative pressure close to the end-user valves.

The plots in figure 3.32, 3.33, 3.34, and 3.35 show how well the model with the given parameters can represent the real test system. One can see that the model is not capable to truly mimic the real system which limits the usability of the model. Before any conclusion is given on the above results the model is verified by applying new data. In the following section, the model is not only verified against new data, it also contains a proper model conclusion where its correctness is discussed along with its limitations.

3.5 Model Verification

The last step in the modeling process is to verify it against new set of data as described in 3.4.3. This new data is referred to as the verification data. It is necessary to apply a new set of data to the model to reveal its correctness. The verification input data has to include different input sequences with different amplitudes, where it is expected to see similar output matching results as achieved in the estimation process. Even though the validation data is no longer used to evaluate the parameter estimation process, it is still important to test the model with a set of different input data to help evaluate the model correctness.

The verification signal for the valves is shown in figure 3.36.

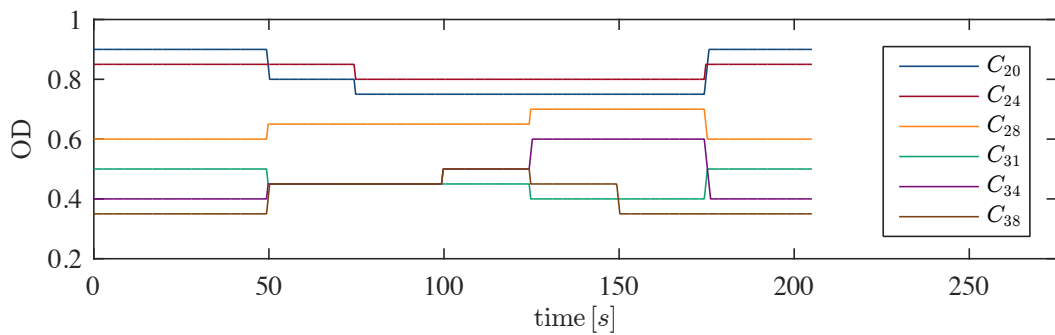


Figure 3.36: The valve input signal which is applied in the parameter estimation.

And the estimation signals for the pumps is shown in figure 3.37.

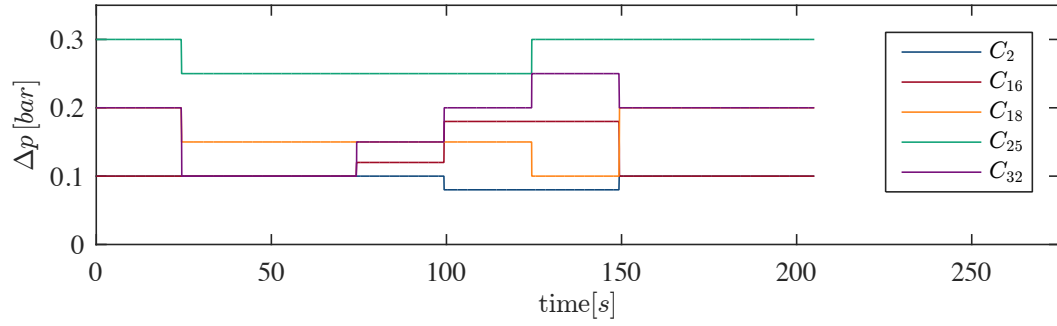


Figure 3.37: The pumps input signal which is applied in the parameter estimation.

Finally, the model outputs are verified against the test system measurements, note that the sensors are implemented correctly at this point. Figure 3.38 shows the pressures at the pump inlets where one can see the $C_{10,25}$ sensor is partly in saturation. Even so, this is not of concern since this data is not used to estimate parameters.

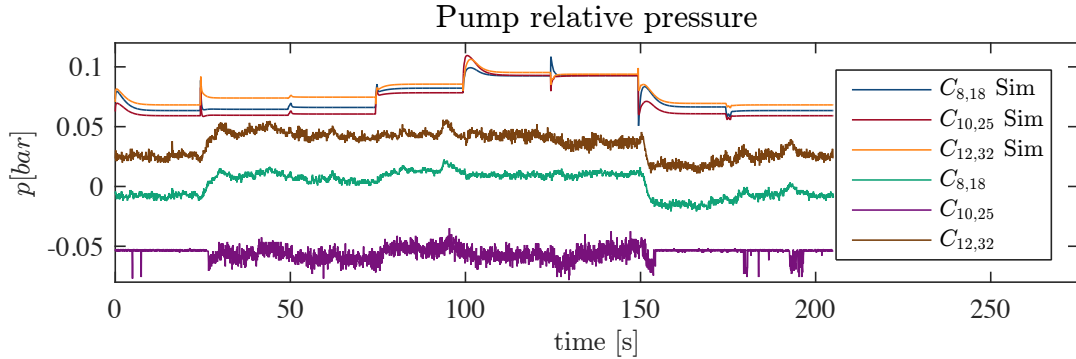


Figure 3.38: Estimation data results showing the actual and simulated relative pressure at the pumps inlet.

Figure 3.39, 3.40, and 3.41 show the pressures at or close to the end-user valves.

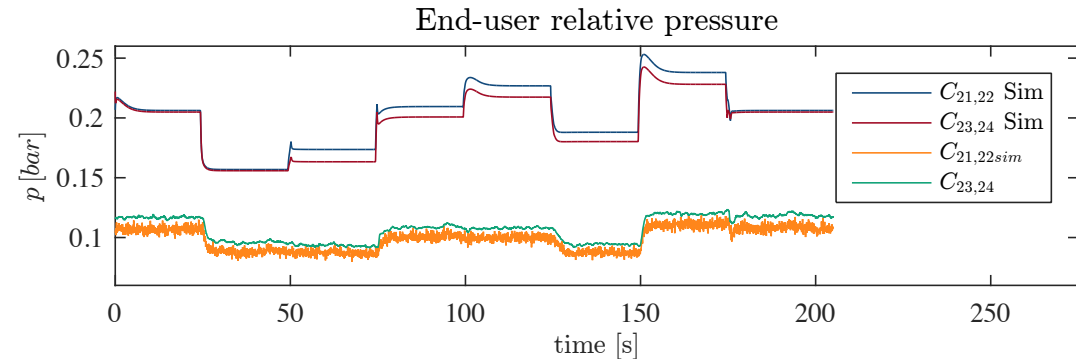


Figure 3.39: Estimation data results showing the actual and simulated relative pressure close to the end-user valves.

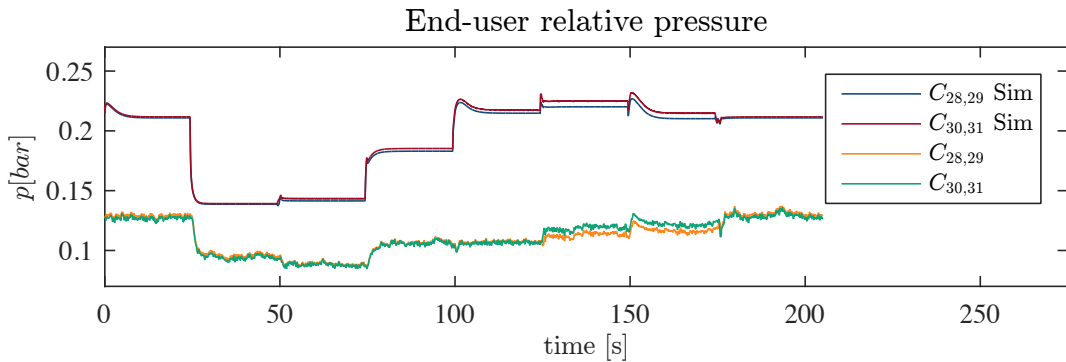


Figure 3.40: Estimation data results showing the actual and simulated relative pressure close to the end-user valves.

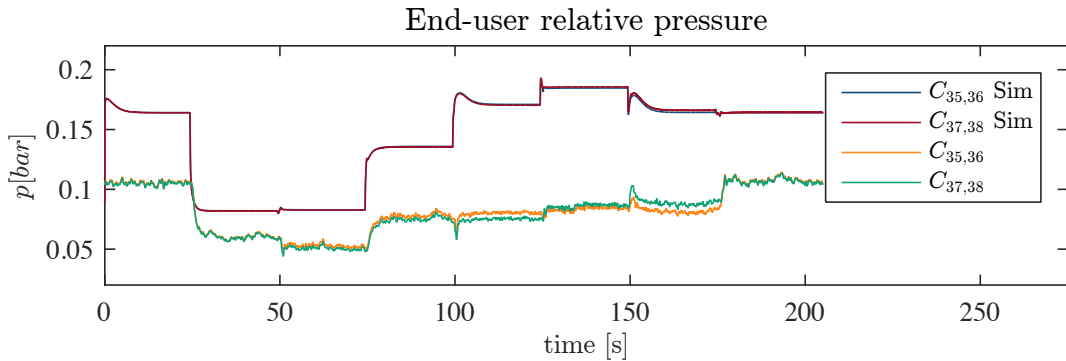


Figure 3.41: Estimation data results showing the actual and simulated relative pressure close to the end-user valves.

The plots in figure 3.36, 3.39, 3.40, and 3.41 show the final model verification and the conclusions which can be made from it and the parameter estimation section results are listed below:

- The model which is a combination of the component models and graph theory is an suitable modelling platform for this type of water distribution network.
- The parameter estimation process is consider to work correctly. The problem accounted where a incorrect sensor implementation and probably a model error in the valve model. It is however not been analysed any further.
- It is clear that relatively small modelling errors and errors in hardware implementation can have a big negative impact when one tries to estimate the over all model.
- The author believes that it is possible to obtain almost correct parameters by first correcting the pipe parameters while the valves are fully open and then afterwards, correct the valve model.
- It is obvious that the model containing the initial parameters can not represent the Water Wall test system. However, the model can represent a system with is slightly different but with the same structure. This means that the model can be used as an simulation platform where control schemes can be designed before they are implemented onto the Water Wall.
- The model is not correct enough to be used in a model based control scheme and not in a fault detection scheme where one compares the system to the model to detect faults.

The model is hereby completed. The resulting model can be used as an simulation platform and a control development platform. The model represents a system which has the same structure and a similar size as the Water Wall test system.

Part II

Control Design

Chapter 4

Steady-state Power Minimization

In this chapter a control system, for a water distribution network of the form presented in part I, is introduced. The controller seek to minimize the steady state power consumption and maintain the desired pressure at the critical points (CP) in the distribution network.

First the control problem is formulated, then a control structure is presented and finally a power optimal controller is designed.

4.1 Control Problem

By introducing additional pumps at key positions in a water distribution network it is possible to reduce the collective energy consumption required for water distribution.

With the system being over actuated there is more freedom in the choice of control signal for the pumps in the network, hence the control problem relies in choosing the optimal control signal which minimizes the total power consumption, while still maintaining a minimum pressure at the end-users.

It is desired to reduce the total power consumption $P(\Delta\mathbf{p}, \mathbf{q})$ of the pumping effort, while still controlling the system output vector \mathbf{y} to a vector of reference values \mathbf{r} . The reference values are the desired pressures the CPs. The CP pressure in each PMA is also the measured output of the system, \mathbf{y} .

The control problem can be formulated as a minimization problem on the form

$$\begin{aligned} \min_{\mathbf{u}, \mathbf{q}} P(\Delta\mathbf{p}, \mathbf{q}) &= \min_{\mathbf{u}, \mathbf{q}} \sum_{i=1}^N P_i(\Delta p_i, q_i) \\ \text{s.t. } \mathcal{J}\dot{\mathbf{q}}_\ell &= -\mathbf{B}\lambda(\mathbf{B}^T \mathbf{q}_\ell) - \mathbf{B}\mu(\mathbf{B}^T \mathbf{q}_\ell, \mathbf{OD}) + \mathbf{B}\alpha(\mathbf{u}) - \mathbf{B}\zeta \\ \underline{\Delta p}_i &\leq \alpha(u_i) \leq \overline{\Delta p}_i \end{aligned} \quad (4.1)$$

Where N is the number of pumps in the system and $P_i(\Delta p_i, q_i)$ is the power consumption of the i^{th} pump in the distribution network, and $\underline{\Delta p}_i$ and $\overline{\Delta p}_i$ are the lower and upper bounds of the pumps operational range.

The solution to the minimization problem is the control signal vector \mathbf{u} which minimizes the power consumption without violating any of the conditions, which the minimization problem is subject to.

4.2 Pressure Control

First and foremost it is necessary to regulate the CP pressures to the reference values.

The water distribution network depicted in figure 3.2 has two supply pumps, which are connected to the main distribution line, another three pumps, here called local pumps, are each connected to a PMA.

It is observed that the pressure regulation can be performed solely by the local pumps, therefore a controller using only the local pumps are used for pressure regulation. However, the physical locations of the local pumping stations and the PMAs within the network are distributed over a large geographical area. Therefore it is desirable to make a distributed control system where the pump controller only relies on locally available information.

A local controller is proposed for each of the local pumps, regulating the pressure to the specified reference pressure at the CP in the PMA which the pump is directly connected to. The control architecture is shown in figure 4.1 for a single local control loop.

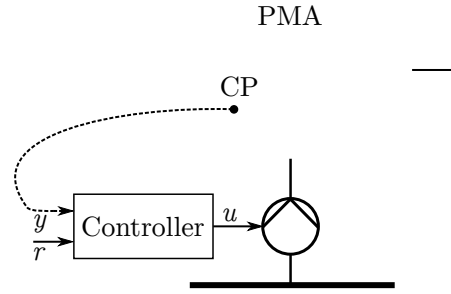


Figure 4.1: A small section of the water distribution network, where a local-loop local controller is used to control the CP pressure within a PMA.

As shown in figure 4.1, each controller only uses a pressure measurement of the CP in the PMA that it is directly connected to, hence it is not necessary to communicate pressure measurements between the local controllers.

The local controller is designed as a standard PI controller.

$$\begin{aligned}\dot{\xi} &= \mathbf{K}_i \mathbf{r} - \mathbf{y} \\ \mathbf{u}_L &= \xi + \mathbf{K}_p(\mathbf{r} - \mathbf{y})\end{aligned}\tag{4.2}$$

Where \mathbf{K}_i is the integral gain matrix and \mathbf{K}_p is the proportional gain matrix, both being diagonal. The control signal vector \mathbf{u} is divided into two separate vectors, one for the local pumps and one for the supply pumps.

$$\mathbf{u} = \mathbf{G}_L \mathbf{u}_L + \mathbf{G}_S \mathbf{u}_S\tag{4.3}$$

Where \mathbf{u}_L is the control vector for the local pumps and \mathbf{u}_S is the control vector for the supply pumps, with $\mathbf{u}_L \in \mathbb{R}^3$ and $\mathbf{u}_S \in \mathbb{R}^2$. \mathbf{G}_L and \mathbf{G}_S are matrices used to map \mathbf{u}_L and \mathbf{u}_S into the control vector $\mathbf{u} \in \mathbb{R}^{33}$, where non-pump entries are zero.

The PI-controller is included in the closed loop system by inserting control vectors in equation 4.21 into the system model equation 3.8.

$$\mathcal{J}\dot{\mathbf{q}}_\ell = -\mathbf{B}\lambda(\mathbf{B}^T \mathbf{q}_\ell) - \mathbf{B}\mu(\mathbf{B}^T \mathbf{q}_\ell, \mathbf{OD}) + \mathbf{B}(\mathbf{G}_L \mathbf{u}_L + \mathbf{G}_S \mathbf{u}_S) - \mathbf{B}\zeta \quad (4.4)$$

Noting that $\alpha(u) = u$, α is omitted.

With the PI-controller as an inner-loop controller in a cascaded control loop, as shown in figure 4.2, it is possible to indirectly control the differential pressure of the local pumps, by control of the supply pumps differential pressure.

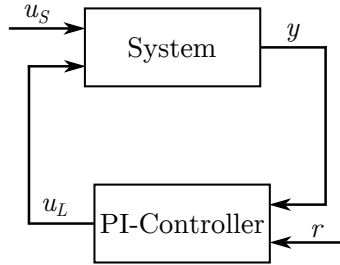


Figure 4.2: A diagram of the cascaded control loop, with an inner-loop PI-controller controlling the CP pressure.

The objective function can be written as $P(\Delta\mathbf{p}, \mathbf{q}) = \sum_{i=1}^N P_i(\Delta p_i, q_i) = \sum_{i=1}^K P_{L,i}(\Delta p_i, q_i) + \sum_{j=1}^M P_{S,j}(\Delta p_j, q_j)$, where K is the number of local pumps and M is the number of supply pumps, with $N = M + K$. The minimization is obtained by choosing the optimal control vector, \mathbf{u}_S , for the supply pumps, with $P_{L,i}$ being the power consumption of the i^{th} local pump and $P_{S,j}$ being the pumper consumption of the j^{th} supply pump.

The minimization problem is then reformulated to include the PI-controller.

$$\begin{aligned}
 \min_{\mathbf{u}_S} P(\Delta\mathbf{p}, \mathbf{q}) &= \min_{\mathbf{u}_S} \left(\sum_{i=1}^K P_{L,i}(\Delta p_i, q_i) + \sum_{j=1}^M P_{S,j}(\Delta p_j, q_j) \right) \\
 \text{s.t.} \quad \mathcal{J}\dot{\mathbf{q}}_\ell &= -\mathbf{B}\lambda(\mathbf{B}^T \mathbf{q}_\ell) - \mathbf{B}\mu(\mathbf{B}^T \mathbf{q}_\ell, \mathbf{OD}) + \mathbf{B}(\mathbf{G}_L \mathbf{u}_L + \mathbf{G}_S \mathbf{u}_S) - \mathbf{B}\zeta \\
 \mathbf{u}_L &= \boldsymbol{\xi} + \mathbf{K}_p(\mathbf{r} - \mathbf{y}) \\
 \dot{\boldsymbol{\xi}} &= \mathbf{K}_i(\mathbf{r} - \mathbf{y}) \\
 \underline{\Delta p_S} \leq u_S &\leq \overline{\Delta p_S} \\
 \underline{\Delta p_L} \leq u_L &\leq \overline{\Delta p_L}
 \end{aligned} \tag{4.5}$$

4.3 Steady-state Optimization Problem

The optimization problem is rewritten into a steady-state optimization problem. This is done in order to simplify the optimization, and because the daily variation in water consumption changes slowly and can be assumed piecewise constant.

The steady-state optimization problem is based on the closed-loop optimization problem in equation 4.5. Since the reference is assumed to be constant, then in steady state $\dot{\mathbf{q}} = 0$ and $\dot{\boldsymbol{\xi}} = 0$. The flow \mathbf{q} along with the integral action control signal $\boldsymbol{\xi}$ are denoted \mathbf{q}^* and $\boldsymbol{\xi}^*$ in steady-state.

$$\begin{aligned}
 \min_{\mathbf{u}_S} P(\Delta\mathbf{p}, \mathbf{q}) &= \min_{\mathbf{u}_S} \left(\sum_{i=1}^K P_{L,i}(\Delta p_i, q_i) + \sum_{j=1}^M P_{S,j}(\Delta p_j, q_j) \right) \\
 \text{s.t.} \quad 0 &= -\mathbf{B}\boldsymbol{\lambda}(\mathbf{B}^T \mathbf{q}_\ell^*) - \mathbf{B}\boldsymbol{\mu}(\mathbf{B}^T \mathbf{q}_\ell^*) + \mathbf{B}(\mathbf{G}_L \boldsymbol{\xi}^* + \mathbf{G}_S \mathbf{u}_S) - \mathbf{B}\boldsymbol{\zeta} \quad (4.6) \\
 \boldsymbol{\xi}^* &= \mathbf{u}_L \\
 \mathbf{r} &= \boldsymbol{\mu}(\mathbf{q}_{CP}^*) \\
 \underline{\Delta p_S} \leq u_S &\leq \overline{\Delta p_S} \\
 \underline{\Delta p_L} \leq u_F &\leq \overline{\Delta p_L}
 \end{aligned}$$

Where \mathbf{q}_{CP} is the end-user flow in the chord to the critical points, thus $\mathbf{y} = \mathbf{q}_{CP}$.

Solving the steady-state optimization problem is of course not optimal for the system during transients, but because the system approaches steady-state very fast, a solution to the steady-state optimization problem is viable solution for the majority of the time, as it is only a fraction of the time that the system is in transition between steady-states.

4.4 Convexity

It is an important factor in the ease of solving the optimization problem, that the problem is convex. If the problem is convex then any local minima is also the global minimum.

For the optimization problem to be convex, the objective function must be convex in the free variables and the optimization constraints must form a convex set.

4.4.1 Objective Function

The objective function represents the power consumption of the pumps in the distribution network. The approximation of the power consumption for a pumping station is given in equation 2.26 in section 2.1.3, it is restated here convenience.

$$\sum_{i=1}^N P_{e,i} = \Delta p_i q_i^* \frac{1}{\eta_i} \quad (4.7)$$

The free variables in the objective function are Δp and q^* . Calculating the derivatives of the objective function with respect to the two free variables shows that P_e is convex for $q^* \in \mathbb{R}^N$ and $\Delta p \in \mathbb{R}^N$, as the function is bilinear. A sum of convex functions is itself a convex function, thus the objective function is indeed convex in q^* and Δp .

4.4.2 Constraints

The first equality constraint of 4.6 is the steady-state equation of the closed loop system. If the functions $\boldsymbol{\lambda}(\mathbf{B}^T \mathbf{q}_\ell^*)$ and $\boldsymbol{\mu}(\mathbf{B}^T \mathbf{q}_\ell^*)$ are constant vectors in steady-state, then this constraint becomes affine in \mathbf{u}_S .

The functions $\boldsymbol{\lambda}(\mathbf{B}^T \mathbf{q}_\ell^*)$ and $\boldsymbol{\mu}(\mathbf{B}^T \mathbf{q}_\ell^*)$ are constant if the chord flows \mathbf{q}_ℓ^* are equal for all \mathbf{u}_S , thus the functions are independent of u_S .

The chord flow vector \mathbf{q}_ℓ can be divided into two vectors \mathbf{q}_{CP} and \mathbf{q}_u .

$$\mathbf{q}_{CP}, \mathbf{q}_u \in \mathbf{q}_\ell, \quad \mathbf{q}_{CP} = [c_{23}, c_{30}, c_{37}]^T, \quad \mathbf{q}_u = [c_9, c_{13}, c_{21}, c_{26}, c_{28}, c_{33}, c_{35}, c_{37}]^T \quad (4.8)$$

The flows \mathbf{q}_{CP}^* are the steady-state flows in the chords which are incident on the CP-nodes. Since the chord is in a series connection with an end-user valve, the flow of the chord is equal to the flow of the valve, which gives that, at steady-state when the CP pressure y_i is equal to the reference pressure r_i , and the flow through the end-user valve incident out of the CP-node is given by $q_{\mu,i}^* = \mu_i^{-1}(r_i)$, thus $q_{CP,i}^* = \mu_i^{-1}(r_i)$ at steady state.

A PI-controller is employed to regulate the CP pressure to the reference pressure using only the forward pumps. These pumps are assumed to be able to maintain $y_i = r_i$ regardless of the pumping effort of the supply pumps.

This concludes that the flow \mathbf{q}_{CP}^* is constant for all \mathbf{u}_S .

The flows of the remaining chords of \mathbf{q}_u^* are unknown as there is no direct relation from the critical point pressures to the flow of these chords.

In order to determine whether the flows \mathbf{q}_u^* are equal for all supply pump control signals \mathbf{u}_S a numerical analysis is performed of simulation results from the system model with the PI-controller regulating the pressure.

The numerical analysis in Appendix D shows that the chord flow vector \mathbf{q}_ℓ^* converges to the same constant value for $u_{S1} - u_{S2} = c$, where c is some appropriate constant $c \in \mathbb{R}^N$. Thus the numerical analysis concludes that under the constraint that $u_{S1} - u_{S2} = c$, \mathbf{q}_ℓ^* is equal and in turn also $\lambda(\mathbf{B}^T \mathbf{q}_\ell^*)$ and $\mu(\mathbf{B}^T \mathbf{q}_\ell^*)$ are constant vectors.

Furthermore it is necessary to also confirm that each row of the term $-\mathbf{B}(\lambda(\mathbf{B}^T \mathbf{q}_\ell^*) + \mu(\mathbf{B}^T \mathbf{q}_\ell^*) + \zeta)$ remains negative for all flows of \mathbf{q}_ℓ^* . Because of the non-linear nature of the pipe friction, the flow within each pipe may change drastically from small changes in pump differential pressure, even the flow direction may change.

Instead of analyzing $-\mathbf{B}(\lambda(\mathbf{B}^T \mathbf{q}_\ell^*) + \mu(\mathbf{B}^T \mathbf{q}_\ell^*) + \zeta)$ for all flows of $\mathbf{q}_\ell^* \in \mathbb{R}$, it is observed that each row in $-\mathbf{B}(\lambda(\mathbf{B}^T \mathbf{q}_\ell^*) + \mu(\mathbf{B}^T \mathbf{q}_\ell^*) + \zeta)$ is the pressure across a fundamental cycle of the system. For the pressure across the fundamental cycle to be a positive value, without the use of a pressure boosting pump, the water source must be at a higher elevation than the end-users.

In such cases, the proposed controller is not applicable, as valves are needed for pressure reduction. Therefor it is not analyzed further whether $-\mathbf{B}(\lambda(\mathbf{B}^T \mathbf{q}_\ell^*) + \mu(\mathbf{B}^T \mathbf{q}_\ell^*) + \zeta)$ remains negative for all flows of \mathbf{q}_ℓ^* .

The remaining equality constraints are all independent of \mathbf{u}_S , thus it can be concluded that the equality constraints form a convex set, when $u_{S1} - u_{S2} = c$ is imposed as an additional constraint on the optimization problem. With this in mind it can be concluded that all of the inequality constraints are affine, and therefore they also form a convex set.

To ensure that the optimization problem is feasible, the two convex sets, one from the equality constraints and one from the inequality constraints, must have a non-empty intersection. However this is not investigated here, as the water distribution system is designed by default to have a non-empty intersection.

If the two convex sets were to have an empty intersection it would be the cause of wrongly designed water distribution network, with for example poorly dimensioned pumps, which would be unable to deliver the required pressure boost, or in cases where the water reservoir is located at a higher elevation than the consumers, and pressure reduction valves should be used instead of pumps.

4.5 Power Optimization

The power optimization functions as an outer-loop controller as previously shown in figure 4.2. The optimization algorithm adjusts the control signal \mathbf{u}_S to the supply pumps, with the objective to minimize the power consumption of the pumping effort of the water distribution network. When the difference pressure of the supply pumps are changed, the local pumps have to follow

suit accordingly, by either reducing or increasing their differential pressures. In this way the local pumps power consumption is indirectly controlled by controlling the supply pumps power consumption.

In this section the optimization method will be explained and the optimization problem will be transformed from a constrained optimization problem to an unconstrained problem, by use of penalty functions.

4.5.1 Gradient Descent

The method chosen to minimize the power consumption is a gradient descent method, similar to the optimization in [Kallesøe 14b].

The gradient descent method takes advantage of the fact that a differentiable function $f(x)$ decreases towards its minimum fastest in the opposite direction its gradient, $-\nabla f(x)$. The gradient descent method approaches the minimum by taking a step in the opposite direction of the gradient at each iteration, as shown in equation 4.9. The gradient descent method will continue to go towards the point where $\nabla f(x) = 0$, which if the function is convex is the global minimum [Antoniou 07].

$$x_{k+1} = x_k - \gamma \nabla f(x_k) \quad (4.9)$$

where x_k is the current iteration of the minimizer function within the search-space and x_{k+1} is the next iteration. γ is a gain factor, with $\gamma > 0$, which controls the length of the step taken in the direction of $-\nabla f(x_k)$. The algorithm is visualized in figure 4.3, where a gradient descent is used to find the minimum at x^* . The gradient descent algorithm here has a constant gain, γ , resulting in only the value of the gradient impacts the step size.

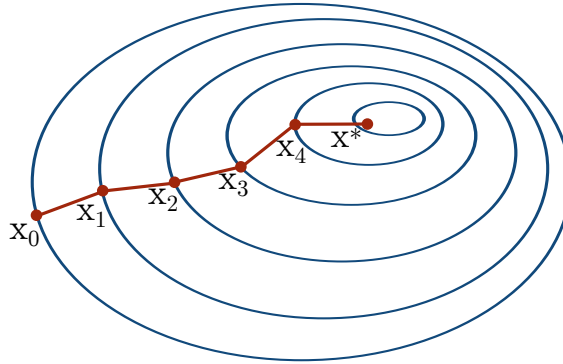


Figure 4.3: Gradient descent minimization with a constant gain γ .

The step size gain, γ , can also be included as a variable, γ_k . This can help with faster convergence of the optimization, by using a large step size when it is far away from the optimum, γ_k is then decreased as the optimization converges towards the minimum in order to avoid overshooting the true optimum.

4.5.2 Soft Constraints

It is not possible to directly include the constrained optimization problem in the gradient descent algorithm. One method for using gradient based optimization on a constrained problem, is by softening the constraints to form an unconstrained problem.

Penalty functions are used to transform the constrained optimization problem

$$\min_{x \in C} f(x) \quad (4.10)$$

into an unconstrained optimization problem

$$\min_{x \in \mathbb{R}^N} \tilde{f}(x) \quad (4.11)$$

By using penalty functions to transform $f(x)$ into $\tilde{f}(x)$, the optimizations problem is expanded from the region, C , which is the intersection of the feasible sets created by the constraints, to all of \mathbb{R}^N . The penalty functions are then created such that $\tilde{f}(x)$ is continuous, differentiable and convex on all of \mathbb{R}^N , thus methods such as gradient descent can be used to solve the optimization problem [Smith 97].

An example of this transformation is shown in figure 4.4, where a constrained problem is transformed into an unconstrained problem.

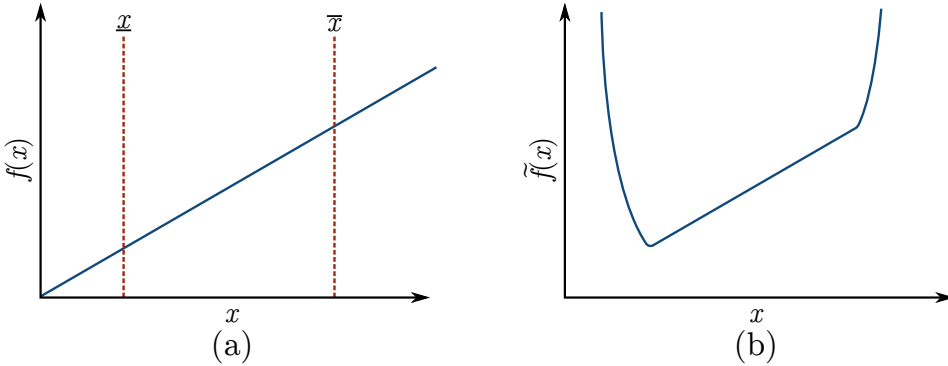


Figure 4.4: (a) Constrained optimization problem, where \underline{x} and \bar{x} form the constraints, the feasibility region C is the interval between the two constraints. (b) Unconstrained optimization problem, where the hard constraints shown in (a) has been included in the objective function by use of penalty functions, thus making the feasibility region all of \mathbb{R}^N .

As shown in figure 4.4, the penalty function will encourage the optimization algorithm to stay within the constraints, without enforcing the optimization algorithm to stay within the feasibility region C as it is done with hard constraints. Also $f(x)$ is identical to $\tilde{f}(x)$ when the optimization variable is within the bounds $\underline{x} \leq x \leq \bar{x}$, but the penalty function included in $\tilde{f}(x)$ makes the cost increase very rapidly when x is outside the allowable region.

However, using penalty functions can change the optimum of the function, such that the optimum of the newly defined function is not necessarily the optimum of the original function. This problem can be observed in figure 4.4, where the minimum of the original function is the intersection of $f(x)$ and \underline{x} , for the newly defined function $\tilde{f}(x)$ the minimum further out the x-axis, as the penalty function makes the cost increase slightly before crossing \underline{x} . Thus it is necessary to be careful when designing penalty functions, as not to alter the minimum too far from the original function.

4.5.3 Unconstrained Optimization Problem

The steady-state constrained optimization problem is given in equation 4.6 which is restated here for convenience.

$$\begin{aligned}
 \min_{\mathbf{u}_S} P(\Delta \mathbf{p}, \mathbf{q}) &= \min_{\mathbf{u}_S} \left(\sum_{i=1}^K P_{L,i}(\Delta p_i, q_i) + \sum_{j=1}^M P_{S,j}(\Delta p_j, q_j) \right) \\
 \text{s.t.} \quad 0 &= -\mathbf{B}\boldsymbol{\lambda}(\mathbf{B}^T \mathbf{q}_\ell^*) - \mathbf{B}\boldsymbol{\mu}(\mathbf{B}^T \mathbf{q}_\ell^*) + \mathbf{B}(\mathbf{G}_L \boldsymbol{\xi}^* + \mathbf{G}_S \mathbf{u}_S) - \mathbf{B}\boldsymbol{\zeta} \\
 \boldsymbol{\xi}^* &= \mathbf{u}_L \\
 \mathbf{r} &= \boldsymbol{\mu}(\mathbf{q}_{CP}^*) \\
 \underline{\Delta p_S} \leq u_S &\leq \overline{\Delta p_S} \\
 \underline{\Delta p_L} \leq u_L &\leq \overline{\Delta p_L} \\
 u_{S1} - u_{S2} &= c
 \end{aligned} \tag{4.12}$$

To obtain the unconstrained optimization problem denoted $\min_{\mathbf{u}_S} (\tilde{P})$, the inequality constraint $\underline{\Delta p_{S,L}} \leq u_{S,L} \leq \overline{\Delta p_{S,L}}$, must be included in the objective function, which can be done using penalty functions.

Recognizing that the constraints that the pumps are subject to can be formulated as constraints on the control signal, the constraints are reformulated as

$$\begin{aligned}
 \underline{u}_L \leq u_L &\leq \overline{u}_L \\
 \underline{u}_S \leq u_S &\leq \overline{u}_S
 \end{aligned} \tag{4.13}$$

A penalty function for the inequality constraint for the control signals is constructed as proposed by [Fletcher 75].

$$S_{i,j}(u) = \begin{cases} \kappa(\underline{u} - u)^2 & , \quad u \leq \underline{u} \\ 0 & , \quad \underline{u} \leq u \leq \overline{u} \\ \kappa(u - \overline{u})^2 & , \quad u \geq \overline{u} \end{cases} \tag{4.14}$$

Where κ is a constant, $\kappa > 0$, which controls how rapidly the penalty cost grows when u is crossing its boundaries, with \overline{u} being the maximum value for u and \underline{u} being the minimum value. The subscript i of S is $i = L, S$, which denotes the penalty functions S for either the supply pumps ($S_{S,j}$) or the local pumps ($S_{L,j}$), with j denoting the j^{th} pump of the respective set. The choice of κ value influences how fast the cost rises, this is shown in figure 4.5 for a quadratic penalty function.

The equality constraint $u_{S1} - u_{S2} = c$ is handled by only using either u_{S1} or u_{S2} as the optimization variable, with the constraint as $u_{S1} = u_{S2} + c$ for u_{S2} as the optimization variable.

The unconstrained optimization problem is then given by including the penalty functions into the objective function.

$$\begin{aligned}
 \min_{u_{S2}} \tilde{P}(\Delta \mathbf{p}, \mathbf{q}) &= \min_{\mathbf{u}_S} \left(\sum_{i=1}^K (P_{L,i}(u_{L,i}) + S_{L,i}(u_{L,i})) + \sum_{j=1}^M (P_{S,j}(u_{S,j}) + S_{S,j}(u_{S,j})) \right) \\
 \text{s.t.} \quad 0 &= -\mathbf{B}\boldsymbol{\lambda}(\mathbf{B}^T \mathbf{q}_\ell^*) - \mathbf{B}\boldsymbol{\mu}(\mathbf{B}^T \mathbf{q}_\ell^*) + \mathbf{B}(\mathbf{G}_L \boldsymbol{\xi}^* + \mathbf{G}_S \mathbf{u}_S) - \mathbf{B}\boldsymbol{\zeta} \\
 \boldsymbol{\xi}^* &= \mathbf{u}_L \\
 \mathbf{r} &= \boldsymbol{\mu}(\mathbf{q}_{CP}^*) \\
 u_{S1} &= u_{S2} + c
 \end{aligned} \tag{4.15}$$

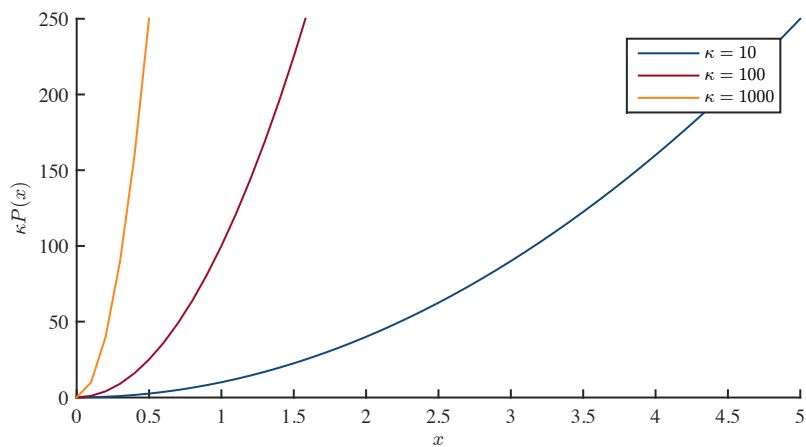


Figure 4.5: A quadratic penalty function with three different κ values, with $\kappa = 10$, $\kappa = 100$, $\kappa = 1000$.

The unconstrained optimization problem is then minimized using gradient descent.

4.6 Power Optimization Controller

In this section the derivation of an optimization algorithm which reduces the combined power consumption of all the pumps will be described. The optimization algorithm makes use of the gradient descent method presented in section 4.5.1, to search for a solution to the unconstrained optimization problem in equation 4.15.

The optimization algorithm uses gradient descent to search for the optimal distribution of pressures delivered by the local pumps and supply pumps. Where the optimal distribution of pressure boosts is the one with the least combined power consumption. It is necessary to run the optimization on-line, as the water flow is varying throughout the day, thus the optimal distribution of pressures between the pumps may also change with varying flow.

The gradient descent uses the gradient of the objective function to calculate the control signal for the supply pumps

$$\mathbf{u}_{S,k+1} = \mathbf{u}_{S,k} - \gamma \left(\frac{d \tilde{P}(\mathbf{u}_{S,k}, \mathbf{u}_{L,k})}{d \mathbf{u}_{S,k}} \right) \quad (4.16)$$

The derivative of the objective function with respect to the control signal is given in equation 4.17.

$$\frac{d \tilde{P}(\mathbf{u}_S, \mathbf{u}_L)}{d \mathbf{u}_S} = \sum_{i=1}^K \left(\frac{d P_{L,i}(u_{L,i})}{d \mathbf{u}_S} + \frac{d S_{L,i}(u_{L,i})}{d \mathbf{u}_S} \right) + \sum_{j=1}^M \left(\frac{d P_{S,j}(u_{S,j})}{d \mathbf{u}_S} + \frac{d S_{S,j}(u_{S,j})}{d \mathbf{u}_S} \right) \quad (4.17)$$

Where the control signal for the local pumps, \mathbf{u}_L , is given by rearranging the steady-state equation for the model.

$$\mathbf{B}\mathbf{G}_L\mathbf{u}_L = \mathbf{B}(\boldsymbol{\lambda}(\mathbf{B}^T \mathbf{q}_\ell^*) + \boldsymbol{\mu}(\mathbf{B}^T \mathbf{q}_\ell^*) + \boldsymbol{\zeta}) - \mathbf{B}\mathbf{G}_S\mathbf{u}_S \quad (4.18)$$

$$\mathbf{u}_L = (\mathbf{B}\mathbf{G}_L)^\dagger(\mathbf{B}(\boldsymbol{\lambda}(\mathbf{B}^T \mathbf{q}_\ell^*) + \boldsymbol{\mu}(\mathbf{B}^T \mathbf{q}_\ell^*) + \boldsymbol{\zeta}) - \mathbf{B}\mathbf{G}_S\mathbf{u}_S) \quad (4.19)$$

From equation 4.16 and 4.17 it is seen that the gradient is calculated based on the power consumption and penalty of both the supply pumps and the local pumps. This dictates that some form of communication between the pumps is necessary.

The pressure controllers previously designed in section 4.2, are designed to operate individually without any communication between each of the local pumps. Similarly it is also desired to keep the communication between the supply pumps and local pumps at a minimum. The desire is therefore to design a power optimization controller with minimum communication between the pumps in the water distribution system.

First the supply pumps communication structure is investigated. The derivative of the supply pumps is given by

$$\frac{d \tilde{P}_{S,j}(u_{S,j})}{d \mathbf{u}_S} = \frac{d P_{S,j}(u_{S,j})}{d \mathbf{u}_S} + \frac{d S_{S,j}(u_{S,j})}{d \mathbf{u}_S} \quad (4.20)$$

Equation 4.20 describes the change of power consumption and penalty for the j^{th} supply pump with respect to the pressures delivered by the supply pumps.

Note that the pressure delivered by the supply pumps are given by

$$\mathbf{u}_S = \begin{bmatrix} u_{S1} \\ u_{S2} \end{bmatrix} = \begin{bmatrix} 1 \\ 1 \end{bmatrix} u_{S2} + \begin{bmatrix} c \\ 0 \end{bmatrix} \quad (4.21)$$

where c is some constant that can be adjusted to give a constant off-set between the supply pumps.

Recalling the assumption that the local pumps alone are able to maintain the output pressure, such that $y_i = r_i$ regardless of the water consumption of the end users, the supply pump pressures \mathbf{u}_S can be chosen freely.

The derivative for each of the supply pumps only depends on locally available information, thus it is possible to calculate the derivative locally. Because $u_{S1} = u_{S2} + c$ the derivative $d\tilde{P}_{S,1}(u_{S,1})/d\mathbf{u}_S = d\tilde{P}_{S,2}(u_{S,2})/d\mathbf{u}_S$, hence it is only necessary to calculate the derivative of u_{S1} or u_{S2} , which can be done at either one of the supply pumps.

The supply pump which then calculates the derivative and updates the control signal, must send the new control signal to the other supply pump. Thus communication between the supply pumps can not be avoided, but it is limited to one-way communication.

Secondly the communication structure of the local pumps regarding the power optimization is investigated. The derivative for the local pumps with respect to the control signal is given by

$$\frac{d\tilde{P}_L(\mathbf{u}_L)}{d\mathbf{u}_S} = \sum_{i=1}^K \left(\frac{dP_{L,i}(u_{L,i})}{d\mathbf{u}_S} + \frac{dS_{L,i}(u_{L,i})}{d\mathbf{u}_S} \right) \quad (4.22)$$

Equation 4.22 describes the change of power consumption and penalty for the i^{th} local pump with respect to the pressures delivered by the supply pumps.

The local pumps can be controlled indirectly using the supply pumps, as shown in figure 4.2, which is also described by equation 4.19. Because the steady-state flow \mathbf{q}_ℓ^* is equal for all \mathbf{u}_S fulfilling $u_{S2} = u_{S1} - c$, a relation from the change in supply pressure the local pump pressure can be found as

$$\frac{d\mathbf{u}_L}{d u_{S2}} = \frac{d\mathbf{u}_L}{d\mathbf{u}_S} \cdot \frac{d\mathbf{u}_S}{d u_{S2}} = -(\mathbf{B}\mathbf{G}_L)^\dagger \mathbf{B}\mathbf{G}_S \cdot \begin{bmatrix} 1 \\ 1 \end{bmatrix} = -\mathbf{R} \quad (4.23)$$

The relation \mathbf{R} describes how the pressure is related between the supply pumps and the local pumps. Using the relation in equation 4.23 the derivative of the objective function for the local pumps can be rewritten to only include locally available information.

$$\frac{d\tilde{P}_{L,i}(u_{L,i})}{d u_{S2}} = \frac{d\tilde{P}_{L,i}(u_{L,i})}{d u_{L,i}} \cdot \frac{d u_{L,i}}{d u_{S2}} = -\frac{d\tilde{P}_{L,i}(u_{L,i})}{d u_{L,i}} \mathbf{R}_i \quad (4.24)$$

Where $\tilde{P}_{L,i}$ is the objective function for the i^{th} local pump and \mathbf{R}_i is the i^{th} row of \mathbf{R} . The relation \mathbf{R} is also used for designing the communication structure which is described in section 4.6.1.

With the gradient of the local pumps being calculated locally, only one-way communication is needed, from the local pumps to the supply pumps.

Finally the gradient of the control signal u_{S2} can be computed using the following equation.

$$\frac{d\tilde{P}(\mathbf{u}_S, \mathbf{u}_L)}{d u_{S2}} = \left(\sum_{j=1}^M \left(\frac{dP_{S,j}(u_{S,j})}{d u_{S2}} + \frac{dS_{S,j}(u_{S,j})}{d u_{S2}} \right) - \sum_{i=1}^K \left(\frac{dP_{L,i}(u_{L,i})}{d u_{L,i}} + \frac{dS_{L,i}(u_{L,i})}{d u_{L,i}} \right) \mathbf{R}_i \right) \quad (4.25)$$

Using equation 4.25 in equation 4.16, the change of the control signal is obtained.

$$\mathbf{u}_{S2,k+1} = \mathbf{u}_{S2,k} - \gamma \left(\frac{d \tilde{P}(\mathbf{u}_{S,k}, \mathbf{u}_{L,k})}{d \mathbf{u}_{S2,k}} \right) \quad (4.26)$$

The penalty functions for the local and supply pumps are constructed as done in equation 4.14, where the derivatives with respect to u_{S2} becomes

$$\frac{d S_{i,j}(u)}{d u} = \begin{cases} 2\kappa(\underline{u} - u) & , \quad u \leq \underline{u} \\ 0 & , \quad \underline{u} \leq u \leq \bar{u} \\ 2\kappa(u - \bar{u}) & , \quad u \geq \bar{u} \end{cases} \quad (4.27)$$

Because the control signals $u_{S1} = u_{S2} + c$ with $c \in \mathbb{R}$, the penalty functions for the supply pumps needs to be changed to include the off-set, c , between the pumps. Furthermore the penalty function must penalize u_{S2} if $u_{S1} - c$ is outside the boundaries, as well as if u_{S2} is outside the boundaries.

$$\frac{d S_{S,j}(u_{S,j})}{d u_{S2}} = \begin{cases} 2\kappa(\underline{u} - \min\{(u_{S2} + c), (u_{S2})\}) & , \quad \min\{(u_{S2} + c), (u_{S2})\} \leq \underline{u} \\ 0 & , \quad \underline{u} \leq (u_{S2}), (u_{S2} - c) \leq \bar{u} \\ 2\kappa(\max\{(u_{S2} + c), (u_{S2})\} - \bar{u}) & , \quad \max\{(u_{S2} + c), (u_{S2})\} \geq \bar{u} \end{cases} \quad (4.28)$$

In this way the penalty functions penalizes the optimization when the inner most boundaries have been crossed.

4.6.1 Controller Communication Structure

The power optimal controller requires information about the local pumps in order to minimize the power consumption of the water distribution network.

It is found in equation 4.24, that it is only necessary to calculate the derivatives of the local pumps power consumption with respect to its own control signal $u_{L,i}$. Which can be done locally at each local pump.

The derivatives are then transmitted to one of the supply pumps, which by multiplying the local pumps derivatives by \mathbf{R} , obtains the derivatives of the local pumps power consumption with respect to the supply pumps control signals \mathbf{u}_S . It is then possible to calculate the derivative of the combined power consumption with respect to the control signal of the supply pumps, as shown in equation 4.25.

This results in a communication structure as shown in figure 4.6, where the local pumps transmit their derivatives to the Power Minimizer, which then calculates the control signal for the supply pumps.

The relation matrix \mathbf{R} , decides which supply pumps each local pump must transmit its own derivative to. \mathbf{R} also contains the gain coefficients applied to each of derivatives to the supply pumps.

Thus the design of the power optimal controller only requires the knowledge of \mathbf{R} , which is given by

$$-(\mathbf{B}\mathbf{G}_L)^\dagger \mathbf{B}\mathbf{G}_S \frac{d \mathbf{u}_S}{d u_{S2}} = -\mathbf{R} \quad (4.29)$$

Equation 4.29 only depends on the graph topology for the system, \mathbf{B} , and the location of the pumps within the graph \mathbf{G}_S and \mathbf{G}_L . Hence the parameters of the pipes, pumps or valves are not

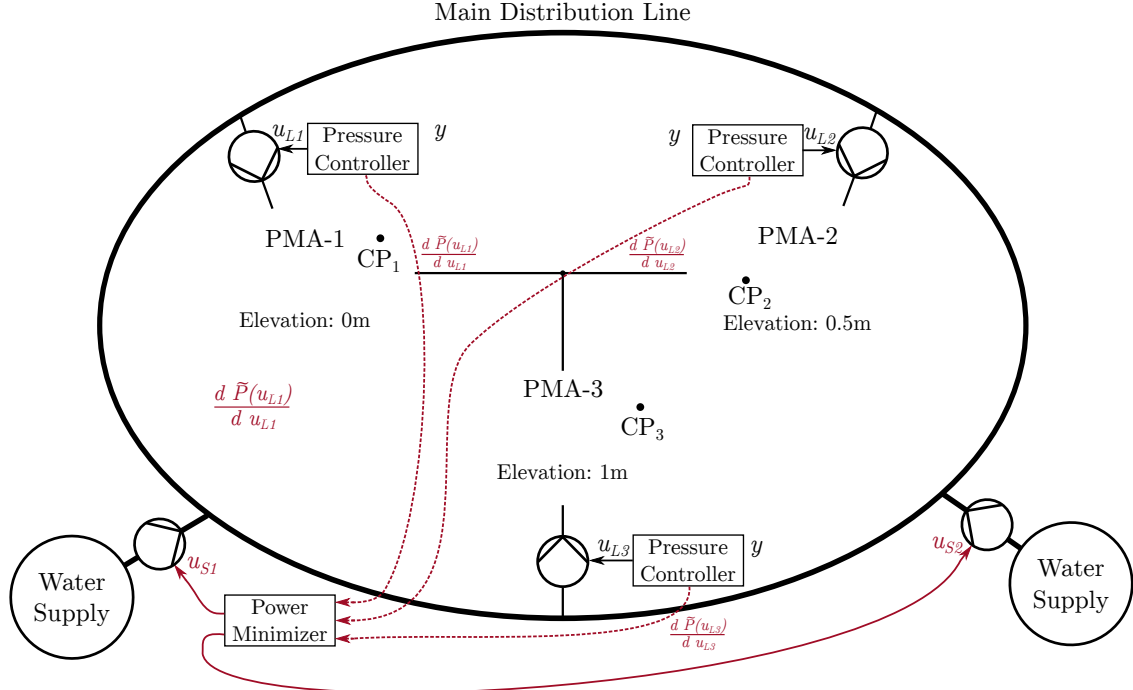


Figure 4.6: The communication structure of the Water Wall for the power optimal controller. The dotted lines represent one-way transmissions of measurements or the local pump derivatives, with fully drawn lines representing control signals.

necessary for designing the controller.

In the case of the Water Wall system, the optimization problem has been reduced to a one-dimensional problem, because of the constraint on the control supply pumps control signals given in equation 4.21. As a consequence the relation matrix \mathbf{R} is a one-dimensional vector instead of a matrix.

Furthermore, the control design using two controllers, a pressure controller for maintaining CP pressure for the local pumps and the power optimization controller for minimizing the power consumption using the supply pumps, offers some robustness to the system with regards to communication failure.

In a situation where the communication between the local pumps and the power optimization controller fails, the pressure controller using the local pumps will still continue to maintain the CP pressure at the set-point, as the pressure controller is independent of the power optimization and the supply pumps. Thus the consumers experience no loss of service or water pressure in the event of communication breakdown, only the power optimality is lost.

Chapter 5

Implementation of the Control System

In this chapter the implementation of the control system in both MATLAB Simulink and on the Water Wall setup is described.

First the implementation of the pressure controller for the local pumps is explained, then the implementation of the power optimization controller is described.

5.1 Pressure Controller

The pressure controller used for maintaining the Critical Point (CP) pressure is implemented on top of the pump speed controller as shown in figure 5.1.

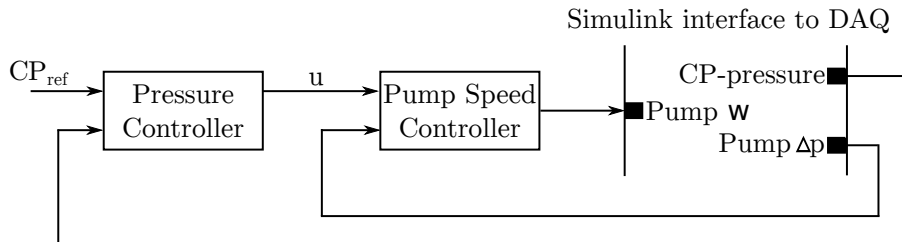


Figure 5.1: Block diagram of the pressure controller for the Water Wall test system, with communication via DAQ boards.

The PI-controller is implemented as shown in figure 5.2 with anti-windup and a saturation block which limits the control signal u to the interval between $\underline{u} = 0$ and $\bar{u} = 0.6$, which is the minimum and maximum pressure boost the local pumps can produce.

The pressure controller is tuned in a similar manner as for the speed controller in section 3.3.2. The tuning parameters of the PI-controller are shown in table 5.1, these are the values for all local pressure controllers.

Local Pumps	$K_{p,L}$	$K_{i,L}$	$K_{a,L}$
C_{18}, C_{25}, C_{32}	1	1.5	1.5

Table 5.1: Tuning parameters for the PI-pressure controllers.

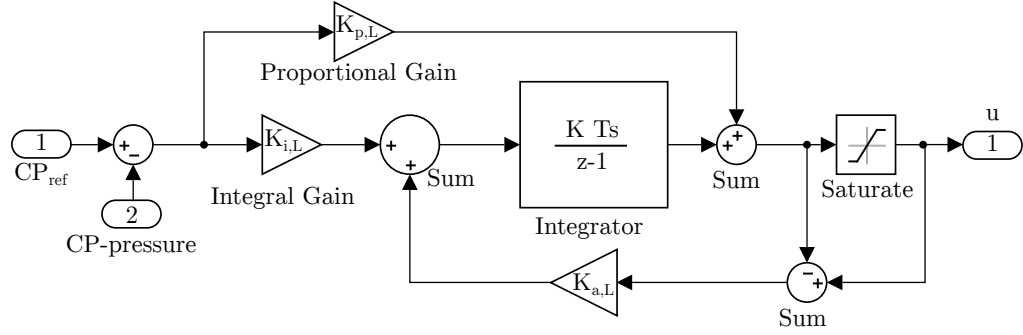


Figure 5.2: A block diagram of the PI-controller used for the pressure controller.

A step-response is made of the pressure controller with a step in reference pressure from 0.08 bar to 0.13 bar . The step-response is shown for the simulation model in 5.3 and for the Water Wall system in figure 5.4

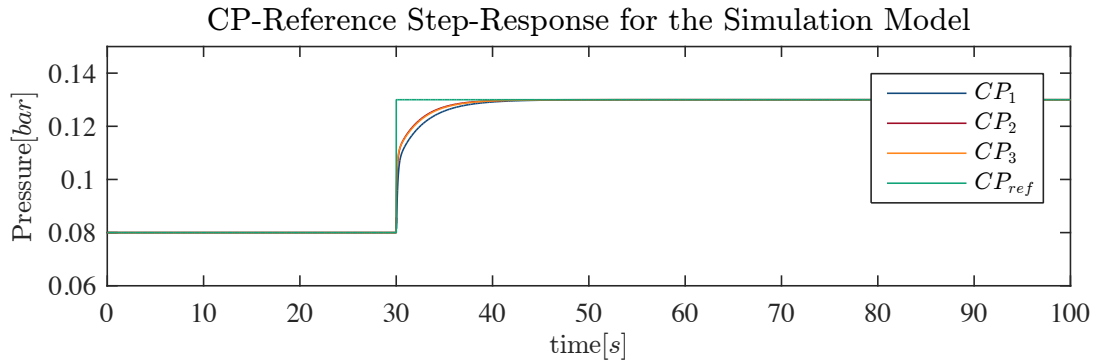


Figure 5.3: A step-response for the simulation model for a change in CP pressure from 0.08bar to 0.13bar .

Comparing the two step-responses it clear to see that the simulation model has a faster rise-time than the Water Wall, this is primarily due to model differences as discussed in section 3.5. It is also noted that there is a delay in the Water Wall system, which also has been discussed previously in section 3.3.2.

However, the rise-time and settling of the pressure is sufficiently fast for the water distribution network, and an increase of the controller gain is not possible due to the delay causing the controller to become unstable.

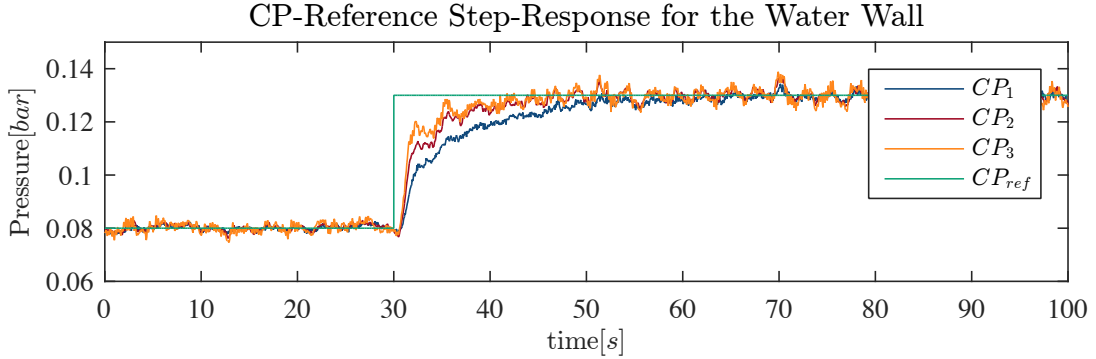


Figure 5.4: A step-response for the Water Wall for a change in CP pressure from 0.08bar to 0.13bar .

5.2 Power Optimization Controller

This section covers the implementation of the power minimization controller on the simulation model in Simulink and on the Water Wall test-system.

5.2.1 Simulation Environment

In the Simulink simulation environment it is first of all necessary to include the sample time T_s in the minimization function, such that the tuning of γ is independent of the simulations discrete step size.

$$\mathbf{u}_{S2,k+1} = \mathbf{u}_{S2,k} - T_s \cdot \gamma \left(\frac{d \tilde{P}(\mathbf{u}_{S,k}, \mathbf{u}_{L,k})}{d \mathbf{u}_{S2,k}} \right) \quad (5.1)$$

The efficiency used in the simulation for the supply pumps and locals pumps are $\eta_S = 0.80$ and $\eta_L = 0.65$ respectively. Although these efficiency values do not agree with the actual efficiency of the pumps in the Water Wall system, which are much lower, these values are chosen based on the expected efficiency of the booster sets used in water distribution networks, this is explained in further details in Appendix C.

5.2.2 Flow Estimation

In order to implement the power optimization controller on the Water Wall system, it is necessary to design and implement a flow estimator, which estimates the flow through each pump. This is necessary because the derivative of each pump is a function of the differential pressure across and the flow through the pump.

The method used for flow estimation is patented by Grundfos [Kallesøe 12, Kallesøe 14a]. It uses measurements of the pump pressure drop, Δp , pump speed, ω , and electrical power consumption, P_e , to estimate the flow q , given that the pump parameters are known.

First, recall the two equations which describe a centrifugal pump.

Equation 5.2 from section 2.1.3 describes the pump differential pressure, Δp , where $\Delta p = p_{in} - p_{out}$.

$$\Delta p = a_{h2} q^2 - a_{h1} q \omega - a_{h0} \omega^2 \quad (5.2)$$

Where a_{h0} , a_{h1} , a_{h2} are constants describing the pump which are considered known and ω is the rotational speed of the pump.

Equation 5.3 from section 2.1.3 describes the pump electrical power consumption P_e .

$$P_e = -a_{P2} q^2 \omega + a_{P1} q \omega^2 + a_{P0} \omega^3 + B_0 \omega^2 + P_0 \quad (5.3)$$

where B_0 and P_0 along with the constants a_{P0} , a_{P1} , and a_{P2} are also considered known.

Equations 5.2 and 5.3 are combined to estimate the value of q where the first step is to make the terms which are multiplied by q^2 in both equations equal. By doing so, it becomes possible to eliminate these terms, that is $a_{h2} q^2$ and $a_{P2} q^2 \omega$, when the two equations are combined later on.

Equation 5.2 is multiplied by a_{P2} .

$$\begin{aligned} \Delta p &= a_{h2} q^2 - a_{h1} q \omega - a_{h0} \omega^2 \\ a_{P2} \Delta p &= a_{P2} a_{h2} q^2 - a_{P2} a_{h1} q \omega - a_{P2} a_{h0} \omega^2 \end{aligned} \quad (5.4)$$

Equation 5.3 is multiplied by a_{h2}/ω .

$$\begin{aligned} P_e &= -a_{P2} q^2 \omega + a_{P1} q \omega^2 + a_{P0} \omega^3 + B_0 \omega^2 + P_0 \\ \frac{a_{h2}}{\omega} P_e &= -\frac{a_{h2}}{\omega} a_{P2} q^2 \omega + \frac{a_{h2}}{\omega} a_{P1} q \omega^2 + \frac{a_{h2}}{\omega} a_{P0} \omega^3 + \frac{a_{h2}}{\omega} B_0 \omega^2 + \frac{a_{h2}}{\omega} P_0 \\ \frac{a_{h2}}{\omega} P_e &= -a_{h2} a_{P2} q^2 + a_{h2} a_{P1} q \omega + a_{h2} a_{P0} \omega^2 + a_{h2} B_0 \omega + \frac{a_{h2}}{\omega} P_0 \end{aligned} \quad (5.5)$$

The next step is to sum equation 5.4 and equation 5.5. Note that q^2 terms are cancelled out.

$$\begin{aligned} \frac{a_{h2}}{\omega} P_e + a_{P2} \Delta p &= a_{h2} a_{P1} q \omega + a_{h2} a_{P0} \omega^2 + a_{h2} B_0 \omega + \frac{a_{h2}}{\omega} P_0 \\ &\quad - a_{P2} a_{h1} q \omega - a_{P2} a_{h0} \omega^2 \\ a_{h2} \frac{P_e}{\omega} + a_{P2} \Delta p &= \underbrace{(a_{h2} a_{P1} - a_{P2} a_{h1})}_{k_1} q \omega + \underbrace{(a_{h2} a_{P0} - a_{P2} a_{h0})}_{k_2} \omega^2 + \underbrace{a_{h2} B_0}_{k_3} \omega + \underbrace{a_{h2} P_0}_{k_4} \frac{1}{\omega} \\ a_{h2} \frac{P_e}{\omega} + a_{P2} \Delta p &= k_1 q \omega + k_2 \omega^2 + k_3 \omega + k_4 \frac{1}{\omega} \end{aligned} \quad (5.6)$$

The last step is to isolate q .

$$\begin{aligned} k_1 q \omega &= a_{h2} \frac{P_e}{\omega} + a_{P2} \Delta p - k_2 \omega^2 - k_3 \omega - k_4 \frac{1}{\omega} \\ q &= \underbrace{\frac{a_{h2}}{k_1}}_{\gamma_1} \frac{P_e}{\omega^2} + \underbrace{\frac{a_{P2}}{k_1}}_{\gamma_2} \frac{\Delta p}{\omega} + \underbrace{\frac{-k_2}{k_1}}_{\gamma_3} \omega + \underbrace{\frac{-k_3}{k_1}}_{\gamma_4} + \underbrace{\frac{-k_4}{k_1}}_{\gamma_5} \frac{1}{\omega^2} \\ q &= \gamma_1 \frac{P_e}{\omega^2} + \gamma_2 \frac{\Delta p}{\omega} + \gamma_3 \omega + \gamma_4 + \gamma_5 \frac{1}{\omega^2} \end{aligned} \quad (5.7)$$

where

$$\begin{aligned} \gamma_1 &= \frac{a_{h2}}{k_1} = \frac{a_{h2}}{a_{h2} a_{P1} - a_{P2} a_{h1}} \\ \gamma_2 &= \frac{a_{P2}}{k_1} = \frac{a_{P2}}{a_{h2} a_{P1} - a_{P2} a_{h1}} \\ \gamma_3 &= \frac{-k_2}{k_1} = \frac{-(a_{h2} a_{P0} - a_{P2} a_{h0})}{a_{h2} a_{P1} - a_{P2} a_{h1}} \\ \gamma_4 &= \frac{-k_3}{k_1} = \frac{-a_{h2} B_0}{a_{h2} a_{P1} - a_{P2} a_{h1}} \\ \gamma_5 &= \frac{-k_4}{k_1} = \frac{-a_{h2} P_0}{a_{h2} a_{P1} - a_{P2} a_{h1}} \end{aligned}$$

Note, equation 5.7 is only valid when a pump is operating below its maximum electrical power consumption, P_{e-max} and if the true rational speed is unknown. When the pump exceeds its maximum power consumption the pump automatically reduces its speed. Consequently, the pump speed input signal is no longer equal to the actual pump speed. Hence, equation 5.2 and equation 5.3 become invalid.

Figure 5.5 illustrates how the pump curves given by equation 5.2 and equation 5.3 are effected when the pump exceeds its maximum power consumption.

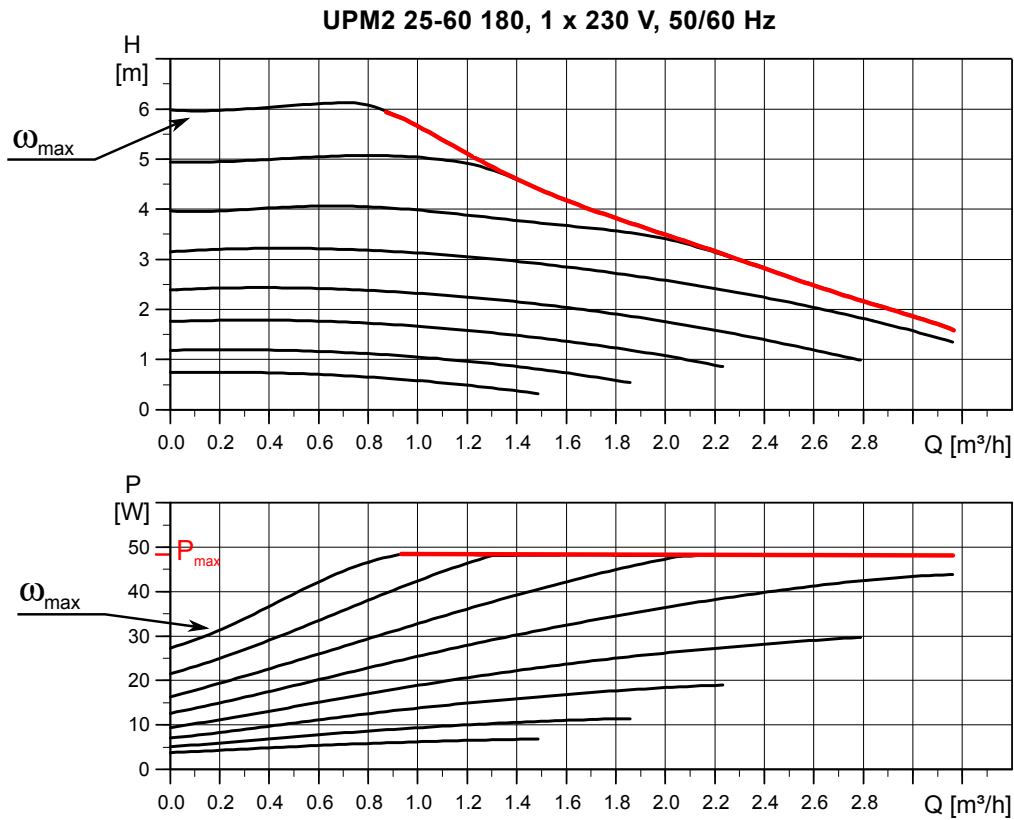


Figure 5.5: A plot showing the pump curve for the Grundfos UPM2 25-60 180 centrifugal pump. The curves are for different pump speeds (ω) where the colour red is used to illustrate how the pump operates at its maximum power consumption. When the pump exceeds its maximum power the pump automatically reduces its speed. Consequently, the pump speed control signal is no longer equal to the actual pump speed. The plot is originally from the pump data sheet [Grundfos 10].

The above demonstration shows that if one does not have access to the true rotational speed of the pump, it is necessary to observe the pump power usage when equation 5.7 is applied. If the pump power usage exceeds P_{e-max} , the flow estimation is no longer valid. Nevertheless, if a pump is regularly operating at P_{e-max} , one should consider to replace the pump with e.g. a bigger pump.

5.2.3 Penalty Functions

The control signal \mathbf{u}_S for the supply pumps is calculated based on the derivatives of all the pumps in the system.

The calculation is done using MATLAB both for the simulation and for the Water Wall. For the

Water Wall, MATLAB receives measurements and sends control signals through the DAQ I/O board as shown in figure 5.6.

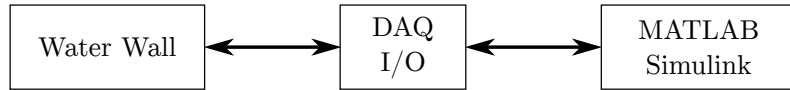


Figure 5.6: The communication between the Water Wall and MATLAB is done through a DAQ I/O board, which sends measurements from the Water Wall to MATLAB and control signals from MATLAB to the Water Wall.

The penalty functions are implemented with quadratic penalties as described in section 4.5.3. However the quadratic penalties does not guarantee that the constraints of $\underline{u} \leq u \leq \bar{u}$ being fulfilled. The penalties merely encourage that the control signal is within the bounds by imposing an additional cost if $u \leq \underline{u}$ or $u \geq \bar{u}$.

One way to make sure the minimum stays within the boundaries of the control signal, is to move the penalty functions inwards, away from the control signal boundaries, as shown in figure 5.7. Where a small interval x has been added and subtracted to the lower penalty and upper penalty boundary respectively.

By properly choosing the interval x and the penalty gain κ , the minimum of the function lies between the control signal boundaries.

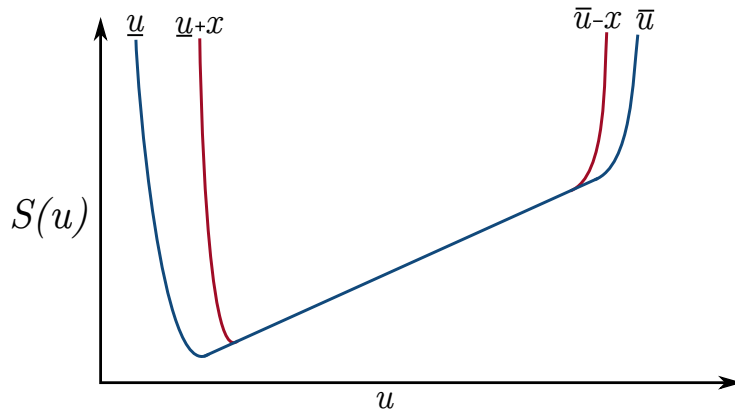


Figure 5.7: The penalty functions shown in red are used to increase the likelihood of u being within the bounds, shown as dotted lines, by increasing the cost when u approaches the bounds, instead of when u crosses the boundaries as it is done with the penalty functions shown in blue.

Secondly, in order for MATLAB being able to always compute the penalty without the problem becoming ill conditioned, an upper bound of the penalty value $S(u)$ is set at 10^5 .

All implementation subjects are hereby covered and it is possible to test the controller, both in simulation and on the Water Wall.

Part III

Test And Verification

Chapter 6

Test Results

This chapter covers the test and verification of the complete control system, being the pressure control of the Critical Points and power optimal control of the supply pumps.

First the results for the Water Wall is presented, next the results obtained from the simulation environment is shown.

6.1 Water Wall

Before it is possible to test the power optimization controller on the Water Wall, the pump flow estimator introduced in 5.2.2 is tested. The flow is calculated from equation 5.7 where measurements of the pump pressure drop, Δp , pump speed, ω , and electrical power consumption, P_e , are applied to the calculation.

The flow estimator is implanted into Simulink as shown in figure 6.1.

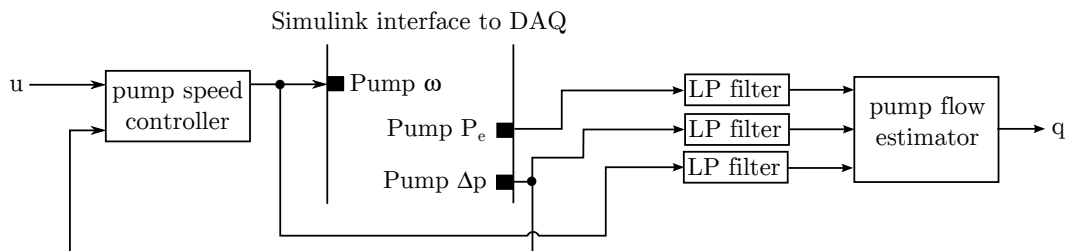


Figure 6.1: The

In figure 6.1, one can see that the signals are fed through a low-pass filter before the flow, q , is calculated. The signals are filtered because the great amount of noise in the pump power signal. The signal is assumed white-noise and the designed low-pass filter is shown in figure 6.2. The filter is designed from the Digital Filter Design block in Simulink where the focus was on a filter design with zero DC gain.

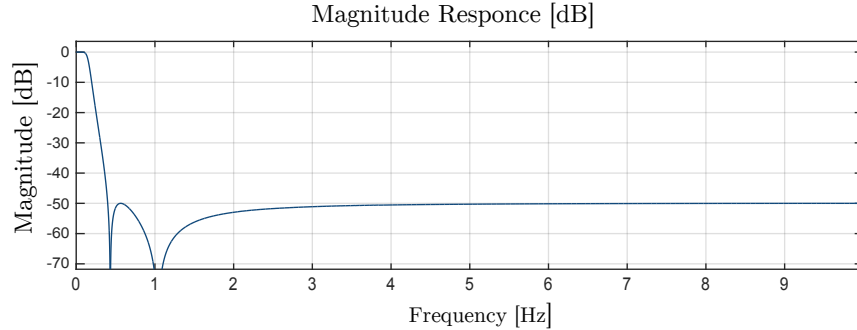


Figure 6.2: The low-pass filter used to filter the pump power consumption signal.

A power consumption measurement from one of the pumps is shown in figure 6.3. It is plotted both with and without a filter.

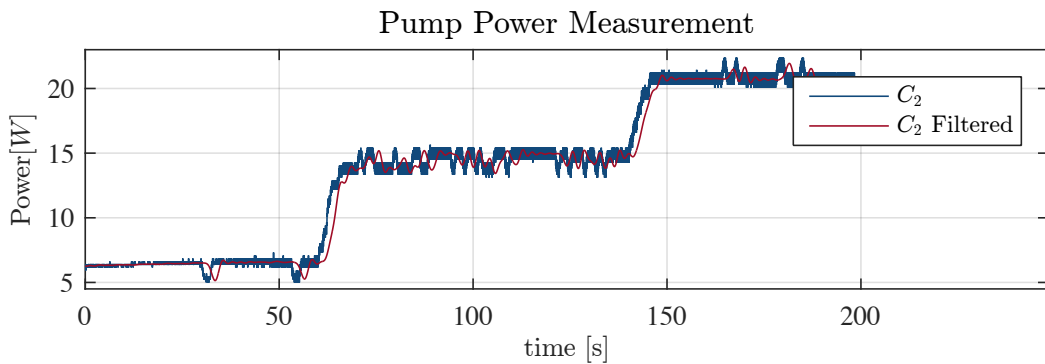


Figure 6.3: Pump Power consumption before and after a low-pass filter.

From figure 6.3, it can be observed that the filter introduces some extra dynamics in the signal transient. Therefore, a low pass filter is also introduced to the two other measurements, Δp and ω , even though they are not as noisy as the pump power signal.

The power optimization controller is only designed to be optimal in steady-state, meaning that the extra dynamics are not of concern. Also, the controller does not depend on the component model, only the systems graphical description. This means that the extra dynamics introduced by the low-pass filters does not have to be included in the power optimization controller.

The next phase is to test the flow estimator with real measurement from the Water Wall. This is done by actuating the pumps with the set-point signals shown in figure 6.4.

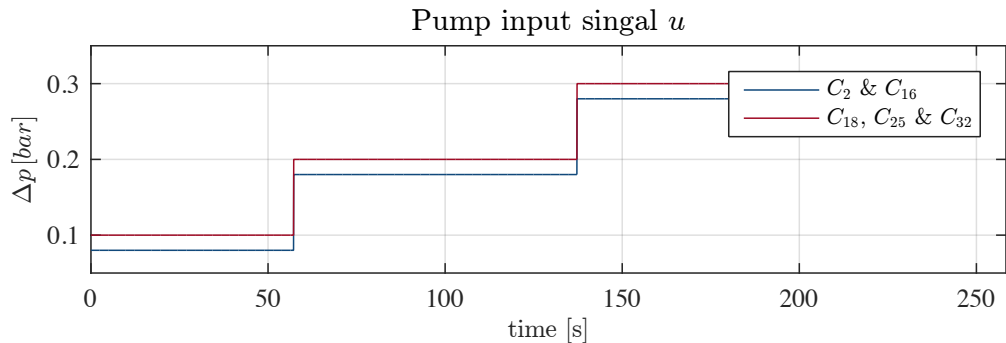


Figure 6.4: The pumps set-point signal which is used to test the flow estimator.

The resulting differential pressure over the pumps is shown in figure 6.5.

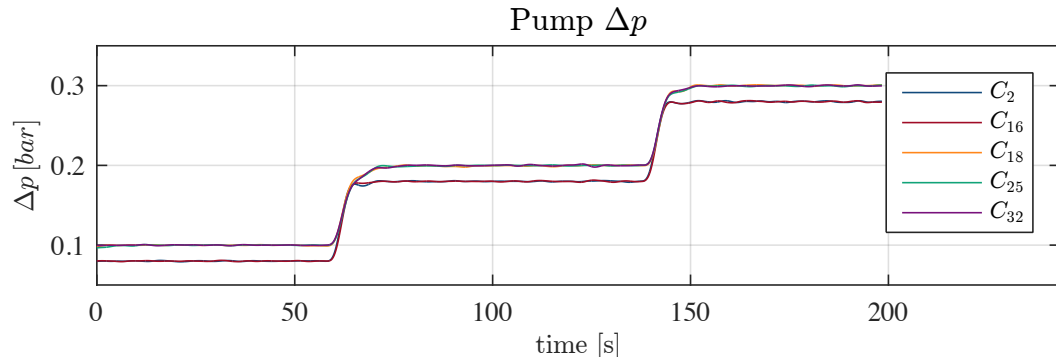


Figure 6.5: Pump differential pressure during the flow estimation test.

The pumps rotational speed signal are plotted in figure 6.6.

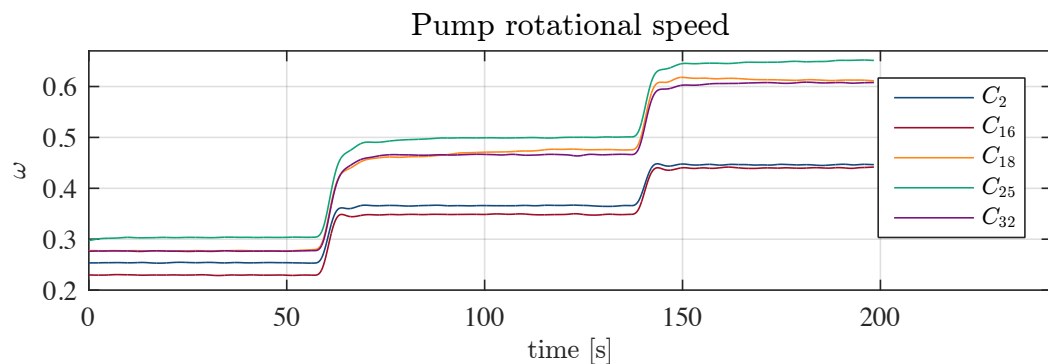


Figure 6.6: Pump speed signal during the flow estimation test.

The pumps power usage are plotted in figure 6.7.

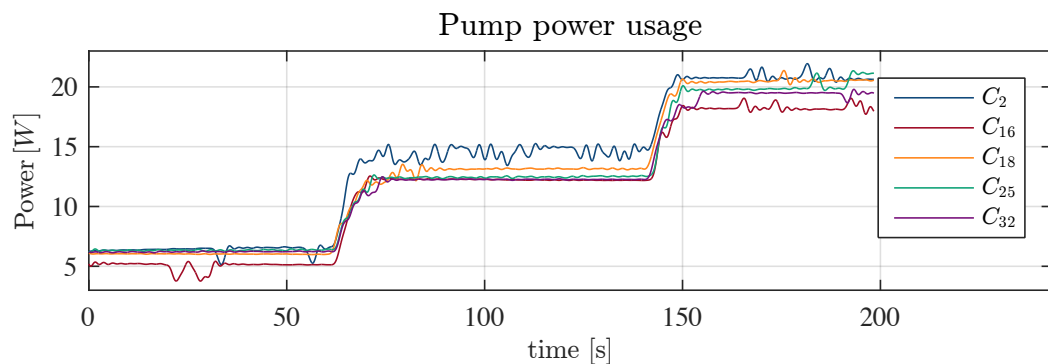


Figure 6.7: Pump power consumption during the flow estimation test.

In figure 6.7 one can observe some variations in the power measurement. However, the pump Δp and ω are relatively stable. Consequently, those variations are assumed to be sensor noise.

At this point, all of the flow estimations input signals, Δp , ω and P , are increasing in sync with the increasing pump set-points shown in figure 6.4. Consequently, it is expected to see the same trend in the flow estimation. The resulting flow estimation is shown in figure 6.8.

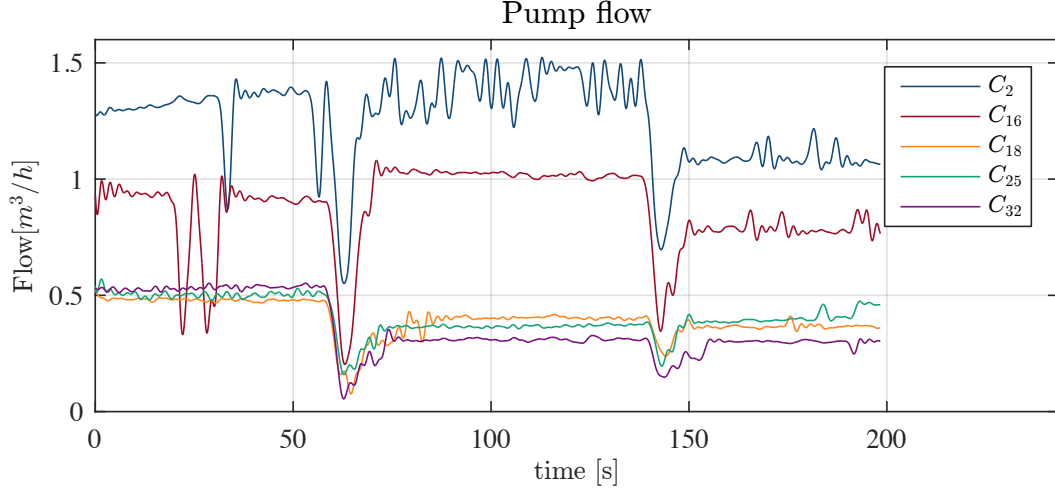


Figure 6.8: The resulting flow in the flow estimation test.

Nonetheless, the flow estimation in figure 6.8 shows not the result which was expected. Before going into details concerning incorrect flow estimation, it is clear to see that the noisy power measurement has a great impact on the flow estimation, as the flow estimation shows the same variation. It is also seen that in transients the estimated flow drops down to very low values before coming back up again. This diving behavior is due the polynomials used in describing the pump models are only valid as statics models.

By analyzing the pump models at the specific speed observed in figure 6.6, one can see why the flow is estimated incorrectly. By taking a sample at time = 170 s in figure 6.6 and figure 6.5, one is interested to see if the:

- The pump C_{18} (UPM2 pump) can deliver a $\Delta p = 0.3 \text{ bar}$ at $\omega = 0.6$.
- The pump C_2 (UPMXML pump) can deliver a $\Delta p = 0.28 \text{ bar}$ at $\omega = 0.44$.

The pump model is plotted for both pump types. It is considered only necessary to show the pressure model which is given by equation 5.2.

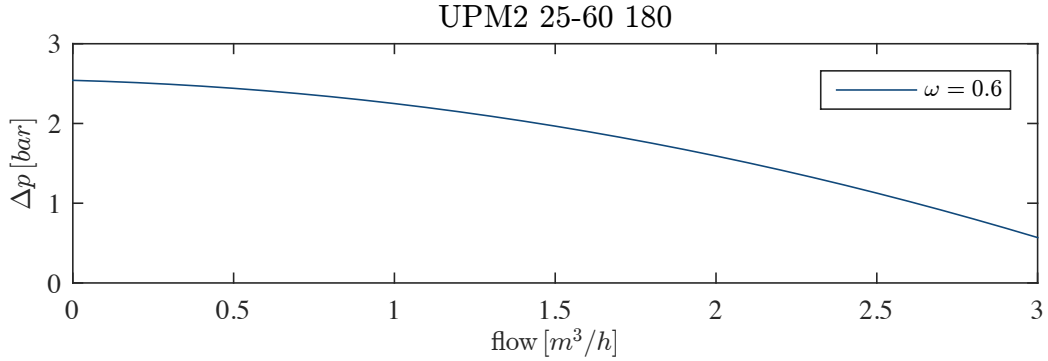


Figure 6.9: Pump model at a given rotational speed ω .

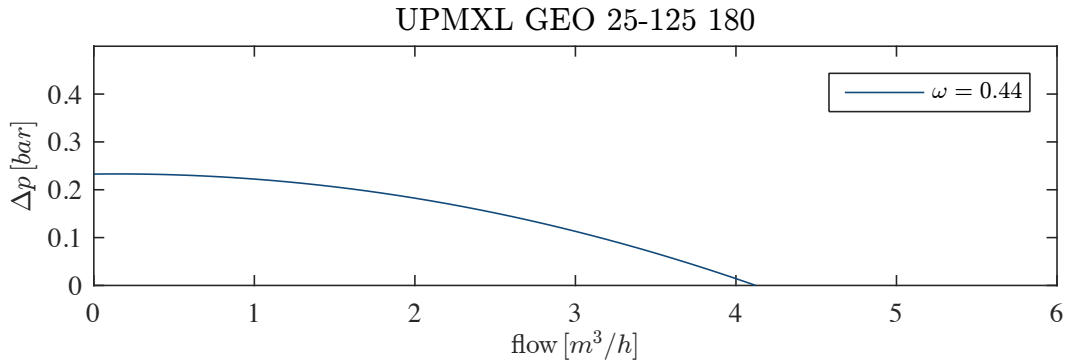


Figure 6.10: Pump model at a given rotational speed ω .

From figure 6.9 and 6.10, one can see that the pump models applied in the flow estimations can not be used to represent the pumps fund on the Water Wall. This statement is drawn from the fact that the pump models can not deliver the expected pressures at the given speeds. Since the flow estimation is not working correctly, the power optimization controller is not implemented onto the Water Wall.

However, it is expected that by obtaining the correct polynomial coefficients for the pump models, it will be possible to solve the problems that occur with the flow estimator.

6.2 Simulation

In this section the results, obtained using the simulation environment with the power optimizing controller, are presented.

The simulation environment is made based on the Water Wall test system. It is developed to simulate the hydraulic dynamics of the Water Wall, with the purpose of being able to easily test and verify control strategies for the water distribution network.

The simulation environment is developed using a graph of the Water Wall connections and component parameters of the pipes, valves and pumps. The diagram of the Water Wall distribution network is presented in Appendix A.2, which form the basis of the graph description, the parameters are presented in Appendix A.1.

The controllers designed in Part II of the report are all implemented in the simulation environ-

ment.

The pressure controllers designed in section 4.2 are controlling the local pump denoted $\{C_{18}, C_{25}, C_{32}\}$, with a pressure feedback from the Critical Points (CPs), which are the pressure measurements at nodes denoted $\{n_{14}, n_{19}, n_{24}\}$, of the system diagram.

The power optimization controller described in section 4.6, controls the two supply pump denoted $\{C_2, C_{16}\}$, using information from the three pressure controllers.

A time-series of the power consumption for a test with the power optimization controller using the simulation environment is shown in figure 6.11. The test is conducted using a step in CP pressure reference from 0.08 bar to 0.13 bar and then from 0.13 bar to 0.08 bar . The CP pressure outputs are shown in figure 6.12, and the control signals for the pumps is shown in figure 6.13.

In figure 6.11, the power consumption can be seen to peak at the transients following a step in reference pressure. When the pressure controllers reach steady-state after approximately 20 s , the power consumption slowly decreases before it converges to a steady-state at approximately 80 s after the step is performed.

The control signals shown in figure 6.13, shows that the power optimization controller slowly increases the supply pumps control signals until one of the local pump control signals meets its minimum boundary of 0. Any further increase of the supply pumps control signals will lead to an excessive pressure at the CP pertaining to the local pump which has reached its minimum control signal.

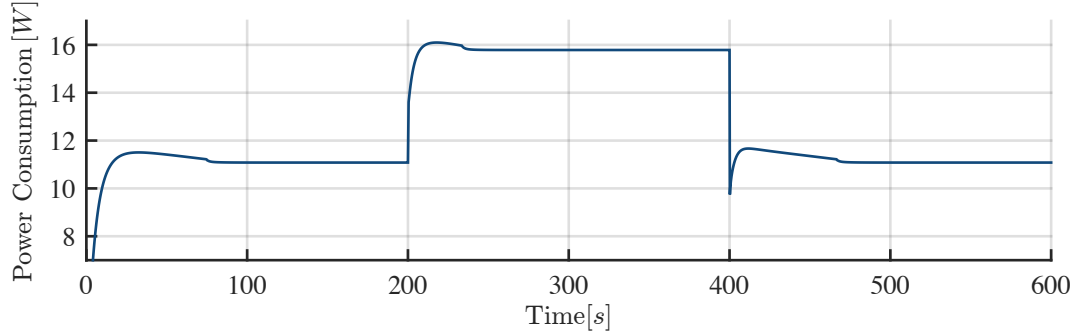


Figure 6.11: Power optimization for a step in CP-reference, where a step from 0.08 bar to 0.13 bar is performed at time 200 s , and a step from 0.13 bar to 0.08 bar is performed at time 400 s .

In figure 6.12 it is seen that the pressure first converges to one pressure, before after some time converging to the correct reference pressure. This behavior seen in the plot is attributed to the control action of the power optimization controller, which increases the differential pressure across the supply pumps in order to minimize the power consumption.

As a consequence of the increased pressure from the supply pumps, the local pump controllers must take action to decrease the pressure delivered by the local pumps, which can be observed in figure 6.13. While this takes place the pressure is constantly slightly above the reference, and finally settles when the power optimization controller has found the minimum.

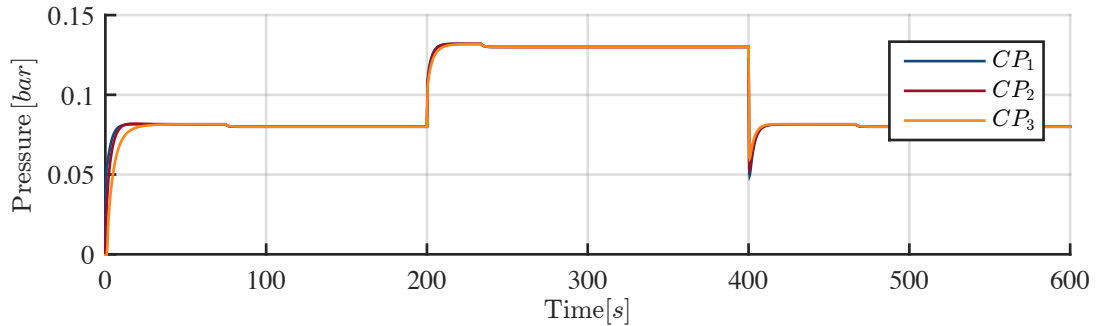


Figure 6.12: CP pressure for a step in CP-reference, where a step from 0.08 bar to 0.13 bar is performed at time 200 s , and a step from 0.13 bar to 0.08 bar is performed at time 400 s .

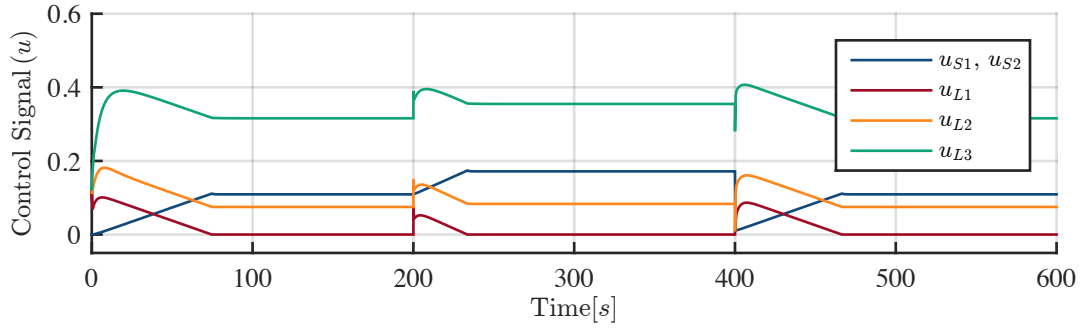


Figure 6.13: Control signals for a step in CP-reference, where a step from 0.08 bar to 0.13 bar is performed at time 200 s , and a step from 0.13 bar to 0.08 bar is performed at time 400 s .

From the control signals shown in figure 6.13, it is possible to see that the power optimization controller indeed finds the optimal distribution of pressure delivered by the pumps in the water distribution network. The two supply pumps are more energy efficient than the three local pumps, thus the controller is more inclined to use the supply pumps. By examining the control signals, it is clear to see that the power optimization controller increases the supply pumps control signal until the control signal u_{L1} reaches zero. This is the optimal distribution of pressures boost delivered by the pumps, as an increase of the supply pumps control signal will result in a too high pressure at CP_1 .

The power optimizing controller design and test is hereby finished. Any further discussion on the subject is brought up in the following chapter.

Chapter 7

Project Closure

In this chapter the finalization of the report is performed, by summing up the findings of this project and concluding on the results obtained.

Lastly a list of possible improvements is discussed and recommendations for further work is given.

7.1 Conclusion and Discussion

This section sums up the sub-conclusions made throughout the report. A discussion of the results obtained is performed, ending with a final conclusion of whether the goal of this project has been fulfilled.

Project Aim

The aim of this report is to develop a distributed control strategy which minimizes the power consumption of a water distribution network. With the control strategy also focusing on minimizing the use of communication between the pumps within the water distribution network.

Power Optimal Control

It is first and foremost proposed in section 1.2 to replace the pressure reducing valves (PRVs) in the water distribution network with pumps. This replacement of the PRVs with pumps creates an over actuated system which has more freedom for control. It also removes the pressure loss of the PRVs, thus avoids an unnecessary waste of energy.

A power optimal controller is designed in section 4.6. It uses gradient descent to obtain the optimal distribution of pressures to be delivered by the pumps in the distribution network, which results in the lowest power consumption, without compromising the end-user pressure requirements.

A time-series plot of power consumption, from a simulation of the power optimization controller using a hydraulic model of a water distribution network, is shown in figure 6.11. The figure shows the power consumption being slowly reduced once the hydraulic system has reached steady-state after a step in reference pressure.

Distributed Controllers

The local pressure controllers designed in section 4.2, are used for controlling the CP pressures within each Pressure Management Area (PMA). The pressure controller is designed to only use a pressure measurement from the CP it pertains to, thus the controller is truly distributed.

In figure 5.3 and 5.4, a step response for a change in reference pressure is shown for the simulation

model and Water Wall, respectively. The step response shows fast convergence for both systems, and convergence for all CP, which concludes that the distributed controllers are able maintain CP pressure in all PMAs regardless of the fact that they are distributed and only rely on local information.

Furthermore the plot shown in figure 6.12, shows that the local controllers are able to sufficiently regulate the CP pressure, even when the power optimization controller affects the pressure distribution in the water distribution system.

A limitation of the local controllers is that they are only able to regulate and maintain CP pressure if the reference for each CP is equal, or confined to a small interval. This limitation arise from the cross-connections between the PMAs giving that a high pressure in one PMA will affect the pressure in other PMAs connected to it. This is especially a problem if there is great hight difference between the PMAs or very low pressure loss in the pipe connections, which is the situation with the Water Wall test system. In real world applications this problem is less likely to occur, as the PMAs will have a larger distance between them, and because the CP pressures in a water distribution network is almost always equal.

Finally the distributed nature of the pressure controller design results in unaffected change of service for the end-users in case of a communication failure or if the power optimization controller experiences an error.

Communication Structure

It is desired to use the minimal amount of communication between the pumps in the distribution network.

A reduced communication structure is obtained by the ingenuity of the power optimization controller, which is designed in section 4.6. The communication structure within the water distribution network is described in section 4.6.1, and depicted in figure 4.6. It shows that the communication necessary is reduced to only requiring a one-way communication from the local pump controllers to the power optimization controller.

Generalized Controller

Throughout the report the formulation has been sought to apply to a general class of water distribution network, namely networks on the form of a main supply ring, with multiple interconnected PMAs and multiple water sources, connected to the main supply ring.

The power optimization controller developed in section 4.6 is designed for this general type of water distribution network.

The main feature of this controller, besides its ability to reduce the power consumption, is that it is designed completely without knowledge of the water distribution network component parameters. As described in section 4.6.1, the controller only requires the knowledge of the distribution networks topology and information of the pump locations within the network.

This is a very important asset of the controller, as most water utility companies have accurate and up-to-date maps or graph representations of their distribution networks topology. Where this is not always the case for the component parameters, as some pipes can be as old as 100 years or more, and the fact that the parameters are time varying, e.g. due to mineral build up in pipes.

One exception to the use of a general formulation is the investigation of convexity of the optimization problem in section 4.4. It was not possible to prove convexity for a general system, however a numerical analysis of the simulation model in Appendix D, shows that for the Water Wall test system the optimization problem is convex.

Parameter Estimation

The subject of parameter estimation is visited in section 3.4. The section also covers what parameters are considered known and which are unknown. The goal is to tune the model parameters until the model gives the same dynamical performance as the Water Wall.

Practical issues prevent the estimation method to obtain the correct parameters. However, the method itself is considered to work. It is also discussed that minor modelling errors can have big impact on the model performance. The section proposes a method to obtain the correct parameters by eliminating the uncertainties in the valve model.

The section ends by defining the initial parameters to be used throughout the project and at the same time, it is shown that those parameters, which are found by analysing the physical system, are not far away from correct and unknown parameters.

System Model

A model of the Water Wall test system is developed in section 3.2. The main purpose of this model is for simulating the water distribution networks hydraulic dynamics, using Simulink and MATLAB.

A model verification of the simulation model is performed in section 3.5 where the initial model parameters are used. Even though the model is not correct enough at this point to give the same dynamical performance as the Water Wall, the model represents a similar system which has the same structure as the Water Wall and is of the same size.

The simulation model sufficiently captures the dynamics of the Water Wall test system, for it to be useful as a tool for development and test of control strategies for the distribution network.

The simulation model does not seem to be of such a precision that it can be used for leakage detection for small flows, or in general to be utilized for fault detection and isolation.

Final Conclusion

The prime focus was to develop and test a distributed control strategy which minimizes the power consumption of a water distribution network. And at the same time, try to keep the complexity of the communication structure at minimum. The power optimization problem is solved by the developed controllers, and verified by a simulation test.

7.2 Perspective

This project proposes an alternative pressure control method for water distribution networks. The method does not only ensure that the users have a sufficient pressure at their end, the power consumptions of the pumps in the system is kept as low as possible. As the power consumption is kept at minimum, the pressure is also kept relatively low in the system. The lower water pressure results in less water lost through leakages in the pipes, and reduces the stress on the pipe wall, meaning less leakages are formed. It is therefore clear that this project has a huge relevance since water distribution networks are utilized in all urban environments.

Improvements

Before any further development on this project is performed, the following points ought to be considered.

- The parameter estimation needs to be performed again as the sensors are hereby implemented correctly. It is though advised to leave the valves fully open while one estimates the pipe parameters. And afterwards, evaluate how correct the valve model is.
- The power optimization controller is designed and tested, however it is not implemented on the Water Wall. For that to be possible, the flow estimation has to be working. It was shown that the pump models are not correct enough for that purpose. Model tuning or new models are therefore required.

Future Work

This project has opened a clear path for this type of an alternative pressure control method for water distribution networks. As for today, pressure in a water distribution networks is not controlled with focus on energy saving.

This project is hereby finished.

Part IV

Appendix

Appendix A

Test System

A.1 Test System Components

The components found in figure A.2 are listed in the following tables.

Datum	Component	Length	Diameter	Material	ε	Δz	fittings	$\sum k_f$
Datum 5	C_4	5m+0.3 m	20 mm	25 mm PEM	0.01 mm	0 m	b, c, c, a, a	4.42
	C_8	10 m	20 mm	25 mm PEM	0.01 mm	0 m	c, b, a, c, b	3.92
	C_9	10 m	20 mm	25 mm PEM	0.01 mm	0 m	c	0.51
	C_{10}	10 m	20 mm	25 mm PEM	0.01 mm	0 m	c, a, a	3.11
	C_{11}	10 m	20 mm	25 mm PEM	0.01 mm	0 m	c, a	1.81
	C_{12}	10 m	20 mm	25 mm PEM	0.01 mm	0 m	c, c, a, c, b	3.63
	C_{13}	10 m	20 mm	25 mm PEM	0.01 mm	0 m	c	0.51
	C_{14}	5m+4 m	20 mm	25 mm PEM	0.01 mm	0 m	a, c	1.81
	C_{19}	2 m	10 mm	15 mm PEX	0.007 mm	0 m	b, c, d, c, e, a	3.57
Datum 1	C_{21}	1 m	10 mm	15 mm PEX	0.007 mm	0 m	c, d, b	1.46
	C_{22}	1 m	10 mm	15 mm PEX	0.007 mm	0 m	c, d, b, e, b	7.68
	C_{23}	2 m	10 mm	15 mm PEX	0.007 mm	0 m	a, b, d, e	2.55
	C_{26}	3 m	10 mm	15 mm PEX	0.007 mm	0.5 m	d, c, a, c, e	2.77
Datum 2	C_{28}	1 m	10 mm	15 mm PEX	0.007 mm	0 m	c, e	0.81
	C_{29}	1 m	10 mm	15 mm PEX	0.007 mm	0 m	b, d, c, b	2.26
	C_{30}	2 m	10 mm	15 mm PEX	0.007 mm	0 m	b, a	2.10
	C_{33}	4 m	10 mm	15 mm PEX	0.007 mm	1 m	b, c, c, d, e	2.27
Datum 3	C_{35}	1 m	10 mm	15 mm PEX	0.007 mm	0 m	b, c, e, d, b, e	3.07
	C_{36}	1 m	10 mm	15 mm PEX	0.007 mm	0 m	a, d, c, e	2.26
	C_{37}	2 m	10 mm	15 mm PEX	0.007 mm	0 m	a, c, d, b, c	3.27
	C_{39}	2 m	10 mm	15 mm PEX	0.007 mm	0.5 m	b, c, c, d, e	2.27
-	C_{42}	2 m	10 mm	15 mm PEX	0.007 mm	0.5 m	c, c, a, d, e	2.77

Table A.1: List of pipe components in figure A.2 and their parameters. More details on the fittings are listed in table A.2, the pipe friction factor f is shown in table A.3 and the average height of roughness inside a pipe wall, ε , is from [Wavin 15] (PEX) and [Wavin 12] (PEM). Note, the $\sum k_f$ is an initial guess which is used in the parameter estimation method in section 3.4.3. Also, the length of pipe C_4 and C_{14} contain their own length and also the length of the pipe connecting the respective pumps, C_2 and C_{16} , to the water supply.

Fitting	symbol	k_f
Tee - Over all loss	$k_{f,a}$	1.3
Tee - Straight through	$k_{f,b}$	0.8
90 ° bend - Diameter/radius ratio 1:1	$k_{f,c}$	0.51
Sudden enlarger - Diameter ratio 1:2	$k_{f,d}$	0.15
Sudden contractor - Diameter ratio 1:2	$k_{f,e}$	0.3

Table A.2: List of the fittings found in the system depicted in figure A.2 along with their form-loss coefficient k_f . The k_f values are found in [Polypipe 08] and [Fischer 11]. Note, the fittings are not depicted in A.2 and are therefore found by studying the physical system.

Pipe material	Diameter	ε	f
25 mm PEM	20 mm	0.01 mm	0.0167
15 mm PEX	10 mm	0.007 mm	0.0180

Table A.3: List of the pipe form-loss coefficient k_f which is dependent on the pipe diameter, mean water flow, water temperature and material, hence the pipe arreage height of roughness ε . The form-loss coefficient is calculated by equation 2.8 where equation 2.7 and equation 2.6 are also applied. The expected water flow is described in 2.1.1 where its mean flow is 1 m/s and the water flowing in the Water Wall described in 3.1 is measured as $T_w = 20^\circ\text{C}$

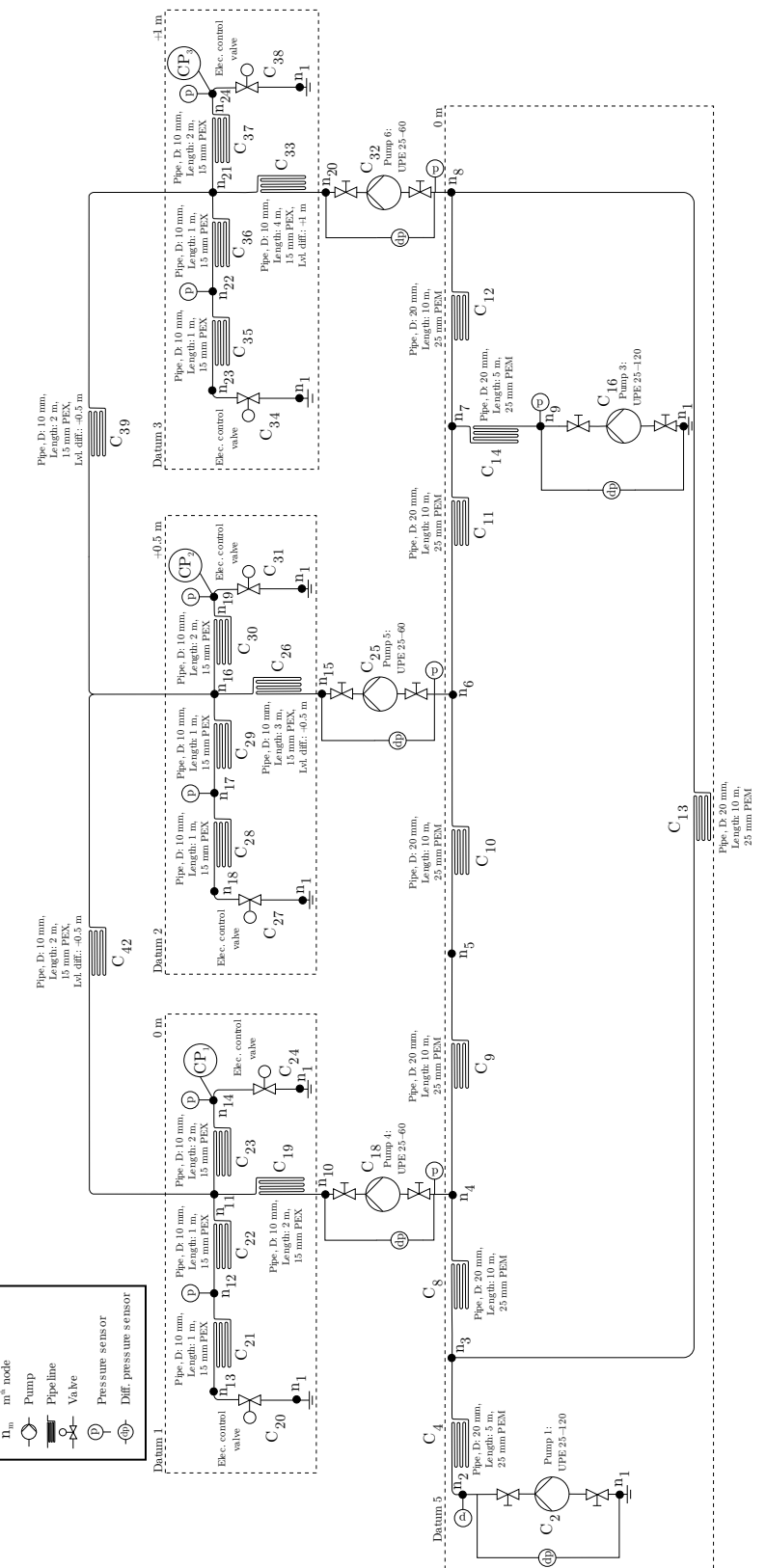
Datum	Component	Valve fitting	k_{vs}	n_{gl}	θ_{off}	θ_{max}	valve motor
Datum 1	C_{20}, C_{24}	Belimo R2015-1-S1	1	3.2	15°	90°	Belimo LRQ24A-SR
Datum 2	C_{27}, C_{31}	Belimo R2015-1-S1	1	3.2	15°	90°	Belimo LRQ24A-SR
Datum 3	C_{34}, C_{38}	Belimo R2015-1-S1	1	3.2	15°	90°	Belimo LRQ24A-SR

Table A.4: List of the valves found in the system depicted in figure A.2 along with their conductivity value k_{vs} , characteristic curve factor n_{gl} , angle of rotation when the valve starts to open, θ_{off} , and the angle of rotation when the valve is fully open θ_{max} . The k_{vs} , n_{gl} , θ_{off} and θ_{max} values are found in [Belimo 11, Belimo 14].

Datum	Component	Pump Type	Constants
Datum 1	C_2, C_{16}	Grundfos UPMXL GEO 25-125 180	$a_{h0} = 1.2024$ $a_{p0} = 65.9475$ $a_{h1} = 0.0098$ $a_{p1} = 46.9126$ $a_{h2} = 0.0147$ $a_{p2} = -3.1342$ $B_0 = 9.8924$ $P_0 = 1.3788$
-	C_{18}, C_{25}, C_{32}	Grundfos UPM2 25-60 180	$a_{h0} = 0.6921$ $a_{p0} = 35.7518$ $a_{h1} = -0.0177$ $a_{p1} = 44.6567$ $a_{h2} = 0.0179$ $a_{p2} = -3.3768$ $B_0 = 0.0698$ $P_0 = 1.0575$

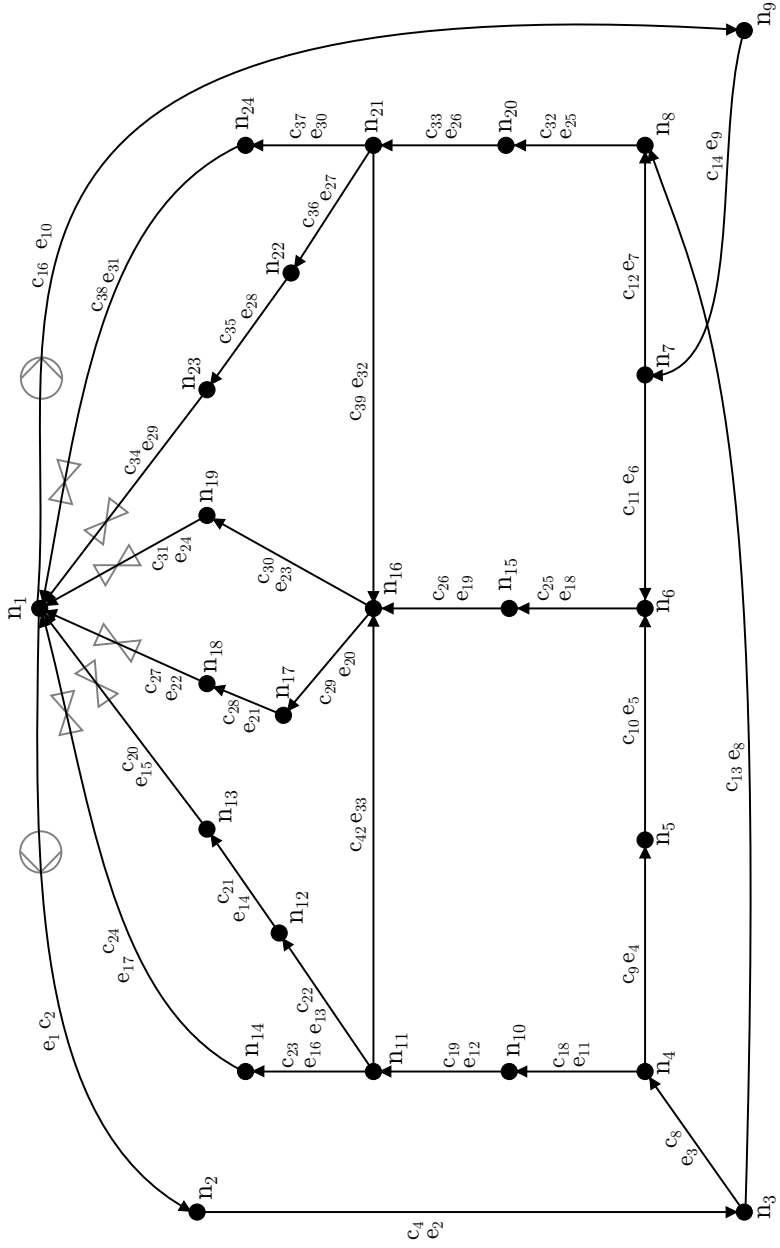
Table A.5: List of the pumps found in the system depicted in figure A.2 along with the constants which describe the pumps. The constants were provided by Grundfos. Note that the constants are scaled so the pump model in equation 2.20 has the units [bar], the rotational speed, ω , is in [1/s] that is valid in the interval [0,1] and lastly, the flow has the unit [m^3/h].

A.2 Test System Topology

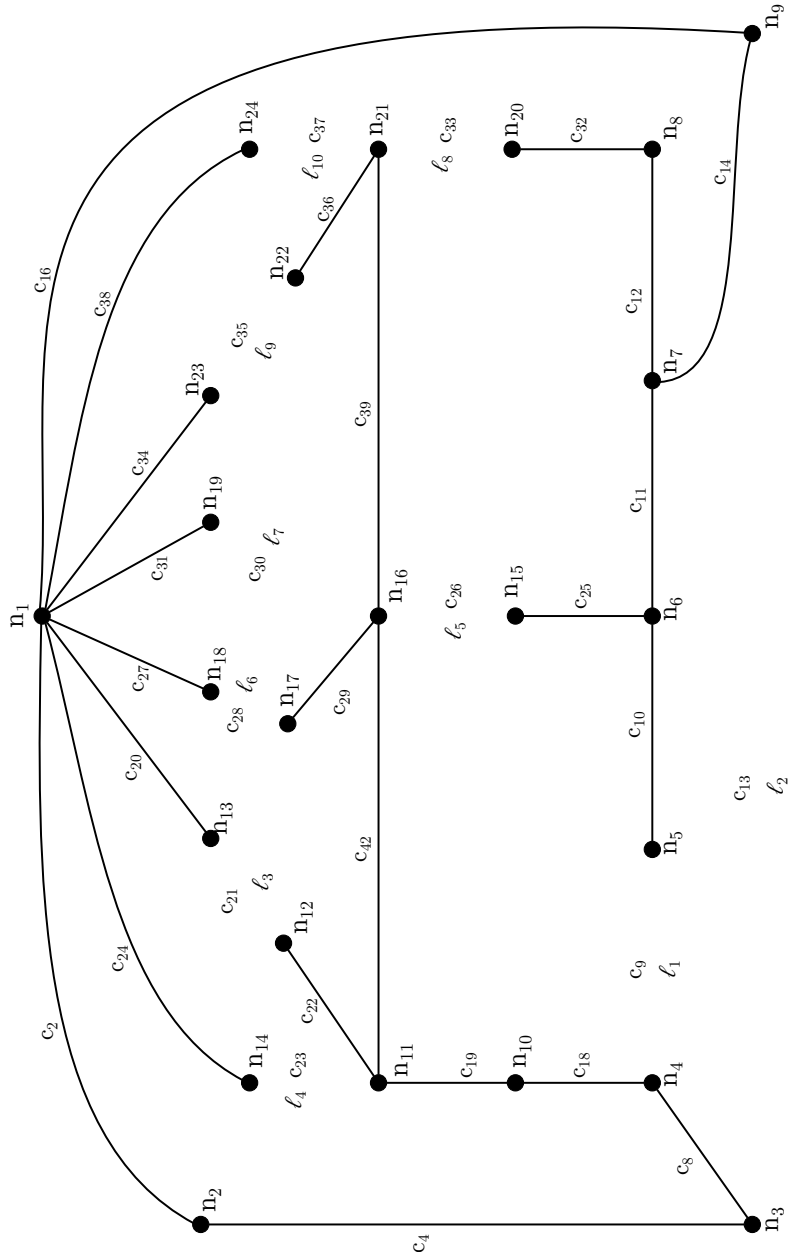


A.2. TEST SYSTEM TOPOLOGY

A.3 Test System Graph



A.4 Test System Spanning Tree



A.5 Test System Incidence Matrix \mathbf{H}

In Appendix A.7 a matrix \mathbf{B} is presented, this matrix has poorly chosen chords, thus it does not fulfill $\mathbf{B} = [\mathbf{I} \quad \mathbf{F}]$. By rearranging the order of the edges in \mathbf{B} a matrix $\mathbf{B}_f = [\mathbf{I} \quad \mathbf{F}]$ is obtained, Appendix A.8. Because the initial cycle matrix \mathbf{B} is of no use, the rearranged cycle matrix \mathbf{B}_f is simply defined as $\mathbf{B}, \mathbf{B} \triangleq \mathbf{B}_f$ in the report.

When rearranging the columns of the cycle matrix \mathbf{B} it is necessary to adapt the incidence matrix \mathbf{H} to the new column arrangement. Similarly to the procedure of \mathbf{B} the incidence matrix \mathbf{H} , shown in Appendix A.5, is rearranged to \mathbf{H}_f , shown in Appendix A.6, and for simplicity \mathbf{H} is then defined as $\mathbf{H}_f; \mathbf{H} \triangleq \mathbf{H}_f$.

	c^2	c^4	c^8	c^9	c^{10}	c^{11}	c^{12}	c^{13}	c^{14}	c^{16}	c^{18}	c^{19}	c^{22}	c^{20}	c^{23}	c^{24}	c^{25}	c^{26}	c^{28}	c^{29}	c^{27}	c^{30}	c^{31}	c^{32}	c^{33}	c^{36}	c^{35}	c^{34}	c^{37}	c^{38}	c^{39}	c^{42}	
$n1$	1	0	0	0	0	0	0	0	1	0	0	0	0	-1	0	0	0	0	0	-1	0	0	0	0	0	0	-1	0	0	0	0		
$n2$	-1	1	0	0	0	0	0	0	0	0	0	0	0	0	0	0	0	0	0	0	0	0	0	0	0	0	0	0	0	0	0		
$n3$	0	-1	1	0	0	0	0	0	0	0	0	0	0	0	0	0	0	0	0	0	0	0	0	0	0	0	0	0	0	0	0		
$n4$	0	0	-1	1	0	0	0	0	0	0	0	0	0	0	0	0	0	0	0	0	0	0	0	0	0	0	0	0	0	0	0		
$n5$	0	0	0	-1	1	0	0	0	0	0	0	0	0	0	0	0	0	0	0	0	0	0	0	0	0	0	0	0	0	0	0		
$n6$	0	0	0	0	-1	0	0	0	0	0	0	0	0	0	0	0	0	0	0	0	0	0	0	0	0	0	0	0	0	0	0		
$n7$	0	0	0	0	0	1	0	0	-1	0	0	0	0	0	0	0	0	0	0	0	0	0	0	0	0	0	0	0	0	0	0		
$n8$	0	0	0	0	0	0	0	-1	0	0	0	0	0	0	0	0	0	0	0	0	0	0	0	0	0	0	0	0	0	0	0		
$n9$	0	0	0	0	0	0	0	0	0	0	0	0	0	-1	0	0	0	0	0	0	0	0	0	0	0	0	0	0	0	0	0		
$n10$	0	0	0	0	0	0	0	0	0	0	0	0	0	0	-1	1	0	0	0	0	0	0	0	0	0	0	0	0	0	0	0		
$n11$	0	0	0	0	0	0	0	0	0	0	0	0	0	0	0	-1	1	0	0	1	0	0	0	0	0	0	0	0	0	0	1		
$n12$	0	0	0	0	0	0	0	0	0	0	0	0	0	0	0	0	-1	1	0	0	0	0	0	0	0	0	0	0	0	0	0		
$n13$	0	0	0	0	0	0	0	0	0	0	0	0	0	0	0	0	0	-1	1	0	0	0	0	0	0	0	0	0	0	0	0		
$n14$	0	0	0	0	0	0	0	0	0	0	0	0	0	0	0	0	-1	1	0	0	0	0	0	0	0	0	0	0	0	0	0		
$n15$	0	0	0	0	0	0	0	0	0	0	0	0	0	0	0	0	0	-1	1	0	0	0	0	0	0	0	0	0	0	0	0		
$n16$	0	0	0	0	0	0	0	0	0	0	0	0	0	0	0	0	0	0	-1	1	0	0	0	0	0	0	0	0	0	0	-1		
$n17$	0	0	0	0	0	0	0	0	0	0	0	0	0	0	0	0	0	0	0	-1	1	0	0	0	0	0	0	0	0	0	0		
$n18$	0	0	0	0	0	0	0	0	0	0	0	0	0	0	0	0	0	0	0	0	-1	1	0	0	0	0	0	0	0	0	0		
$n19$	0	0	0	0	0	0	0	0	0	0	0	0	0	0	0	0	0	0	0	0	-1	1	0	0	0	0	0	0	0	0	0		
$n20$	0	0	0	0	0	0	0	0	0	0	0	0	0	0	0	0	0	0	0	0	0	-1	1	0	0	0	0	0	0	0	0		
$n21$	0	0	0	0	0	0	0	0	0	0	0	0	0	0	0	0	0	0	0	0	0	0	-1	1	0	0	0	0	0	0	0		
$n22$	0	0	0	0	0	0	0	0	0	0	0	0	0	0	0	0	0	0	0	0	0	0	-1	1	0	0	0	0	0	0	0		
$n23$	0	0	0	0	0	0	0	0	0	0	0	0	0	0	0	0	0	0	0	0	0	0	0	-1	1	0	0	0	0	0	0	0	
$n24$	0	0	0	0	0	0	0	0	0	0	0	0	0	0	0	0	0	0	0	0	0	0	0	0	-1	1	0	0	0	0	0	0	0

A.6. TEST SYSTEM INCIDENCE MATRIX \mathbf{H}_f

A.6 Test System Incidence Matrix H_f

A.7 Test System Circuit Matrix B

A.8 Test System Circuit Matrix B_f

Appendix B

Unit Transformation

The SI-units for flow [m^3/s] and pressure [Pa] in equation 2.11 are converted to [m^3/h] and [bar] which are the units used throughout this project. The unit transformation procedure is described in the following equations where the symbols for flow and pressure belonging to the SI-units are denoted as q_{si} and p_{si} . The transformation results in equation B.2 which is then applied in equation 2.12.

First, equation 2.11 is recalled as:

$$\frac{L \rho}{A} \frac{dq_{si}}{dt} = \Delta p_{si} - \left(f \frac{8 L \rho}{\pi^2 D^5} + k_f \frac{8 \rho}{\pi^2 D^4} \right) |q_{si}| q_{si} - \Delta z g \rho \quad (\text{B.1})$$

The first step is transform the pressure unit where $1 \cdot p [\text{bar}] = \frac{p_{is}}{10^5} [\text{Pa}]$

$$\begin{aligned} \frac{L \rho}{A \cdot 10^5} \frac{dq_{si}}{dt} &= \frac{\Delta p_{si}}{10^5} - \left(f \frac{8 L \rho}{\pi^2 D^5 \cdot 10^5} + k_f \frac{8 \rho}{\pi^2 D^4 \cdot 10^5} \right) |q_{si}| q_{si} - \frac{\Delta z g \rho}{10^5} \\ \frac{L \rho}{A \cdot 10^5} \frac{dq_{si}}{dt} &= \Delta p - \left(f \frac{8 L \rho}{\pi^2 D^5 \cdot 10^5} + k_f \frac{8 \rho}{\pi^2 D^4 \cdot 10^5} \right) |q_{si}| q_{si} - \frac{\Delta z g \rho}{10^5} \end{aligned}$$

The second step is to transform the flow unit where $1 \cdot q [\text{m}^3/\text{h}] = 3600 \cdot q_{si} [\text{m}^3/\text{s}]$

$$\frac{L \rho}{A \cdot 10^5} \frac{d}{dt} \left(\frac{q}{3600} \right) = \Delta p - \left(f \frac{8 L \rho}{\pi^2 D^5 \cdot 10^5} + k_f \frac{8 \rho}{\pi^2 D^4 \cdot 10^5} \right) \left| \frac{q}{3600} \right| \frac{q}{3600} - \frac{\Delta z g \rho}{10^5}$$

Resulting in

$$\frac{L \rho}{A \cdot 10^5 \cdot 3600} \frac{dq}{dt} = \Delta p - \left(f \frac{8 L \rho}{\pi^2 D^5 \cdot 10^5 \cdot 3600^2} + k_f \frac{8 \rho}{\pi^2 D^4 \cdot 10^5 \cdot 3600^2} \right) |q| q - \frac{\Delta z g \rho}{10^5} \quad (\text{B.2})$$

Appendix C

Water Wall Pump Efficiency

As discussed in section 2.1.3, the pumping units in a water distribution network are assumed to be booster sets which are operated via differential pressure reference signal u . Section 2.1.3 also covers how to find the total energy efficiency, η for a single pump via equation 2.25 by applying the pump differential pressure, Δp , given in equation 2.20, the pump electrical power consumption, P_e , given in equation 2.24 and the flow through the pump, q . Equation 2.25 recalled in the following equation:

$$\eta = \frac{P_{\text{hydraulic}}}{P_e} = \frac{\Delta p \cdot 10^5 \cdot q \cdot 3600^{-1}}{P_e} \cdot 100$$

The pumps located on the Water Wall described in 3.1 are assumed to be booster sets even though they are only consist of a single pump. This means that the pumping units on the Water Wall do not have a constant efficiency over a wide range of flow as illustrated in 2.8. Even so, equation 2.26 which calculates the pump electrical power consumption, P_e , requires a constants efficiency value. A efficiency plot for the two pump types found on the Water wall are shown in figure C.1 and C.2 where the pump speed is set to $\omega = [0.1, 0.2, \dots, 0.8]$. Note that the pump constants are given in table A.5.

By analysing the efficiency plots one can see that it is hard to find a constant efficiency that can represent each pump type. Consequently, the pumps efficiency is defined from typical booster set efficiency value. The UPMXL pump represent a booster set which maintains a pressure in the water network main distribution lines. Meaning that a UPMXL pump represent a booster set containing relatively big pumps which usually have a combined efficiency around 80% [Kallesøe 15]. The UPM2 pump represent a booster set containing relatively small pumps where the purpose is to maintain a desired pressure in a small part of the whole distribution network. A typical efficiency for such a booster set is between 60 % and 70 % where the efficiency of 65 % is defined for the UPM2 pump [Kallesøe 15]. The resulting efficiency for each pump type is listed in table C.1.

Pump type	$\bar{\eta}$
Grundfos UPMXL GEO 25-125 180	$\eta_{\text{UPMXL}} = 0.8$
Grundfos UPM2 25-60 180	$\eta_{\text{UPM2}} = 0.65$

Table C.1: The defined efficiency for the two pump types located in the system.

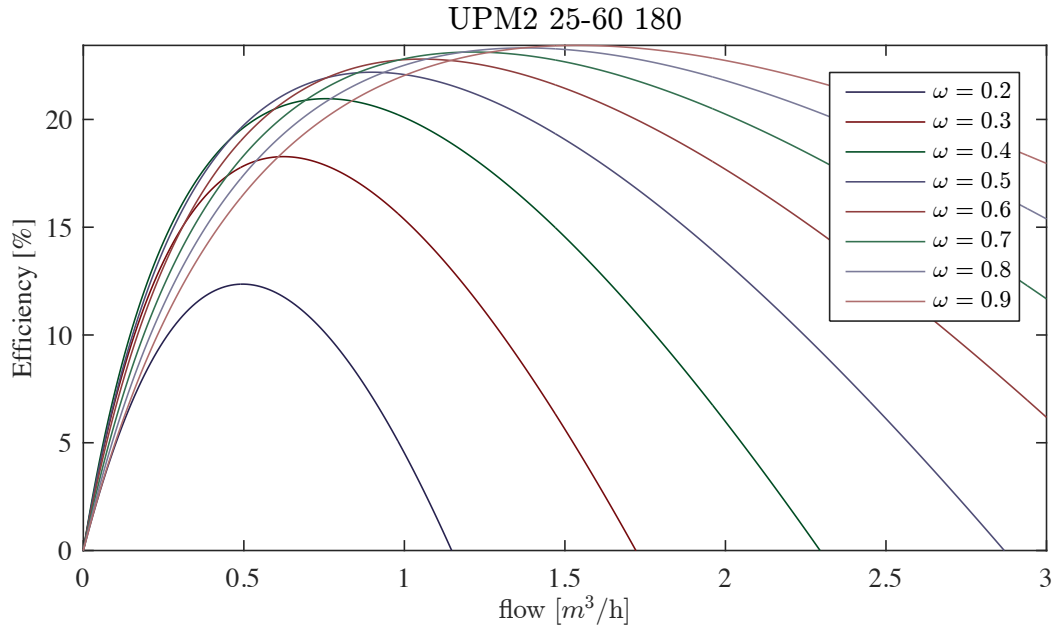


Figure C.1: An efficiency plot of UPM2 25-60 180 Grundfos pump showing its the efficiency for different rotational speeds ω . More information on the pump is found in table A.5.

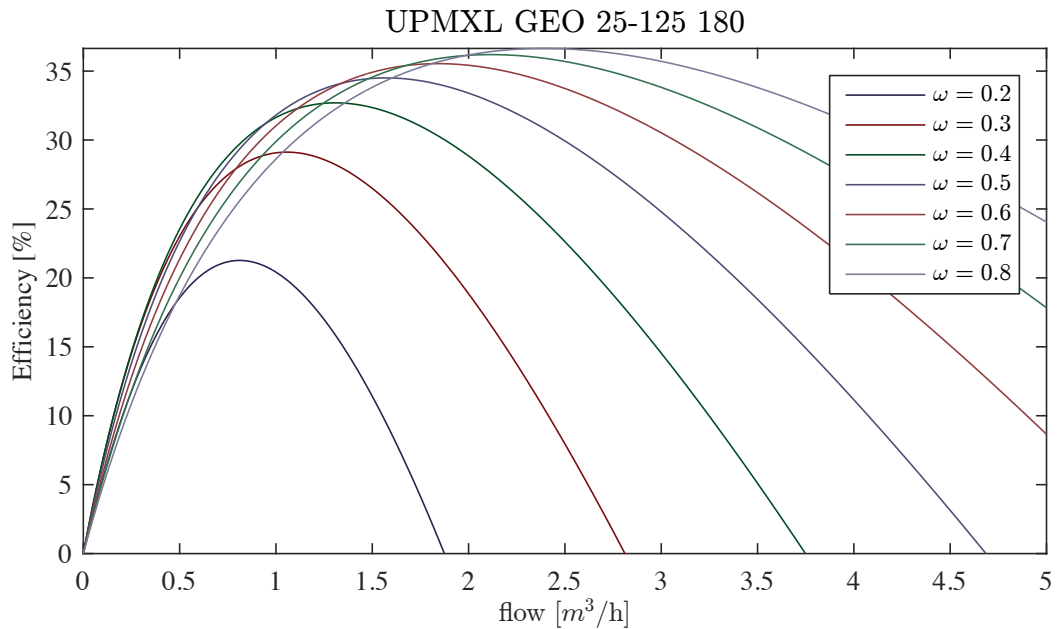


Figure C.2: An efficiency plot of UPMXML GEO 25-125 180 Grundfos pump showing its the efficiency for different rotational speeds ω . More information on the pump is found in table A.5.

Appendix D

Numerical Analysis of Chord Flows

There is a desire to determine whether $\mathbf{B}\lambda(\mathbf{B}^T \mathbf{q}_\ell^*)$ and $\mathbf{B}\mu(\mathbf{B}^T \mathbf{q}_\ell^*)$ are constant for all control signal \mathbf{u}_S given to the supply pumps for $\underline{\Delta p} \leq \mathbf{u}_S \leq \bar{\Delta p}$, in order to investigate convexity of the optimization problem.

The functions $\lambda(\mathbf{B}^T \mathbf{q}_\ell^*)$ and $\mu(\mathbf{B}^T \mathbf{q}_\ell^*)$ are constant if the chord flows \mathbf{q}_ℓ^* are constant for all \mathbf{u}_S . From simulation results of the system a numerical analysis of the flow convergence has been conducted. The simulation results are presented here.

D.1 Equal End-user OD Simulation Results

The simulation is performed with a 75 % OD for all end-user valves. The supply pumps differential pressures have been varied between each test to see whether the chord flows converge to the same steady state values.

D.1.1 Simulation-1 Results

$$u_{S1} = u_{S2} = 0.15 \Rightarrow \Delta p_{c2} = \Delta p_{c16} = -0.15 \text{ bar}$$

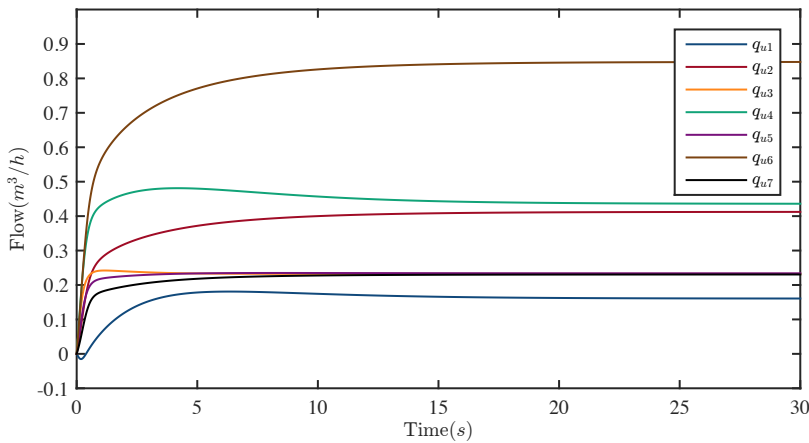


Figure D.1: Simulation results for \mathbf{q}_u flows with $\Delta p_{c2} = \Delta p_{c16} = -0.15$ bar and all end-user OD at 75 %.

D.1.2 Simulation-2 Results

$$u_{S1} = u_{S2} = 0.3 \Rightarrow \Delta p_{c2} = \Delta p_{c16} = -0.3 \text{ bar}$$

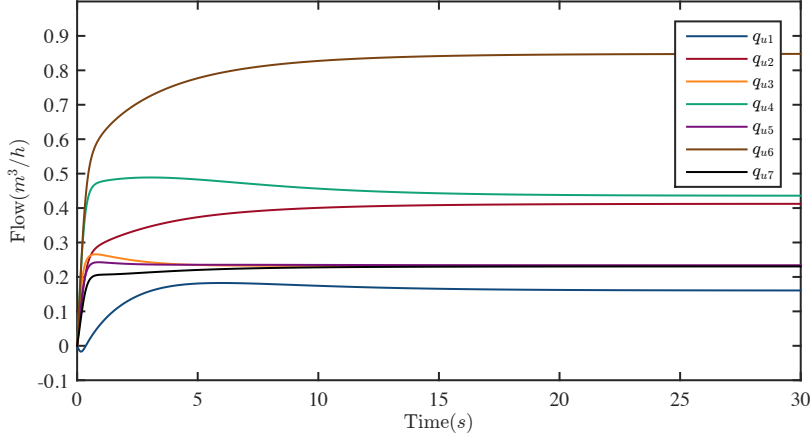


Figure D.2: Simulation results for q_u flows with $\Delta p_{c2} = \Delta p_{c16} = -0.3$ bar and all end-user OD at 75 %.

D.1.3 Simulation-3 Results

$$u_{S1} = u_{S2} = 0.5 \Rightarrow \Delta p_{c2} = \Delta p_{c16} = -0.5 \text{ bar}$$

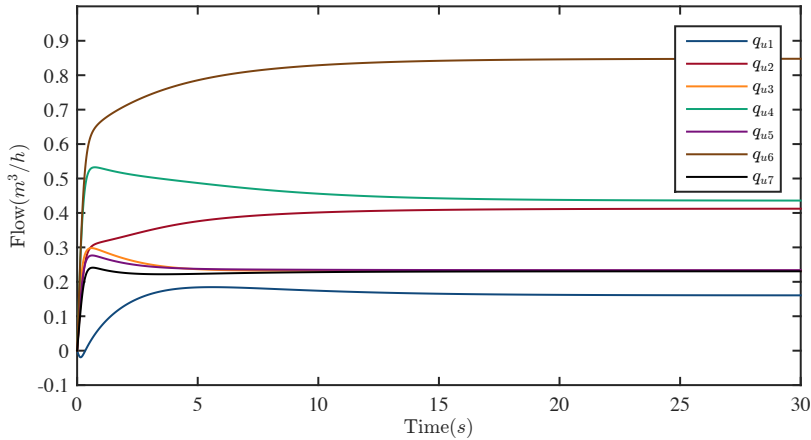


Figure D.3: Simulation results for q_u flows with $\Delta p_{c2} = \Delta p_{c16} = -0.5$ bar and all end-user OD at 75 %.

D.1.4 Convergence Error

A sum of square root error for the simulations are calculated as

$$\mathbf{e}_{i,j} = \sqrt{(\mathbf{q}_i - \mathbf{q}_j)^2} \quad (\text{D.1})$$

$$\mathbf{e}_{total} = \frac{1}{n+k} \sum_{i=1}^n \left(\mathbf{e}_{i,j} + \sum_{j=1}^k \mathbf{e}_{i,j} \right)$$

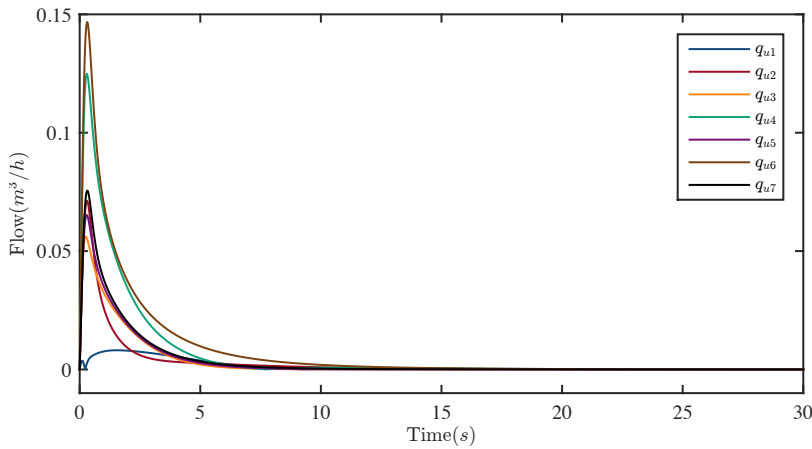


Figure D.4: Sum of square root error of the flow vectors from the previous three simulation results.

D.2 Unequal End-user OD Simulation Results

The simulation is performed with different OD for all end-user valves with $c_{20} = 25\%$, $c_{24} = 50\%$, $c_{27} = 75\%$, $c_{31} = 25\%$, $c_{34} = 50\%$, $c_{38} = 75\%$ open. The supply pumps differential pressures have been varied between each test to see whether the chord flows converge to the same steady state values.

D.2.1 Simulation-1 Results

$$u_{S1} = u_{S2} = 0.15 \Rightarrow \Delta p_{c2} = \Delta p_{c16} = -0.15 \text{ bar}$$

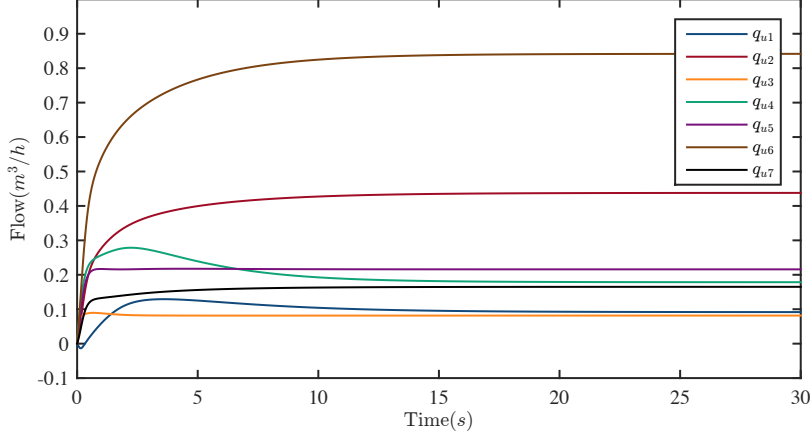


Figure D.5: Simulation results for \mathbf{q}_u flows with $\Delta p_{c2} = \Delta p_{c16} = -0.15$ bar and different end-user valve open degrees.

D.2.2 Simulation-2 Results

$$u_{S1} = u_{S2} = 0.3 \Rightarrow \Delta p_{c2} = \Delta p_{c16} = -0.3 \text{ bar}$$

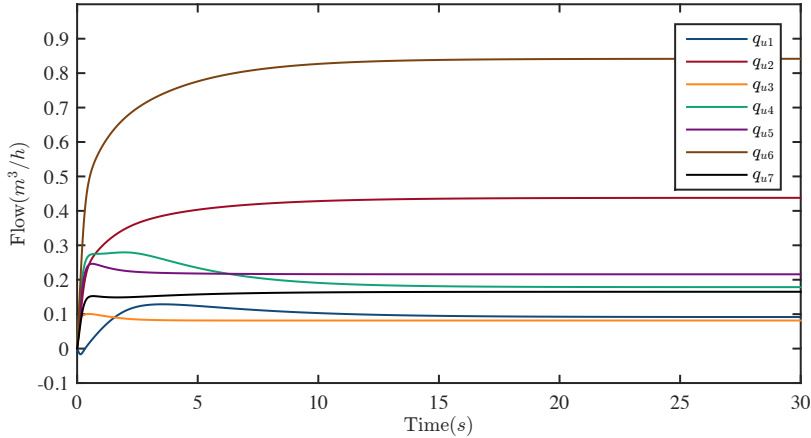


Figure D.6: Simulation results for \mathbf{q}_u flows with $\Delta p_{c2} = \Delta p_{c16} = -0.3$ bar and different end-user valve open degrees.

D.2.3 Simulation-3 Results

$$u_{S1} = u_{S2} = 0.5 \Rightarrow \Delta p_{c2} = \Delta p_{c16} = -0.5 \text{ bar}$$

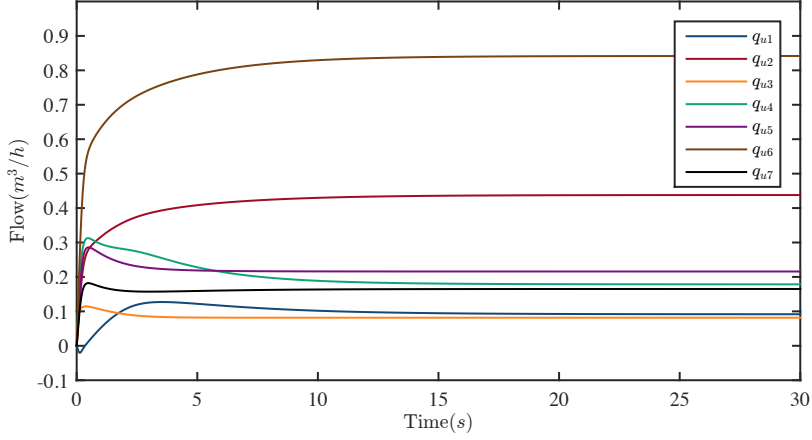


Figure D.7: Simulation results for \mathbf{q}_u flows with $\Delta p_{c2} = \Delta p_{c16} = -0.5$ bar and different end-user valve open degrees.

D.2.4 Convergence Error

A sum of square root error for the simulations are calculated as

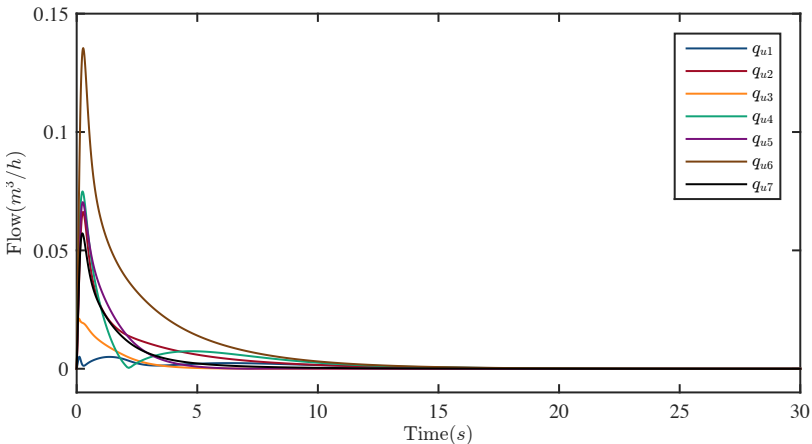


Figure D.8: Sum of square root error of the flow vectors from the previous three simulation results.

D.3 Constant Difference Between Supply Pumps Simulation Results

It has been observed that instead of limiting the pumps control signal to be equal, instead it may be possible to have a constant difference and still converge to the same steady state flows. Thus instead of maintaining the relation $u_{S1} = u_{S2}$, the relation $u_{S1} - u_{S2} = c$, where c is some constant.

The simulation is performed with different OD for all end-user valves with $c_{20} = 25\%$, $c_{24} = 50\%$, $c_{27} = 75\%$, $c_{31} = 25\%$, $c_{34} = 50\%$, $c_{38} = 75\%$ open. The supply pumps differential pressures have been varied between each test to see whether the chord flows converge to the same steady state values.

D.3.1 Simulation-1 Results

$$c = -0.15, \quad u_{S1} = 0.1, \quad u_{S2} = 0.25$$

$$u_{S1} - u_{S2} = -0.15 \Rightarrow \Delta p_{c2} = -0.1 \text{ bar}, \quad \Delta p_{c16} = -0.25 \text{ bar}$$

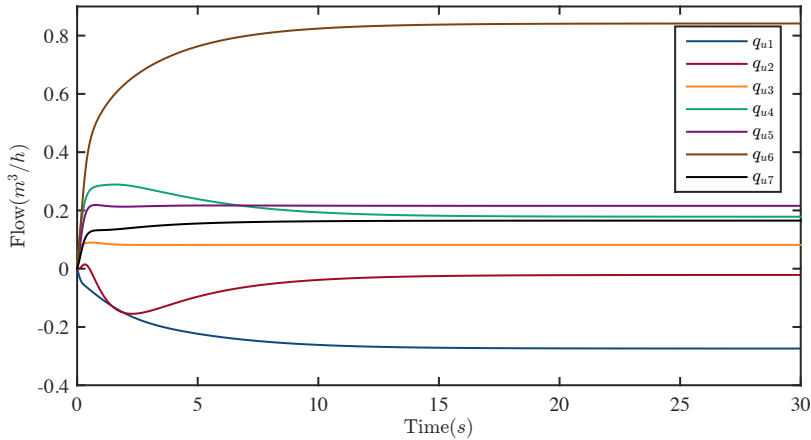


Figure D.9: Simulation results for \mathbf{q}_u flows with $u_{S1} - u_{S2} = -0.15 \Rightarrow \Delta p_{c2} = -0.1 \text{ bar}, \quad \Delta p_{c16} = -0.15 \text{ bar}$.

D.3.2 Simulation-2 Results

$$c = -0.15, \quad u_{S1} = 0.3, \quad u_{S2} = 0.45 \\ u_{S1} - u_{S2} = -0.15 \Rightarrow \Delta p_{c2} = -0.3 \text{ bar}, \quad \Delta p_{c16} = -0.45 \text{ bar}$$

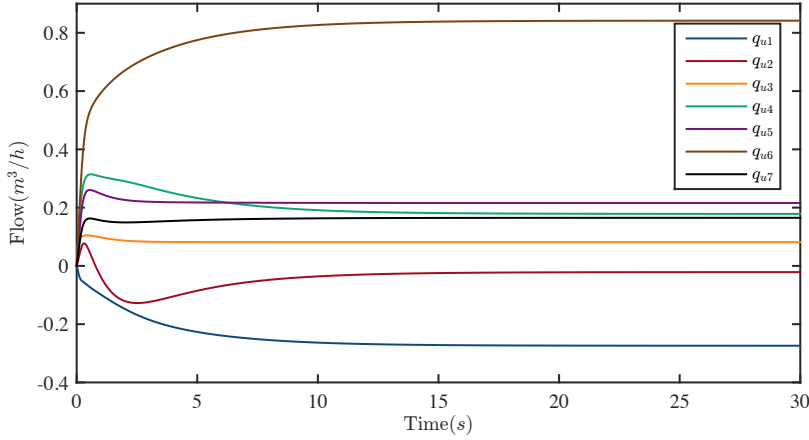


Figure D.10: Simulation results for \mathbf{q}_u flows with $u_{S1} - u_{S2} = -0.15 \Rightarrow \Delta p_{c2} = -0.3 \text{ bar}, \quad \Delta p_{c16} = -0.45 \text{ bar}$.

D.3.3 Simulation-3 Results

$$c = -0.15, \quad u_{S1} = 0.0, \quad u_{S2} = 0.15 \\ u_{S1} - u_{S2} = -0.15 \Rightarrow \Delta p_{c2} = 0.0 \text{ bar}, \quad \Delta p_{c16} = -0.15 \text{ bar}$$

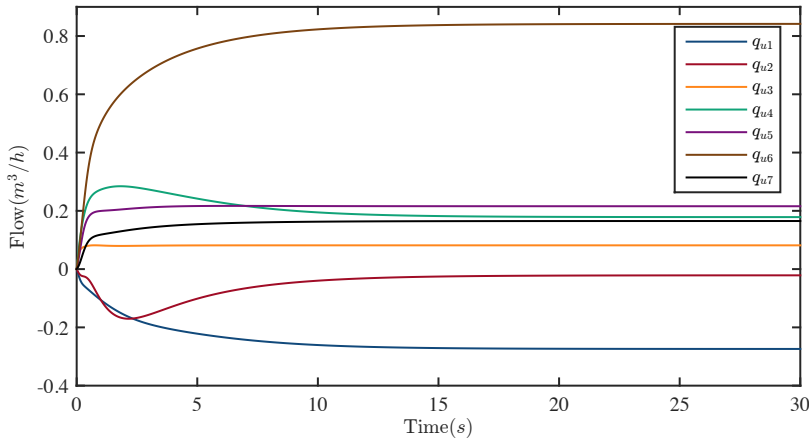


Figure D.11: Simulation results for \mathbf{q}_u flows with $u_{S1} - u_{S2} = -0.15 \Rightarrow \Delta p_{c2} = 0.0 \text{ bar}, \quad \Delta p_{c16} = -0.15 \text{ bar}$.

D.3.4 Convergence Error

A sum of square root error for the simulations are calculated as

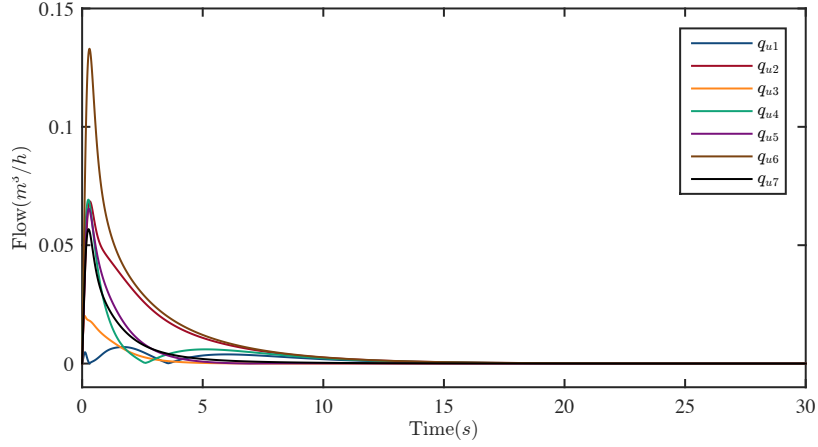


Figure D.12: Sum of square root error of the flow vectors from the previous three simulation results.

D.3.5 Conclusion

The conclusion is that the flow \mathbf{q}_ℓ^* is not constant for all \mathbf{u}_S . But the flow vector \mathbf{q}_ℓ^* is constant for $u_{S1} - u_{S2} = c$ where c is some constant. Thus imposing $u_{S1} - u_{S2} = c$ as an additional constraint on the optimization problem makes \mathbf{q}_ℓ^* constant.

Appendix E

Water Wall Setup Guide

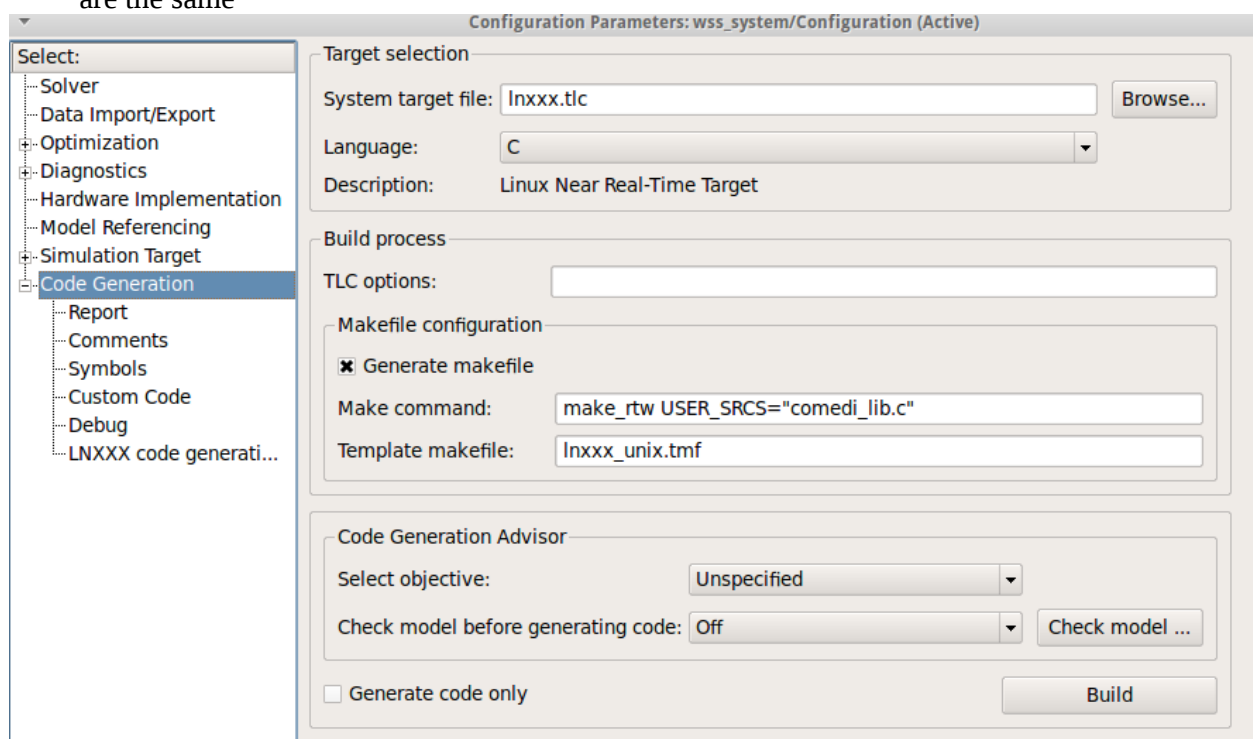
This is a short guide to setup the AAU Water Wall with a Linux PC.

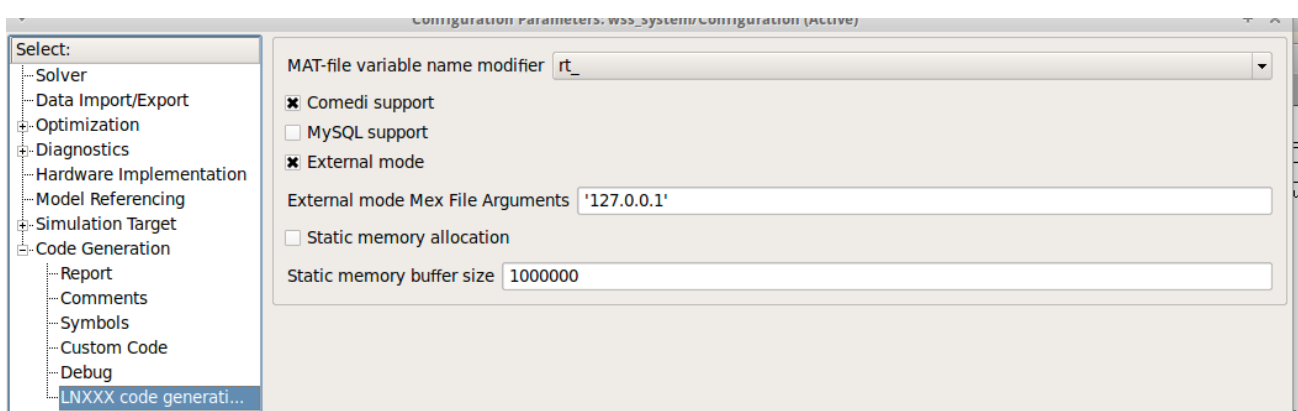
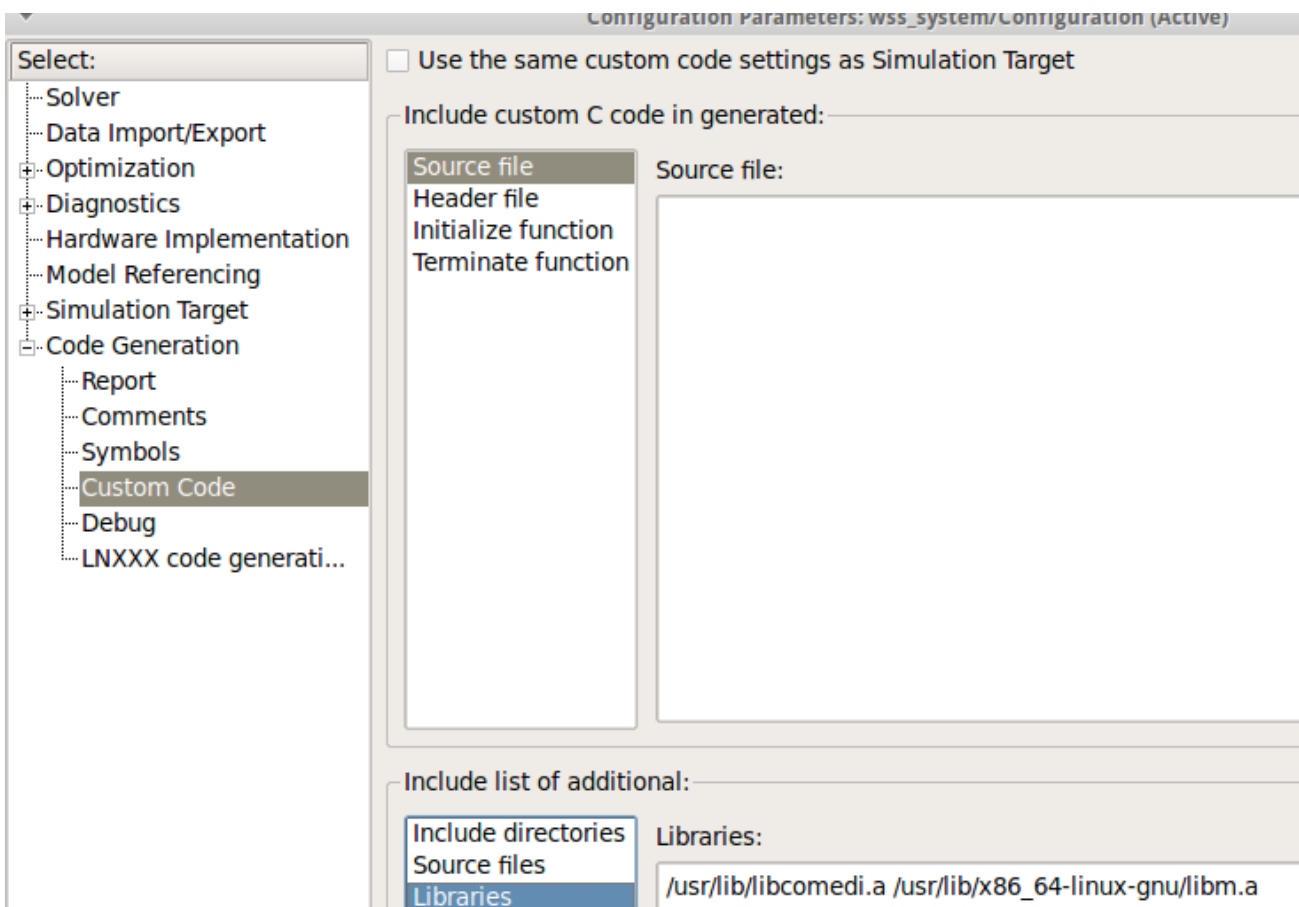
All drivers needed which are not included in MATLAB, Simulink or Linux can be found on the project CD.

- Connect a PC to the USB interface
- Turn on the Water Wall with the switch on the left side of the Water Wall
- Follow the guide on the next page

How to get the wAAUter wall to work with simulink realtime (AKA simulink Coder)

1. Install MATLAB R2012a and make sure that the Simulink Coder is a part of the installation
2. via software center : install libcomedi0 and libcomedi-dev
3. Make sure that folders 'bits' and 'sys' are inside the /usr/include. IF NOT make symbolic links. In our case, they exist in '/usr/include/x86_64-linux-gnu'.
4. Make a copy of the comedilib folder to 'your_path/MATLAB/R2012a/toolbox/'
5. Make a copy of the lnxxx folder to 'your_path/MATLAB/R2012a/rtw/c/src/'
6. Make a copy of the tcpip folder to 'your_path/MATLAB/R2012a/rtw/c/src/ext_mode' and 'your_path/MATLAB/R2012a/rtw/ext_mode'
7. In MATLAB 'addpath your_path/MATLAB/R2012a/toolbox/comedi'
8. open the simulink file 'wss_system.mdl' in MATLAB
GoTo Tools-->Code Generation-->options and make sure that the setting in the following figures are the same





9. click OK :) and press Ctrl+b for build.
10. Now a folder called 'wss_system_lnxxx_rtw' and 'slprj' are created along with a 'wss_system' file
11. Open a terminal and go to the folder including the simulink file and 'wss_system'
12. sudo ./wss_system -tf inf -w
13. In simulink GoTo simulation--> Connect to target
14. Lastly, GoTo simulation--> Start Real-Time Code
15. Now, what happens in simulink happens on the WALL!

Part V

Literature

Bibliography

- [Antoniou 07] Andreas Antoniou & Wu-Sheng Lu. Practical Optimizaztion, Algorithms and Engineering Applications. Springer, First edition, 2007.
- [Association 10] American Water Works Association. Water Transmission and Distribution - Principles and Practices of Water Supply Operations. TIPS Technical Publishing, Inc, Fourth edition, 2010.
- [Belimo 11] Belimo. *Technical data sheet R2..xx-S.* 2011.
- [Belimo 14] Belimo. *Notes for project planning. 2-way and 3-way characterised control valves*. 2014.
- [Belmio 10] Belmio. *Technical data sheet LRQ24A-SR.* 2010.
- [Boysen 11] Herman Boysen. *Technical paper. Kv: What, why, how, whence?* Rapport technique, Danfoss, 2011.
- [C. Kallesøe 11] J. Aarestrup C. Kallesøe & K. Rokkjær. *Energy optimization for booster sets.* World Pumps 0262 1762/11, 2011.
- [Deo 74] Narsingh Deo. GRAPH THEORY with Applications to Engineering and Computer Science. Prentice-Hall, Inc, 1974.
- [DePersis 07] Claudio DePersis, Tom Nørgaard Jensen, Romeo Ortega & Rafal Wisniewski. *Output Regulation of Large-Scale Hydraulic Networks.* JOURNAL OF LATEX CLASS FILES, vol. 6, no. 1, 1 2007.
- [Desoer 69] Charles A. Desoer & Ernest S. Kuh. Basic Circuit Theory. McGraw-Hill Book Company, 1st edition, 1969.
- [Encyclopedia 04] of World Biography Encyclopedia. *Konstantin Eduardovich Tsiolkovsky.* 2004. http://www.encyclopedia.com/topic/Konstantin_Eduardovich_Tsiolkovsky.aspx.
- [EPA 13] United States Environmental Protection Agency EPA. *Strategies for Saving Energy at Public Water Systems.* 2013. EPA 816-F-13-004.
- [Feldman 09] Mordecai Feldman. *Aspects of Energy Efficiency in Water Supply Systems.* Proc. 5th IWA Water Loss Reduction Specialist Conference, 2009.
- [Fischer 11] Georg Fischer. *GF Technical Manual For PE Piping Systems in Utilities.* 2011.
- [Fletcher 75] R. Fletcher. *An ideal penalty function for constrained optimization.* Journal of Institue of Mathematics and Applications, 1975.

- [Franklin 10] Gene F. Franklin, J. David Powell & Abbas Emami-Naeini. Feedback control of dynamic systems. Pearson, 2010.
- [GIZ 11] GIZ. Guidelines for Water Loss Reduction - A focus on pressure management. Deutsche Gesellschaft für Internationale Zusammenarbeit (GIZ) GmbH, 2011.
- [Goldstein 02] R. Goldstein & W. Smith. Water and Sustainability: U.S. Electricity Consumption for Water Supply & Treatment - The Next Half Century. Electric Power Research Institute, 2002.
- [Group 06] World Bank Group. *The Challange of Reducing Non-Revenue Water in Developing Countries*. 2006.
- [Grundfos 06] Grundfos. The Centrifugal Pump. GRUNDFOS Management A/S, 2006.
- [Grundfos 10] Grundfos. *Grundfos Data Booklet UPML, UPMXL*. 2010.
- [Horn 85] Roger A. Horn & Charles A. Johnson. Matrix Analysis. Cambridge University Press, First edition, 1985.
- [Hunt 95] Bruce Hunt. Fluid Mechanics For Civil Engineers. Department of Civil Engineering, University Of Canterbury Christchurch, New Zealand, 1995.
- [Kallesøe 05] Carsten Skovmose Kallesøe. Fault Detection and Isolation in Centrifugal Pumps. Aalborg Universitet, 2005.
- [Kallesøe 07] Carsten Skovmose Kallesøe. *Simulation of a District Heating*. 2007.
- [Kallesøe 12] Carsten Skovmose Kallesøe. *Method For Determining Characteristic Values, Particularly of Parameters, of a Centrifugal Pump Aggregate Driven by an Electric Motor And Integrated in a System*, 2012.
- [Kallesøe 14a] Carsten Skovmose Kallesøe. *Method For Detecting The Flow Rate Value of a Centrifugal Pump*, 2014.
- [Kallesøe 14b] Carsten Skovmose Kallesøe, Rafael Wisniewski & Tom Nørgaard Jensen. *A Distributed Algorithm for Energy Optimization in Hydraulic Networks*. Proceedings of the 19th IFAC World Congress, 2014, vol. 19, pages 11926–11931, 2014.
- [Kallesøe 15] Carsten Skovmose Kallesøe. *Grundfos knowledge*, 2015.
- [Keller 11] Urs Keller. *METHOD FOR THE HYDRAULIC COMPENSATION AND CONTROL OF A HEATING OR COOLING SYSTEM AND COMPENSATION AND CONTROL VALVE THEREFOR*, 2011.
- [KJ Astrom 94] and T Hagglund KJ Astrom. PID Controllers: Theory, Design, and Tuning . 1994.
- [Knudsen 08] Torben Knudsen, Klaus Trængbæk & Carsten Skovmose Kallesøe. *Plug and Play Process Control Applied to a District Heating System*. Elsevier IFAC Publications / IFAC Proceedings series, vol. 1, pages 1474–6670, 2008.
- [Lem 96] Gary A Lem, Gregory C Brown & Jogesh Warrior. *VALVE POSITIONER WITH PRESSURE FEEDBACK, DYNAMIC CORRECTION AND DIAGNOSTICS*, 1996.
- [Ljung 87] Lennart Ljung. System identification - theory for the user. PTR Prentice Hall, Englewood Cliffs, New Jersey 07632, 1987.
- [Persis 09] Claudio De Persis & Carsten Skovmose Kallesøe. *Pressure Regulation in Non-linear Hydraulic Networks by Positive Controls*. Proceeding of the 9th European Control Conference, 2009.

- [Persis 11] Claudio De Persis & Carsten Skovmose Kallesøe. *Pressure Regulation in Nonlinear Hydraulic Networks by Positive and Quantized Controls*. IEEE TRANSACTIONS ON CONTROL SYSTEMS TECHNOLOGY, vol. 19, no. 6, page 1371, 11 2011.
- [Petursson 15] Bjarni Geir Petursson. Boiler Feed System - Modelling and Control Analysis. Aalborg Universitet, 2015.
- [Polypipe 08] Polypipe. *Efast PVCu and ABS. High performance PVCu and ABS Pressure Pipe Systems*. 2008.
- [Nørgaard Jensen 14] Tom Nørgaard Jensen, Rafael Wisniewski, Claudio De Persis & Carsten Skovmose Kallesøe. *Output Regulation of Large-Scale Hydraulic Networks with Minimal Steady State Power Consumption*. Control Engineering Practice, vol. 22, pages 103–113, 2014.
- [Smith 97] Alice E. Smith & David W. Coit. Handbook of Evolutionary Computation, chapitre Constraint-Hnadling Techniques - Penalty Functions. Oxford University Press & Institute of Physics Publishing, 1997.
- [Swamee 08] Prabhata K. Swamee & Ashok K. Sharma. Design of Water Supply Pipe Networks. A John Wiley and Sons, 2008.
- [Tahavori 12] Maryamsadat Tahavori, Tom Nørgaard Jensen, Carsten Kallesøe, John Leth & Rafael Wisniewski. *Toward model-based control of non-linear hydraulic networks*. Journal of Vibration and Control, page 2146, 2012.
- [Thornton 07] J. Thornton & A. O. Lambert. *Pressure Management Extends Infrastructure Life and Reduces Unnecessary Energy Costs*. 2007.
- [Trifunovic 06] Nemanja Trifunovic. Introduction to Urban Water Distribution. Taylor & Francis, 2006.
- [Vinther 12] Kasper Vinther, Casper Hillerup Lyhne, Erik Baasch Sørensen & Henrik Rasmussen. *Evaporator Superheat Control With One Temperature Sensor Using Qualitative System Knowledge*. 2012.
- [Wavin 12] Wavin. *Tryktechnisk haandbog. FOR WAVIN PE-uPVC TRYKRØRSSYSTEMER*. 2012.
- [Wavin 15] Wavin. *K1 Tigris Press-fit Plumbing Product and Installation Guide*. 2015.

